工學博士 學位論文

Sensitivity Based Cooperative Operation for Grid Connected Converter and Distributed Generator Considering Losses in the Radial DC Distribution System

放射形 直流 配電系統에서 損失을 考慮한 系統 連繫 컨버터와 分散電源의 敏感度 基盤 協助 運營 技法

2016年 2月

서울大學校 大學院

電氣·컴퓨터 工學部

鄭 湖 龍

工學博士 學位論文

Sensitivity Based Cooperative Operation for Grid Connected Converter and Distributed Generator Considering Losses in the Radial DC Distribution System

放射形 直流 配電系統에서 損失을 考慮한 系統 連繫 컨버터와 分散電源의 敏感度 基盤 協助 運營 技法

2016年 2月

서울大學校 大學院

電氣·컴퓨터 工學部

鄭 湖 龍

Sensitivity Based Cooperative Operation for Grid Connected Converter and Distributed Generator Considering Losses in the Radial DC Distribution System

指導敎授 文 承 逸

이 論文을 工學博士 學位論文으로 提出함

2016年 **2**月

서울大學校 大學院
電氣·컴퓨터工學部
鄭 湖 龍

鄭湖龍의 工學博士 學位論文을 認准함

2016年 **2**月

委 員 長 _____(인)

副委員長 _____(인)

委 員 _____(인)

委 員 _____(인)

委 員 _____(인)

Abstract

Sensitivity Based Cooperative Operation for Grid Connected Converter and Distributed Generator Considering Losses in the Radial DC Distribution System

Ho-Yong Jeong
School of Electrical Engineering and Computer Science
The Graduate School
Seoul National University

This dissertation proposes a cooperative control scheme for grid connected converter (GCC) and distributed generator (DG) considering line and conversion losses in the radial DC distribution system and novel formulations of approximate expression for voltage sensitivity and line loss sensitivity.

Interesting and possibilities of the DC distribution system is increasing due to its advantages. In the DC distribution system, transmittable power can be increased and overall system loss is smaller comparing with the AC distribution system. The DC distribution system is also suitable for smart grid (SG) environment from the perspective of energy efficiency, sustainability, and flexibility and this is one of important technical issues in SG. Possibility and feasibility of the DC distribution system is studied in many researches. However, there are technical issues on the DC distribution system and these should be considered from the perspective of stable and economic operation. Loads in the DC distribution system are fed through DC/AC or DC/DC converter, which have constant-power load (CPL)

behavior, and CPL behavior cause voltage instability due to negative incremental resistance characteristics of CPL. Voltage control methods have studied to prevent voltage instability. However, these studies have drawbacks of limit of voltage regulation capability and efficient voltage control. Especially, line and conversion loss is an important factor in the DC distribution system from view point of efficient operation because large power delivered by power converter. However, most of conventional researches do not focused on both line loss over the conductor and conversion loss.

The Purpose of research in this dissertation is to control voltage within suitable range considering total loss reduction in the radial DC distribution system. Before establishing control scheme, novel sensitivity expressions on voltage and line loss are formulated based on linear approximation and reasonable assumptions. Verification on proposed formulation is presented and it is indicated that an accuracy of proposed expression presents a good result. Analytic analysis of voltage sensitivity is presented and results are utilized to construct a voltage control strategy. In addition, these formulations are useful for fast speed controller because the computation effort can be reduced.

Based on approximate sensitivity expression and analysis result, cooperative voltage control scheme considering total losses in the radial DC distribution system is proposed. The structure of the overall control scheme is illustrated and roles and interaction of voltage control equipment are explained. A model for an optimal scheduling is presented and objective function and constraints are formulated. The Control strategies for loss reduction and voltage regulation are established and control modules are designed to realize proposed strategy. In addition, the loss sensitivity on total with regard to voltage control equipment is formulated and it represents the actual loss sensitivity due to changes in electrical quantities of the voltage control equipment.

The proposed method applied to the test system to verify effectiveness and tested under various conditions using MATLAB and PSCAD/EMTDC. The results

have shown that the entire bus voltages are regulated and loss can be reduced under varying load and generation condition.

The cooperative voltage control scheme can be implemented within the radial DC distribution system and provide a useful control scheme from the perspective of stability and economic operation.

Keyword: DC distribution system, Cooperative voltage control, Loss reduction, Voltage sensitivity, Loss sensitivity

Student Number: 2009-20897

Table of Contents

List of Tables

List of Figures

Abbreviation

Chapter 3

g_{ij}	Conductance of the line between bus *i* and bus *j*
g_{ii}	Conductance of a constant resistive load at bus *i*
G_{ij}	Element of an *G*-Bus matrix at *i*-th row and *j*-th column
V_{slack}	Slack bus voltage
n	Number of buses in the DC distribution system
$P_{L,i}$	The load power of constant power load at bus *i*
$[J]$	Jacobian matrix for the DC power system
V_i	Bus voltage at bus *i*
P_i	Net bus real power (*i.e.*, generation minus the load consumption)
$\{R_i\}$	Set of line resistances located on the shortest path between the slack bus and bus *i*
R_{ij}	Element of an *R*-Bus matrix at *i*-th row and *j*-th column

Chapter 4

N_T	Number of time intervals
N_K	Number of voltage control equipment
P_{DG}^{loss}	Converter internal loss of DG
P_{GCC}^{loss}	Converter internal loss GCC
P_{line}^{loss}	Line loss over the conductors in the DC distribution system
a_k	Coefficient for converter internal loss equation of *k*-th DG
b_k	Coefficient for converter internal loss equation of *k*-th DG
c_k	Coefficient for converter internal loss equation of *k*-th DG

a_{GCC}	Coefficient for converter internal loss equation of *GCC*
b_{GCC}	Coefficient for converter internal loss equation of *GCC*
c_{GCC}	Coefficient for converter internal loss equation of *GCC*
V_{max}	Maximum allowed voltage
V_{min}	Minimum allowed voltage
SOC	State-of-charge (SOC) of energy storage system
SOC_{max}	Maximum SOC
SOC_{min}	Minimum SOC
SOC_{meas}	Measured SOC
SOC_{final}	SOC at end of last time interval
P_{DG}	Output power of DG
P_{DG}^{min}	Minimum output power of DG
P_{DG}^{max}	Maximum output power of DG
P_{GCC}	GCC output power at secondary side
P_{GCC}^{min}	Minimum GCC output power
P_{GCC}^{max}	Maximum GCC output power
P_{DG}^{meas}	Measured DG output power
P_{GCC}^{meas}	Measured GCC output power
P_{DG}^{ref}	Reference output power of DG
P_{GCC}^{ref}	Reference output power of GCC
T_{period}	Time period of a scheduling
C	Capacity of battery (Wh)
P_{avg}	Average delivered power from the battery during a time interval
$P_{DG,ref}^{reg}$	DG Output power reference for voltage regulation
$P_{DG,ref}^{loss}$	DG Output power reference for loss reduction
$P_{DG,ref}^{sch}$	Scheduled DG output power reference
$V_{GCC,ref}^{reg}$	GCC Output voltage reference for voltage regulation

$V_{GCC,ref}^{loss}$	GCC Output voltage reference for loss reduction
$V_{GCC,ref}^{sch}$	Scheduled GCC output voltage reference
V_{high}	Highest bus voltage
V_{low}	Lowest bus voltage
V_{max}	Maximum voltage limit
V_{min}	Minimum voltage limit
V_{max}^{loss}	Maximum voltage limit for loss reduction control
V_{min}^{loss}	Minimum voltage limit for loss reduction control
W_{margin}	Marginal width for voltage regulation
$\Delta P_{GCC}^{by\,P_{DG}}$	Variation of the GCC output due to the DG output power
$\Delta P_{GCC}^{by\,P_{GCC}}$	Variation of the GCC output due to the GCC output voltage
P_{total}^{loss}	Total loss including line loss and converter internal losses of voltage control equipment
V_{DG}^{target}	Target voltage should be regulated by DG
V_{GCC}^{target}	Target voltage should be regulated by GCC
SW_{DG}^{pos}	Positive power flag signal for loss reduction controller of DG
SW_{DG}^{neg}	Negative power flag signal for loss reduction controller of DG
SW_{GCC}^{pos}	Positive voltage flag signal for loss reduction controller of GCC
SW_{GCC}^{neg}	Negative voltage flag signal for loss reduction controller of GCC
V_{high}^{reg}	Magnitude of highest voltage should be regulated
V_{low}^{reg}	Magnitude of lowest voltage should be regulated
$P_{DG,high}^{reg}$	Required output power of DG to regulate highest voltage violation
$P_{DG,low}^{reg}$	Required output power of DG to regulate low voltage violation
$V_{GCC,high}^{reg}$	Required output voltage of GCC to regulate highest voltage violation
$V_{GCC,\mathrm{low}}^{reg}$	Required output voltage of GCC to regulate lowest voltage violation
$P_{DG,upper}^{reserve}$	Upper reserve of the DG output power
$P_{DG,lower}^{reserve}$	Lower reserve of the DG output power

$\Delta P_{DG,high}^{loss}$	Estimated loss variation due to highest voltage regulation
$\Delta P_{DG,low}^{loss}$	Estimated loss variation due to lowest voltage regulation
VR	Voltage regulation

Chapter 5

x	Actual value delivered to local controller
$x_{meausred}$	Measured value gathering by supervisory controller
T_d	Communication delay between supervisory controller and local controller
V_{GCC}^{ref}	Voltage reference of conventional voltage regulation controller for GCC
V_{DG}^{ref}	Voltage reference of conventional voltage regulation controller for DG

Appendix A

$V_{Drop,k}$	Voltage drop between the slack bus and bus *k* due to bus injection current at bus *k*

Chapter 1. Introduction

1.1. Motivation of This Dissertation

1.1.1. Motivation of researches on the DC distribution system

Initially, Thomas A. Edison was shown an arc light system in Boston in 1878, and developed all necessary components for a complete low-voltage (LV) DC distribution system to deliver electricity to power both lights and machines. The drawback of this DC system was limited distance of feeder due to low voltage. Since then, George Westinghouse has built the AC power system and incorporated the patents of AC transformer and two-phase induction machine. The first poly-phase AC power system was introduced to distribute electrical power at the world fair in Chicago 1893. In the AC power system, the voltage can be boosted easily by the transformer. Therefore, the AC power system can deliver the electricity to long distance and transmittable power was increased, and it becomes a commonly used power system.

Nevertheless, the DC system is still remained and high voltage (HV) DC system, which is effective in large power transmission for long distance, is a representative system. In addition, there has been growing interest in DC network over the past several years. There have been many reports of investigations of the advantages of DC distribution systems over AC systems and possibilities of LVDC distribution system are discussed. Higher transmission powers and transmission distances can be achieved with the LVDC system and it is proved that the transmittable power can be increased by as much as 10 times [1, 2]. Line losses decrease and cable cross-sections become smaller, therefore, the total constructing and operating cost of the DC distribution system can be decreased [2]. Meanwhile, requirement for the DC distribution system is increasing as environment of the

power grid is changed. A concept of smart grid (SG) is introduced to enhance the conventional power system and benefits are anticipated, which are improving power reliability and quality, enhancing capacity and efficiency of the existing electric power network, enabling predictive maintenance and self-healing responses to system disturbance, and are anticipated [3]. From a concern of power distribution, DC distribution system will be important part it has various advantages in SG environment. When renewable energy resources (RESs) which utilize the DC power such as a photovoltaic (PV) generator are incorporated into a DC distribution system, energy conversion can be eliminated, which results in a saving of 2.5–10% of the generated energy [4]. Distributed energy resources (DERs), energy storage systems (ESSs), and electric vehicles (EVs) can be utilized efficiently in a DC distribution system because they utilize DC power [5]. Such advantages motivate further study into the applications of DC distribution systems, including residential home, commercial facilities, industrial area, and shipboard power systems, and they proved the feasibility of the DC distribution system [6-12]. Furthermore, Studies discussed the integration of DER in the DC distribution system, and it is presented that high power quality network can be constructed [13, 14].

DC distribution systems can have various grid layouts, including radial, ring and meshed grids, which affect their vulnerability to faults [8]. Furthermore, in naval shipboard systems, a zonal distribution architecture can be applied to satisfy the requirements for survivability, low weight, reduced manning, and low costs [10]. In conventional distribution systems, radial distribution is most commonly used, and this structure can be used if the DC distribution system replaces a conventional AC distribution system, which is the focus of this dissertation.

1.1.2. Specific topics in this dissertation

Voltage Instability Problem

In the DC distribution system, loads are generally fed through DC/AC or

DC/DC converters, which have constant-power load behavior if the converter maintains continuous load consumption under rapid current and voltage variations. Constant power loads (CPLs) tend to draw constant power load regardless of the bus voltage, and therefore, it has a negative incremental resistance [15]. This is the reason of voltage instability in the DC distribution system and research to enhance the voltage stability in the DC distribution system is presented [16].

Voltage Regulation in the DC network

Because of a voltage instability problem, many researches are carried out concerning voltage control in the DC network and there are standard for steady state voltage tolerance limit [17]. Therefore voltage regulation is a fundamental control object in the DC network for stable operation. In conventional studies, researches only focus on voltage control in small scale DC network such as nanogrid which consists of a common bus and microgrid. However, voltage problem in larger scale DC distribution system should be investigated because DC network is expanded becomes larger and new kind of voltage problem can occur.

Loss Reduction

Loss reduction is one of a common object in many researches on optimal operation and control in the distribution system. Researches focus on reducing line loss and conversion loss in whole distribution system. There were various concerns on loss reduction in planning, operation, and control. These efforts are more important nowadays because the concerns about high gas price and global warming, energy efficiency are focusing. In addition, loss reduction is meaningful for efficient operation to reduce operation cost in the distribution system.

Researches on Voltage and Loss Sensitivities

Voltage sensitivity represents the relation between voltage and electrical quantities and provides useful information on system characteristic. The voltage is

a major variable in DC network because it determines current and power flow between buses and reflects stability. Loss sensitivity is also important from concern of efficient operation of DC network. Generally, Jacobian matrix is used to calculate these sensitivities while there methods have limitations when analyzing sensitivities and understanding system characteristic.

1.2. Highlights and Contributions

This dissertation proposes a cooperative control scheme for GCC and DG considering line and converter losses in the radial DC distribution system. Its contributions can be divided into three areas, described as follows.

Formulation of the approximate voltage sensitivity in the radial DC distribution system

Voltage is a primary variable in the DC distribution system and it affect overall characteristic of the system. Therefore, study on the voltage characteristic is helpful to understand system phenomenon and establish operation and control strategy in the DC distribution system. In this dissertation, a novel approximate expression of the voltage sensitivities are formulated and analytic analysis of the voltage sensitivity is presented based on these formulations.

Formulation of the approximate line loss sensitivity in the radial DC distribution system

In a similar way as shown in formulation of approximate voltage sensitivity expression, a formulation and verification of approximate expression of line loss sensitivity are presented. This expression is a basis of cooperative voltage control scheme.

Cooperative control scheme for voltage regulation

Cooperative voltage control scheme to regulate voltage problem in larger scale radial DC distribution system is proposed. Proposed method utilizes GCC and DG and voltage control equipment can regulate both maximum and minimum voltage violation by proposed control strategy considering voltage sensitivity characteristic.

Cooperative control scheme for loss reduction

Loss reduction strategy based on proposed approximate sensitivity expression is integrated to proposed voltage regulation method. Therefore, voltage control equipment can reduce total system loss while maintain overall bus voltages within suitable range. Proposed method deals with loss reduction from concern of a scheduling and real-time control. Methodology of proposed cooperative control scheme is illustrated and specific control modules are designed to realize cooperative control scheme.

1.3. Dissertation Organization

Chapter 1 consists of the general introduction, motivation, highlights and contributions, and describes the organization of this dissertation.

Chapter 2 reviewed technical issues on specific topics in this dissertation. Technical issues in the DC distribution system including voltage problem, loss reduction problem, an importance of sensitivity analysis is presented

Chapter 3 proposed a novel formulation of approximate voltage sensitivities with regard to the slack bus voltage and bus injection power. Accuracy of proposed formulation is compared to actual value to verify approximate voltage sensitivities. Based on formulations, analytic analysis on the voltage sensitivity is described.

Chapter 4 presents a novel formulation of approximate loss sensitivities with regard to the slack bus voltage and bus injection power. Proposed formulation is verified by comparing actual loss sensitivity.

Chapter 5 describes proposed cooperative voltage control scheme considering

the voltage regulation and loss reduction. Methodology of proposed scheme is illustrated and explanation of scheduling process and local controller are presented. Detail design and function of each module in the local controller is presented.

Chapter 6 presents case studies. The improvement of the voltage regulation and loss reduction using the proposed methods is identified.

Chapter 7 concludes this dissertation and discusses future extensions.

Chapter 2. Technical Issues on Specific Topics in This Dissertation

The main purpose of this dissertation is to develop a cooperative voltage control scheme in the DC distribution system. In proposed method, control scheme considering voltage regulation and loss reduction is presented. Specifically, this dissertation focuses on topics on the radial DC distribution system: researches on voltage and loss sensitivities and a cooperative voltage control for long distance distribution system considering loss reduction. Before presenting above topics, technical issues are discussed in here and necessities of proposed studies are presented.

2.1. Voltage Control

2.1.1. Voltage Control in the AC distribution Network

Structure of AC distribution system

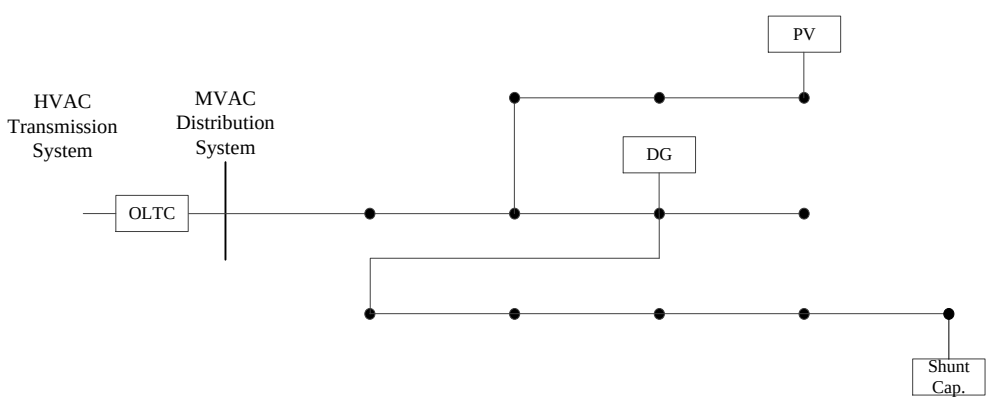

Figure 2.1. Typical structure of radial AC distribution system

In the AC distribution system, DNO should maintain bus voltages within appropriate range for stabile and reliable power distribution. However, voltage

problem occurs due to long distance distributed line and large load power. Figure 2.1 illustrates typical structure of radial AC distribution system. Distribution system is connected to higher voltage AC (HVAC) transmission system through on-load tap changing (OLTC) transformer. Typical distribution system is radial structure and shunt capacitor and DERs are connected.

Conventional Voltage control strategy in AC distribution system

In conventional voltage control strategy, OLTC and shunt capacitor are utilized. OLTC can control whole bus voltage by changing its tap and tap position of OLTC is usually controlled depending on load consumption power. For example, DNO increases tap position of OLTC in peak load time interval because overall bus voltages are decreased due to large load current. In conventional AC distribution system, power is only delivered from OLTC to EOL bus because there were not DERs. Because distribution system has radial structure, voltage of drop is accumulated power is delivered to end-of-line (EOL), and voltage problem might occur at EOL bus if line distance is too long or large load power is consumed. This problem is can be resolved by shunt capacitor which provides reactive power compensation.

Effect on voltage control strategy due to DERs

However, DERs are connected in the distribution network recently and voltage regulation strategy becomes more complex. Changes in generation power of RESs induce voltage variation in the distribution network and it causes power quality problem such as flicker. Moreover, current flows reversely, from EOL to OLTC, due to large generation power of DERs. In this case, conventional rule based voltage control strategy cannot be applied. Conventional voltage control method established based on assumption which EOL voltage is smaller than other bus voltage. However, this assumption is not satisfied in recent distribution network environment and various voltage control method which utilizes DERs are

introduced considering DERs. If DERs is dispatchable and controlled by DNO, voltage can be regulated by controlling both active power and reactive power of DERs [18, 19].

2.1.2. Voltage Control in the DC distribution Network

Structure of DC distribution system

Distinct characteristic of voltage control methods in the DC distribution network is that only active power is utilized. Reactive power is negligible in the DC distribution system and active power compensator, which means controllable power sources such as DGs, is required for voltage control. In addition, distribution system is connected to utility grid through GCC and it can control DC side voltage as OLTC in the AC distribution system. Figure 2.2 illustrate typical structure of radial DC distribution system including GCC and DERs.

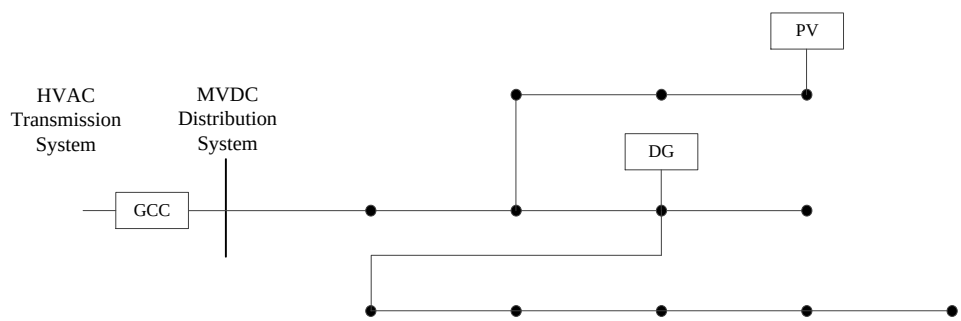

Figure 2.2. Typical structure of radial DC distribution system

Voltage regulation standard

In DC distribution system, the bus voltage should be maintained within appropriate range for stable operation and IEC 60092-101 recommended that maintain the steady state DC voltage within 10% voltage tolerance limit [17]. Figure 2.3 illustrates DC voltage tolerance in steady state and when there is a fault. Larger voltage tolerance is acceptable during a short time when fault is occurred and cleared. However, voltage should be recovered within 10% tolerance limit 1

second after fault is occurred and maintained within this tolerance limit in steady state.

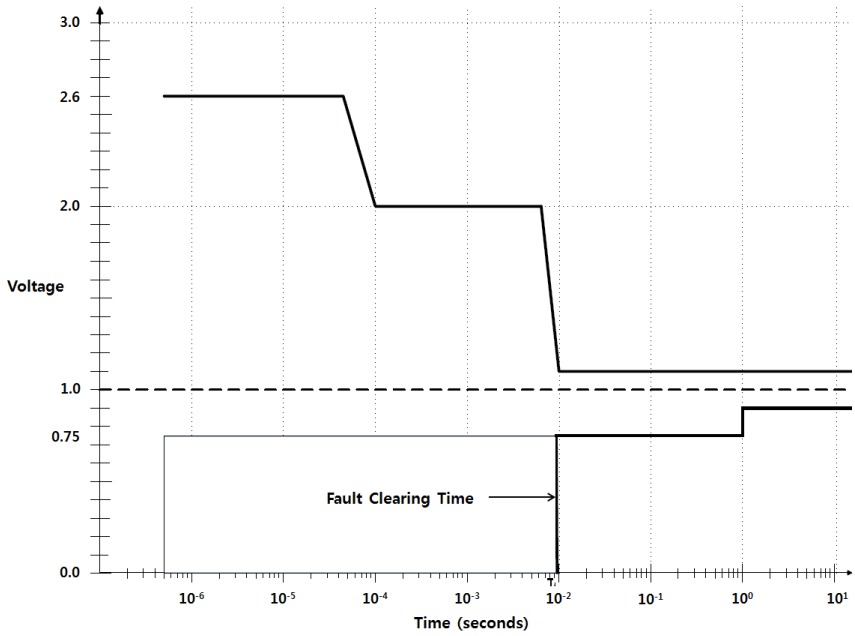

Figure 2.3. DC voltage tolerances worst case envelope

Classification of voltage control method

Three kinds of voltage control methods can be classified, constant voltage control, constant power control, and droop control method.

With constant voltage control, voltage reference is entered to voltage control equipment and it provides active power to maintain the target bus voltage to reference voltage. Voltage references can be determined by various control object and method, for example, voltage references is determined by DBS voltage control in [20] and fuzzy control in [21] to regulate bus voltage. Common structure of this controller is illustrated in Figure 2.4.

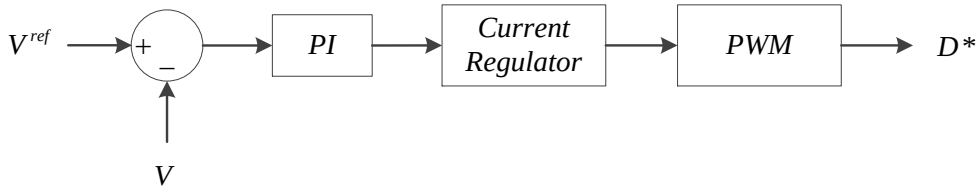

Figure 2.4. Structure of constant voltage controller

In constant power control, output power of converter is regulated by power reference. Generally, this control method is applied to master / slave control scheme and DERs which is controlled by this method does not participate in voltage control. However, this control is useful to voltage control if certain power reference of DER is determined by voltage control strategy.

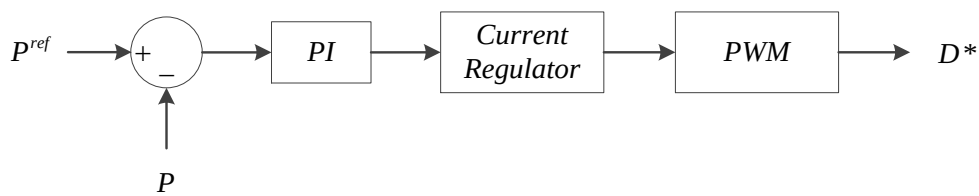

Figure 2.5. Structure of constant power controller

Droop control is most common voltage control scheme in the AC and DC distribution system and it is useful to power sharing of a number of DERs. Communication is not required because control is implemented with only local measurement of voltage control equipment. However, control is affected by droop coefficient and result of voltage control performance might be poor if inappropriate droop coefficient is chosen. In the DC distribution system, active power versus voltage droop control is widely used, which is presented in Figure 2.6. Modified droop control methods is utilized in some research and droop control considering SOC of ESS is presented in [22, 23]. In these researches, droop coefficient of each ESS is determined by its SOC and output power deviation becomes smaller if SOC margin of ESS is decreased.

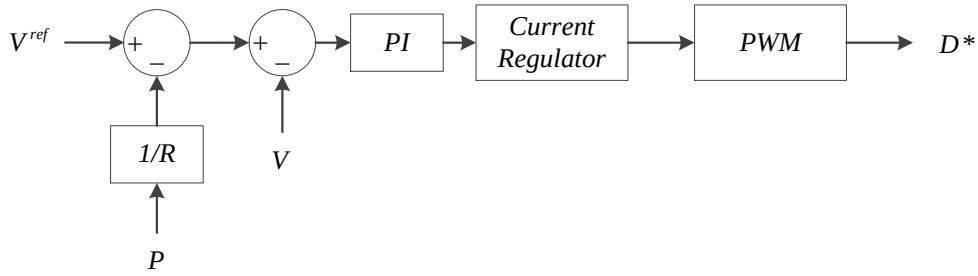

Figure 2.6. Structure of active power – voltage droop controller

Conventional researches on voltage control method

There are many researches on voltage control in DC distribution system or DC microgrid. These researches focus on how to maintain bus voltage within allowed range for stable and reliable operation of the DC network. Master / slave concept is introduced in [24]. The merits of this scheme are stiff voltage regulation and precise load sharing. However, the limitations are also obvious. First, the implementation of the scheme relies on communication between the two modules, master and slave modules. Second, the master module failure may disable the entire system. In addition, all modules are control dependent. Control of low voltage bipolar type DC microgrid for super high quality distribution is proposed [14]. The DC voltages are controlled with bi-directional voltage source converter, which is same as GCC shown above, when the DC network is connected to the utility grid. The DC microgrid is disconnected from the utility grid if a voltage problem detected, and voltage is controlled by electric double-layer capacitor in the DC side. Several types of droop controls have been proposed for the parallel operations [24-27]. Modified droop concepts are proposed if ESS utilized in DC microgrid and these are based on adaptive droop considering SOC of ESS [22, 23]. These researches are based on voltage-power droop or voltage-current droop in the converter and fast communication is not required for voltage control. Voltage control method for using fuzzy control and gain-scheduling technique is presented [21]. This research is developed from [14] and authors accomplished both power

sharing and energy management simultaneously by the proposed method. A distributed control strategy based on DC bus signaling (DBS) was presented [20, 28, 29]. DBS based method controls sources and GCC with regard to the DC bus voltage level. The source and storage interface converters operate autonomously based on the voltage level of the dc bus. Each converter is assigned to a voltage threshold to trigger the point at which it begins discharging or charging [28]. The voltage control mode or state is chosen with regard to the DC bus voltage level, and control strategies of GCC, battery and PV are determined by definition of each mode or state [20, 29].

These conventional researches are summarized by voltage control method in Table 2.1.

No.	Ref.	Control Method.	Communication Required	Constant Voltage	Constant Power	Droop Control
1	[24]	Master / slave	O	O	O	
2	[14]	Const. V(GCC) and droop(DER)	O	O		O
3	[24]	Const. V(GCC) and droop by gain scheduling(DER)	X	O		O
4	[25]	Const. V (GCC) and droop(DG)	X	O		O
5	[21]	Droop	X	O		O
6	[26]	Droop	X			O
7	[27]	Droop	X			O
8	[28]	DBS	X			O
9	[29]	DBS	X			O
10	[20]	DBS	X	O		

Table 2.1. Summary of voltage control methods

Characteristic of conventional voltage control methods

The methods in most of conventional researches have common characteristic

and drawbacks.

- A number of voltage control methods are based on droop control and it has a drawback. In conventional researches, droop control is commonly used for active power sharing for generators or DGs to regulate the frequency. The frequency in the AC network at each bus is almost same and a difference of these values is very smaller than nominal frequency. Therefore, each generator or DG can control common electrical quantity, frequency. However, voltage is not identical at each bus, and overall voltage in the long distance distribution system or microgrid can't be maintained within allowed range if voltage is controlled by only few DGs based on droop control.
- Conventional studies focus on small scale DC power system such as DC nanogrid or microgrid. In these studies, DC system including only few DC bus or a common bus and an object of these studies is regulate the DC bus voltage to certain value. However, in larger scale DC distribution system, length of feeder becomes longer and line voltage drop increases. In these system configurations, voltage problem can occur at multiple buses. Furthermore, the bus voltages can exceed both maximum and minimum tolerance limit if there is reverse power flow on feeder due to large amount of power generated by DG or generation power of RES. In these cases, conventional voltage control method cannot regulate overall bus voltages.
- Most of conventional researches focus on maintaining the DC bus voltage to nominal value or allowed range. However, various control objects can be established while maintain voltage to appropriate range and details are discussed in later section.

2.2. Loss Reduction in the DC Distribution System

Consuming power reduction in the AC distribution system

In the AC system, from the viewpoint of frequency control, object of the frequency control is to maintain frequency near nominal value. However, in the DC distribution system, the frequency is not considered and the bus voltage is primary electrical variable for stable operation. The allowed range of the bus voltage is relatively wider and less strict, in both AC and DC distribution system, than that of frequency in the AC system. For example, grid code in South Korea limits the frequency within between 60 ± 0.2 Hz, which has tolerance limit of $\pm 0.33\%$ [30]. Whereas, American national standard for electric power systems and equipment – voltage ranges (ANCI C84.1) presents that service voltage limits in the distribution system are 95% and 105% of nominal voltage, respectively [31]. Therefore, various control strategies can be applied for efficient operation while maintaining the bus voltage. The conservation voltage reduction (CVR) and loss reduction is a typical application of these kinds of control.

CVR is the control method to reduce load energy consumption by lowering voltages of the distribution system and one of most cost-effective ways to save energy. If bus voltage becomes lowered by CVR, load consumption power is decreased because of resistive and constant power consuming component of load in the AC distribution system. CVR can also reduce peak demand and losses while maintaining suitable voltage range [32-34]. However, when a power converter at load side is tightly regulated, it behaves like a CPL in the dc distribution system. Therefore, in this case, energy consumption reduction due to the CVR control is not effective.

There are various researches on loss reduction for distribution or microgrid. Optimal allocation of combined DG and capacitor for loss minimization in the distribution system is presented [35] and algorithm for the reconfiguration of distribution feeder for loss minimization is proposed [36]. These researches are approaching to loss minimization problem from perspective of system planning. Researches from perspective of optimal scheduling are presented such as optimal scheduling for ESS charging / discharging [37].

Loss reduction in the DC distribution system

Unlike operation in the AC distribution system, usefulness of CVR is poor in the DC distribution system because loads are connected through DC/DC or DC/AC converter to the grid and they consume constant power regardless of bus voltage. Therefore, loss reduction is an only useful application to reduce consuming power in the DC distribution system.

There are few studies on loss reduction in the DC network presented. The long term optimal operation such as system planning has been studied. Optimal allocation and economic analysis of energy storage system in DC microgrid are presented [38]. In this study, optimal sizing and allocation of ESS is determined using genetic algorithm (GA) and economical effect is evaluated. A hybrid programming for distribution reconfiguration of dc microgrid is proposed [39]. Efficient network configuration can be obtained to reduce loss and the problem is optimized in a stochastic searching using evolutionary programming (EP). The result is applied to OPF as initial condition and optimal switching between nodes is determined by OPF.

In short-term operation and control for loss reduction, optimal scheduling and control methods are proposed. Droop method consider line loss over the conductor in DC microgrid is proposed [40]. In this research, adaptive virtual resistance is adopted to minimize conversion loss of power converter and optimal value of virtual resistance is obtained in optimal scheduling step. Optimal power flow (OPF) strategy by hierarchical control for DC microgrid is presented [41]. Optimal voltage references of converters are determined by proposed optimal condition and hierarchical control strategy is presented to reduce line losses.

Drawbacks in conventional studies

There are some drawbacks in the conventional researches. First, researches shown above cannot reflect variation of generation and load consumption, and

second, conversion loss is not considered.

Optimal reference of virtual resistance and output voltage of converter is determined in optimal scheduling step [40, 41]. However, reference is not changed in real-time control step despite there is unexpected load and generation variations and control scheme in [41] does not guarantee optimal result if output power of DER is reached to maximum or minimum limit.

In addition, object of most of researches is to reducing only line loss, or conversion loss. Line loss is generally larger than 1~2% of total load in the distribution system and it is significant portion of power consumption in the DC distribution network. In addition, conversion loss is also important and not able to be negligible. The impact of conversion loss in the DC distribution system is discussed [42]. In this research, it is presented that conversion efficiency of power converters is important factor and the efficiency has almost a linear relationship with the total loss. From the DNO's concern, the line loss not only is operating cost of the DC distribution system but also conversion loss should be considered. For example, GCC deliver whole load consumption power from utility grid if there are no additional generation power in the distribution system. In this case, impact of internal loss of GCC is very significant and DNO should focus on this problem for economic operation of the distribution system.

2.3. Voltage Sensitivities Analysis

Voltage affects both current and the voltage drop over the conductors, and line loss is also affected by the voltage. Therefore, voltage is a primary variable that reflects system conditions, and affects power flow and voltage stability in a DC distribution system. Here, this dissertation focuses on the relationship between voltage magnitude and electrical quantities, which may elucidate the characteristics of a DC distribution system.

Such a relationship, expressed as the voltage sensitivity, provides a linear relation between voltage deviations and electrical quantities. The voltage–reactive

power (V-Q) sensitivity is generally used for steady-state analyses of AC power systems, and V-Q sensitivity is often used in planning, operation, assessment, and control of power systems [19, 43-52]. Moreover, voltage sensitivity can be utilized in medium- or low-voltage distribution networks with high penetrations of DERs, which underlines the importance of optimal control in a distribution network. Optimal control of a power system is often based on a linear optimal problem, where sensitivity coefficients link the control variables and the controlled quantities. Therefore, voltage sensitivity is useful for solving these types of problems [53].

Voltage sensitivity can also be used to analyze DC distribution systems. The real power and voltage magnitudes are important variables that reflect various phenomena in a DC distribution system. Therefore, this dissertation presents formulation and analysis of voltage sensitivity in the DC radial distribution system. An analysis of such relationships is helpful to describe and understand such systems. In addition, the proposed formulations can be used to solve practical problems in the DC network. A cooperative voltage control scheme using grid-connected converters (GCCs) and DERs in a DC distribution system has been reported [54]. The authors analyzed voltage sensitivity in response to changes in the injected power from the DERs, and a voltage control scheme was constructed based on analytic voltage sensitivity analysis to reduce required amount of power of DERs for voltage regulation. Moreover, the proposed formulation can be used for simple calculation of the voltage sensitivity in radial DC distribution systems. The voltage sensitivity can be calculated directly from measurements without power flow calculation by proposed formulation. The calculated voltage sensitivity could be utilized for voltage control. Voltage control method based on multi agent system (MAS) has been reported and voltage sensitivity is utilized [55, 56]. In these researches, agents calculate voltage sensitivity factor from the inverse of the Jacobian matrix for active power control of DERs and such process could be simplified using proposed formulation to reduce calculation efforts.

Generally, the voltage sensitivity can be obtained during power flow calculation process. Calculation of the voltage sensitivity using Jacobian matrix in the AC power system is introduced [57, 58]. Similarly, the voltage sensitivity in the DC power system can be calculated with inverse of Jacobian matrix. The voltage sensitivity using Jacobian matrix provides exact value of the voltage sensitivity. However, this calculation has some drawback. First, undesired calculation effort is required if a target system or a research does not utilize power flow calculation. Introduced calculation methods require information on Jacobian matrix and power flow calculation should be carried out until it provides converged solution. In addition, the voltage sensitivity calculated from Jacobian matrix does not provide information for analytical analysis. Introduced voltage sensitivity calculation method only provides the value of voltage sensitivity. Therefore, it is hard to analyze and understand the relation between the voltage and electrical quantities.

2.4. Loss Sensitivities Analysis

Loss sensitivity represents the linear relationship between loss and electrical quantities. Loss sensitivity is usually utilized as a primitive factor for loss reduction analysis in the power system, and many researches related to loss reduction, based on loss sensitivity, in the power system are presented [46, 48, 59]. Line loss sensitivity is usually calculated using Jacobian matrix, and line loss sensitivity with regard to bus voltage is equal to the sum of column of Jacobian matrix as (2.1).

$$\frac{\partial P_{line}^{loss}}{\partial V_i} = \sum_{k=1}^{n} \frac{\partial P_k}{\partial V_i} \quad for\ k\ is\ not\ slack\ bus \tag{2.1}$$

and loss sensitivity with regard to bus injection power is derived as follows:

$$\frac{\partial P_{line}^{loss}}{\partial P_i} = \sum_{k=1}^{n} \frac{\partial V_k}{\partial P_i} \frac{\partial P_{line}^{loss}}{\partial V_k} \tag{2.2}$$

As shown above, conventional method requires Jacobian matrix for loss sensitivity calculation, and power flow calculation is also essential to obtain

Jacobian matrix. Therefore, it is suitable to planning method to reduce loss using power flow calculation such as optimal power flow, and most of the studies focus on it. However, this calculation has a similar drawback presented in issues on voltage sensitivity. Calculation effort is required to obtain the line loss sensitivity because inverse of Jacobian matrix is required to calculate this sensitivity, and it cause bad effect on fast calculation in the controller.

In addition, conversion loss is an important issue in the DC distribution system. Most of load power is delivered by GCC and significant conversion loss is caused. Converter internal loss regarding to output power or current of converter could be modeled as a quadratic equation by regression analysis of experimental results. It is presented that converter losses of the power converter is modeled as the quadratic equation as a function of the absolute value of output power [60, 61]. Therefore, the loss sensitivity of converter is expressed as a partial derivative of loss equation, which is expressed as a linear equation.

If there are various kinds of the voltage control equipment in the DC distribution system, effects on voltage sensitivity between each other due to variation of electrical quantities of voltage control equipment should be considered. For example, let assume that there are one GCC and DG in the DC distribution system. A variation in DG output power changes GCC output power because generation and load consumption should be balanced in the DC distribution system. This variation also changes the line loss over the conductor. As a result, a variation in DG output power affects output power of GCC and converter internal loss sensitivity of GCC will be changed.

Chapter 3. Formulation for Approximated Expression for Sensitivities in the Radial DC Distribution System

3.1. Formulation for Approximated Voltage Sensitivity for a Radial DC Distribution System

The power flow in a DC distribution system can be described using a voltage sensitivity analysis. Such an analysis is the basis of the steady-state description upon which conventional voltage sensitivity analyses are based. However, a number of difficulties arise with an analytical study based on the conventional method and this problem is addressed in this section.

3.1.1. Power Flow and Voltage Sensitivity Analysis for a DC Distribution

The Y-Bus matrix is widely used to describe various steady-state analyses in AC power systems, such as power flow calculations, sensitivity analyses, and stability assessments. In the same manner, the G-Bus matrix can be used to describe DC power systems [58]. As shown below, the conductance matrix is similar to the admittance matrix for an AC system, the only difference being the absence of reactive components. The G-Bus matrix is defined as follows:

$$G = \begin{bmatrix} G_{11} & G_{12} & \cdots & G_{1n} \\ G_{21} & G_{22} & \cdots & G_{2n} \\ \vdots & \vdots & \ddots & \vdots \\ G_{n1} & G_{n2} & \cdots & G_{nn} \end{bmatrix} \tag{3.1}$$

where

$$G_{ii} = \sum_{j=1}^{n} g_{ij} \; and \; G_{ij}\big|_{i \neq j} = -g_{ij}$$

3.1.2. Power Flow Analysis in a DC Distribution System

Figure 3.1 shows a diagram of a simple DC distribution system interconnected with a higher-voltage AC or DC system via a GCC, where the secondary terminal of the GCC is located at bus 1. The voltage at this bus is assumed to be constant because the secondary terminal voltage of GCC can be controlled continuously; this point is therefore considered the slack bus. Buses 2 to 6 include DC power loads that are connected to the system using DC/DC or DC/AC converters. It is assumed that each load is a constant-power load, and that these loads can be converted to current loads, where the currents are inversely proportional to the bus voltages. Based on these assumptions, the following sets of nodal equations are obtained:

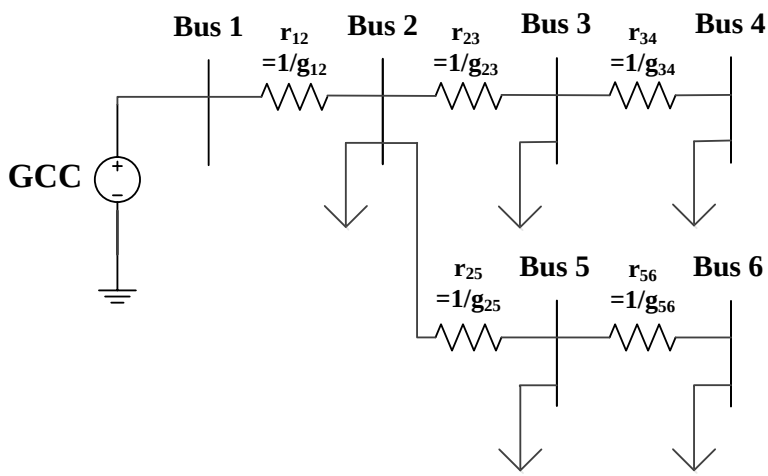

Figure 3.1. A simple radial DC distribution system

$$
\begin{aligned}
&g_{12}(V_2 - V_1) + g_{23}(V_2 - V_3) + g_{25}(V_2 - V_5) + P_{L,2} / V_2 = 0 \\
&g_{23}(V_3 - V_2) + g_{34}(V_3 - V_4) + P_{L,3} / V_3 = 0 \\
&g_{34}(V_4 - V_3) + P_{L,4} / V_4 = 0 \\
&g_{25}(V_5 - V_2) + g_{56}(V_5 - V_6) + P_{L,5} / V_5 = 0 \\
&g_{56}(V_6 - V_5) + P_{L,6} / V_6 = 0
\end{aligned}
\tag{3.2}
$$

To obtain general voltage equations for a DC power system, the above expressions are rearranged as follows. The voltage equation for bus 2 can be expressed as:

$$P_2 = g_{12}(V_2^2 - V_1V_2) + g_{23}(V_2^2 - V_3V_2) + g_{25}(V_2^2 - V_5V_2) \tag{3.3}$$

and

$$P_2 = -P_{L,2} = G_{22}V_2^2 - \sum_{k=1,k\neq 2}^{n} G_{2k}V_k \tag{3.4}$$

From (3.3) and (3.4), the following general equation for the voltage at bus *i* is obtained:

$$P_i = G_{ii}V_i^2 + V_i \sum_{k=1,k\neq i}^{n} G_{ik}V_k \tag{3.5}$$

where

$$V_i = \frac{-\sum_{k=1,k\neq i}^{n} G_{ik}V_k \pm \sqrt{\left(\sum_{k=slack,k\neq i}^{n} G_{ik}V_k\right)^2 + 4G_{ii}P_i}}{2G_{ii}} \tag{3.6}$$

3.1.3. Voltage Sensitivity Calculation in a DC Distribution System

The voltage–reactive power sensitivity is widely used in steady-state analyses of AC power systems because the bus reactive power and the voltage magnitude are typically strongly correlated. In [58], a voltage–reactive power sensitivity analysis of an AC power system was reported, and the voltage sensitivity was derived using a Jacobian matrix. In the same manner, the voltage sensitivity of a DC power system can be determined. In a steady-state analysis of a DC power system, the reactive power and voltage angle can be neglected. Therefore, only the relationship between the voltage magnitude and real bus power is considered in the voltage sensitivity analysis, and a linearized form of the power flow equations can be used; i.e.,

$$\Delta P = [J]\Delta V \tag{3.7}$$

In this expression, the relationship between the deviation of the real bus power and voltage magnitude is represented directly by the Jacobian matrix. The voltage

sensitivity is obtained as follows:

$$\Delta V = [J]^{-1}\Delta P \tag{3.8}$$

The Jacobian matrix gives the sensitivities of the real bus power to deviations in the bus voltage magnitude. The elements of the Jacobian matrix in (3.7) and (3.8) can be obtained from (3.5), and are expressed as follows:

$$J_{ij} = \frac{\partial P_i}{\partial V_j} = G_{ij}V_i \quad for\, i \neq j \tag{3.9}$$

and

$$J_{ii} = \frac{\partial P_i}{\partial V_i} = 2G_{ii}V_i + \sum_{k=1,k\neq i}^{n} G_{ik}V_k \quad for\, i = j \tag{3.10}$$

The expression for the voltage sensitivity of a DC power system is far simpler than the equivalent expression for an AC power system because the phase angle and reactive power can be neglected. However, as with an AC power system, the inverse matrix of the Jacobian matrix must be calculated to obtain the voltage sensitivity. Therefore, the conventional analysis has the drawback that it is difficult to describe the voltage sensitivity analytically, and hence it is difficult to find a direct relation between the voltage deviation and the deviation of the electrical quantities. In other words, it cannot provide useful information to analyze the voltage sensitivity, and the voltage sensitivity must be calculated from the inverse of the Jacobian matrix.

3.1.4. Approximation of Expression of Voltage Sensitivity Equation

Two kinds of voltage sensitivity equations are formulated depending on the bus injection power and the slack bus voltage, respectively. Each sensitivity is formulated as following equation.

$$\frac{\Delta V_i}{\Delta P_j} \approx \frac{V_i^2}{V_i^2 + R_{ii}P_i}\left(\frac{R_{ij}}{V_j} - \sum_{k=1,k\neq i}^{n} \frac{R_{ik}P_k}{V_k^2}\frac{\Delta V_k}{\Delta P_j}\right) \tag{3.11}$$

$$\frac{\Delta V_i}{\Delta V_{slack}} \approx \frac{V_i^2}{V_i^2 + R_{ii}P_i}\left(1 - \sum_{k=1,k\neq i}^{n} \frac{R_{ik}P_k}{V_k^2 + R_{kk}P_k}\right) \tag{3.12}$$

These equations are expressed as function of bus voltages, bus injection power, and line resistances. Detailed derivation is introduced in Appendix A.

Chapter 4. Cooperative Operation Scheme Considering Loss Reduction and Voltage Regulation in the Radial DC Distribution System

4.1. Structure of Proposed Cooperative Operation Scheme

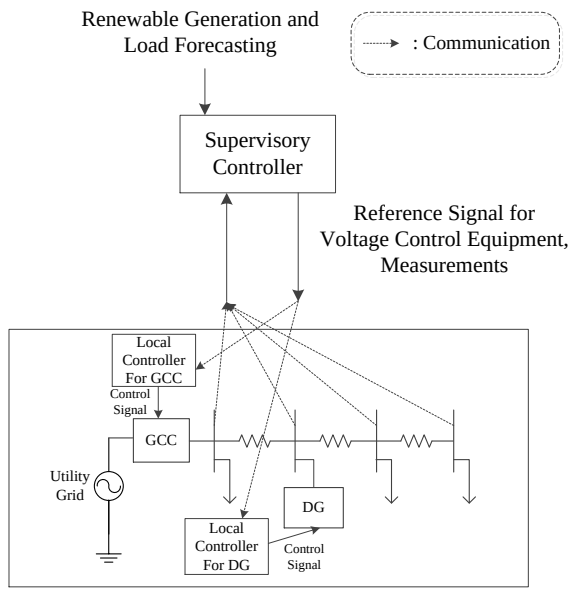

Figure 4.1 Structure of proposed cooperative voltage control scheme

The structure of proposed cooperative voltage control scheme is shown Figure 4.1. Proposed control scheme is centralized control scheme with communication. To realize this structure, communication between supervisory controller and measure equipment at each bus, and voltage control equipment is essential. Communication system can support two-way flows of information in the smart grid environment. Two types of communication system, wireless and wire-line communication, is classified in [62]. Wireless communication technologies can be used in plenty of applications in SG because of its development. Wireless mesh networks (WMN), cellular communication systems, satellite communications, Wi-Fi, and Zigbee are strong candidates for SG. In addition, optical fiber

communication, and power line communication (PLC) are candidate for wire-line communication technologies. These kinds of communication technologies can be applied in the SG environment to provide a fast, reliable, secure, and self-healing communication system covering the entire power grid.

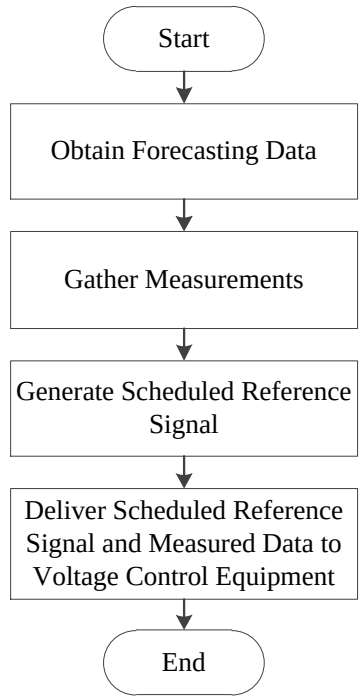

Figure 4.2 Flow chart of supervisory controller

Figure 4.2 presents flow chart of supervisory controller. Supervisory controller gathers measurements from each bus and voltage control equipment status. There is a scheduler for the voltage control equipment in the supervisory controller, which accomplishes optimized scheduling to reduce the whole loss of the system during certain time interval. The scheduled reference signal, the aim of which is to reduce the whole system loss within allowed voltage range, is generated based on load and generation forecasting by supervisory controller. It can be generated by a kind of optimized scheduling method such as dynamic programming (DP), genetic algorithm (GA), and linear programming (LP), and a scheduling using DP is presented in this dissertation.

This dissertation considers four types of power converter in the DC

distribution system, GCC, converter of DG owned by DNO, converter of DG not owned by DNO, and load side converter. The loss in load side converter is the und loss because DNO cannot control consumer load consumption except particular situations such as load shedding. The loss in the converter of DG not owned by DNO is also not dispatchable and it can be considered as the loss due to negative load consumption. The loss in the converter of DG owned by DNO is considerable controllable quantity and it could be operated depending on control strategy of DNO. The loss in the GCC also can be controlled by DNO, and control strategy can be voltage regulation, loss reduction of the whole system, and minimization power flow from the utility grid.

The supervisory controller delivers scheduled reference signal for each time interval, which is presented in Figure 4.3, to the local controller of voltage control equipment, the GCC and DG owned by DNO. The voltage control equipment is operated to meet scheduled results. In addition, measured voltage and bus injection power from each bus are delivered to local controller.

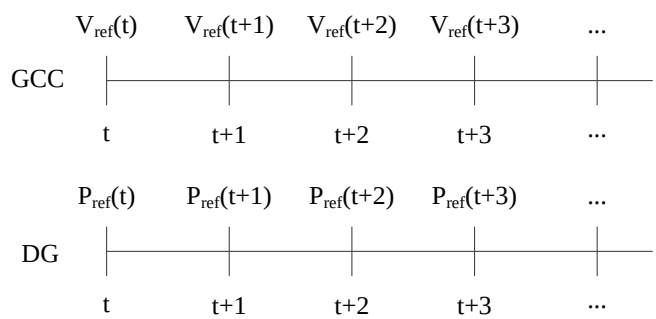

Figure 4.3 Scheduled reference signal generated by supervisory controller

However, there might be a difference between actual load and generation power and forecasted results in the distribution system. Therefore, the scheduled reference signal always does not provide optimized solution and additional control is required to achieve control purpose. In addition, voltage problem can occur if there is large deviation of load and generation mismatch. Therefore, local control is required to generate control signal depending on actual system condition. The

proposed control scheme consists of loss reduction control module, voltage regulation module, and preprocessing modules. Loss reduction module provides reference of voltage control equipment to reduce total loss in the DC distribution system. The reference is generated based on loss sensitivity, voltage sensitivity, and violation condition of bus voltages. Voltage regulation module activates regulation signal if any bus voltage exceeds voltage limits. Regulation signal is determined estimated loss due to voltage regulation and reserve capacity of voltage control equipment. Preprocessing modules generate required input data for loss reduction and voltage regulation modules and provide activation signal of these modules.

4.2. Scheduler for the Voltage Control Equipment

In this section, an optimal scheduling process for the voltage control equipment is introduced. There are many researches on an optimal scheduling for DG or the voltage control equipment, and many optimization methods such as dynamic programming (DP), genetic algorithm (GA), particle swarm optimization (PSO), and linear programming (LP) is utilized. In this dissertation, DP is chosen for an optimal scheduling method, and objective function and constraints to formulate for a DP model are presented.

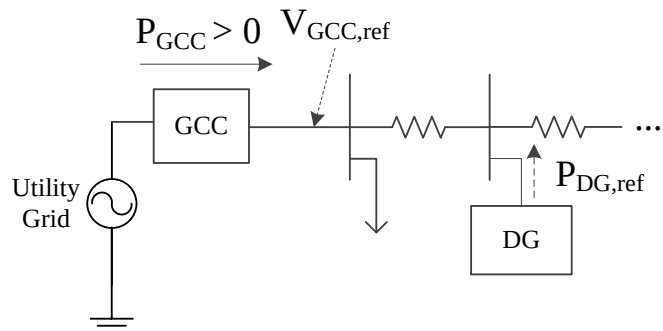

Figure 4.4 Reference signal for the voltage control equipment

Figure 4.4 presents reference signal for the voltage control equipment. A scheduler generates scheduled reference signal of the voltage control equipment,

the reference of GCC output voltage and the reference output power of DG, for each time interval. The GCC output voltage is equivalent to voltage at the secondary side of GCC, and also identical to the slack bus voltage. Equipment status data delivered from the voltage control equipment and load and RES generation forecasting data for scheduled time interval are required for optimal scheduling. Forecasting data are essential to generate network data for each time interval. If there is an ESS in the distribution system, current state of charge (SOC) is also required to generate scheduled reference signal considering SOC constraints.

Object of a scheduling is to minimize the whole system loss during certain time interval. Conventional researches only focus on reduction or minimization of line losses over the conductor. However, internal loss due to power conversion in the GCC and DG is not too small to be neglected because massive power is delivered by this equipment. Therefore, the whole system loss includes line losses over the conductors and internal loss of GCC and DG in this dissertation. Objective function to minimize these losses is formulated as:

$$\text{objective function}: \min \sum_{t=1}^{N_T}\sum_{k=1}^{N_K} P_k(t) + \sum_{t=1}^{N_T}\sum_{k=1}^{N_K} P_{DG,k}^{loss}(t) + \sum_{t=1}^{N_T} P_{GCC}^{loss}(t) \tag{4.1}$$

$$P_{DG,k}^{loss}(t) = a_k \left|P_{DG,k}(t)\right|^2 + b_k \left|P_{DG,k}(t)\right| + c_k \tag{4.2}$$

$$P_{GCC}^{loss}(t) = a_{GCC} \left|P_{GCC}(t)\right|^2 + b_{GCC} \left|P_{GCC}(t)\right| + c_{GCC} \tag{4.3}$$

From (4.1), k denotes index for the bus number or DGs number, and t denotes the index for time interval. N_T and N_K is the number of time interval, and DG or bus. Terms in an objective function denote line losses, internal loss of DGs, and internal loss of GCC. Line losses, which is equivalent to a sum of bus injection power at all buses, can be calculated with power flow results for each state. The internal losses of GCC and DG can be express as a quadratic equation [60, 61], and these are modeled as (4.2) and (4.3).

There are constraints to secure stable operation of the distribution system and

the voltage control equipment. In steady state condition, the bus voltages at all of the bus are should be maintained within suitable range [17]. Therefore, the bus voltage violation is considered for constraint as:

$$V_{min} \le V_k(t) \le V_{max} \quad \forall \ k \text{ and } t \tag{4.4}$$

If a DG is ESS, SOC of ESS at each time interval should be considered because charging and discharging capability of ESS is limited by its SOC. A constraint concerning SOC of ESS is presented as:

$$SOC_{min} \le SOC_k(t) \le SOC_{max} \quad \forall \ k \text{ and } t \tag{4.5}$$

Current SOC and final SOC at last time interval is also considered. A constraint for current SOC is essential to meet the current status of ESS, however, final SOC is optional in accordance with operation strategy. These constraints are expressed as follows:

$$SOC_k(0) = SOC_{meas,k} \quad \forall \ k \tag{4.6}$$

$$SOC_k(N_T) = SOC_{final,k} \quad \forall \ k \tag{4.7}$$

Output power of DG is limited by the maximum output power of its converter. A constraint concerning output power is presented as:

$$P_{DG,k}^{min} \le P_{DG,k}(t) \le P_{DG,k}^{max} \quad \forall \ k \text{ and } t \tag{4.8}$$

Generally, minimum power of DG is zero or positive value. However, minimum power can be a negative value, which might be a negative value of maximum power, if the type of DG is ESS and negative value of minimum power means that ESS can discharge absolute value of negative minimum power. The GCC also have a delivered power constraint and it has a form as:

$$P_{GCC}^{min} \le P_{GCC}(t) \le P_{GCC}^{max} \quad \forall \ t \tag{4.9}$$

In this case, minimum power of GCC should be negative value considering reverse power flow from the DC distribution system to utility grid, and direction of positive power is defined as shown in Figure 4.4. Finally, current output power of

DG and GCC is considered. These constraints are presented as:

$$P_{DG,k}(0) = P_{DG,k}^{meas} \quad \forall \ k \tag{4.10}$$

$$P_{GCC}(0) = P_{GCC}^{meas} \tag{4.11}$$

To calculate the converter internal loss of ESS, actual output power of ESS should be known to calculated internal loss by (4.2). At each SOC state converter output power and internal loss of ESS is presented as follows:

$$P_{DG,k}^{ref}(t) + P_{DG,k}^{loss}(t) = C_k \frac{SOC_k(t) - SOC_k(t-1)}{T_{period}} \tag{4.12}$$

Right hand side in (4.12) is average power delivered from the battery during a time interval and (4.13) is defined to simplify this expression. Left hand side of the above equation is arranged as (4.14) and (4.15) by definition shown in (4.2).

$$P_{avg,k}(t) = C_k \frac{SOC_k(t) - SOC_k(t-1)}{T_{period}} \tag{4.13}$$

$$a_k P_{DG,k}^{ref}(t)^2 + (1+b_k) P_{DG,k}^{ref}(t) + c_k = P_{avg,k}(t) \quad \text{for} \quad P_{DG,k}^{ref}(t) \geq 0 \tag{4.14}$$

$$a_k P_{DG,k}^{ref}(t)^2 + (1-b_k) P_{DG,k}^{ref}(t) + c_k = P_{avg,k}(t) \quad \text{for} \quad P_{DG,k}^{ref}(t) < 0 \tag{4.15}$$

Because the converter internal loss equation includes the absolute value of converter output power, two equations are derived according to the sign of ESS output power. From (4.14) and(4.15), reference power of ESS is derived as follows:

$$P_{DG,k}^{ref}(t) = \frac{-(1+b_k) + \sqrt{(1+b_k)^2 - 4a_k(c_k - P_{avg,k}(t))}}{2a_k} \quad \text{for} \quad P_{DG,k}^{ref}(t) \geq 0 \tag{4.16}$$

$$P_{DG,k}^{ref}(t) = \frac{-(1-b_k) + \sqrt{(1-b_k)^2 - 4a_k(c_k - P_{avg,k}(t))}}{2a_k} \quad \text{for} \quad P_{DG,k}^{ref}(t) < 0 \tag{4.17}$$

In (4.16) and (4.17), a criterion to choose reference of ESS is a sign of reference power, however, it is unknown until calculate these equations. Therefore, the reference signal of ESS output power is determined according to a sign of

reference values after calculating these equations.

The optimization state transition route for DP is illustrated in Figure 4.5 to Figure 4.5. State transition routes consist of each state of the voltage control equipment and each state is a variable of SOC, output power of DG, and output power of GCC. Current status of the voltage control equipment determines the initial state of each route, and final state is also determined if required SOC of ESS at final state is entered by the operator.

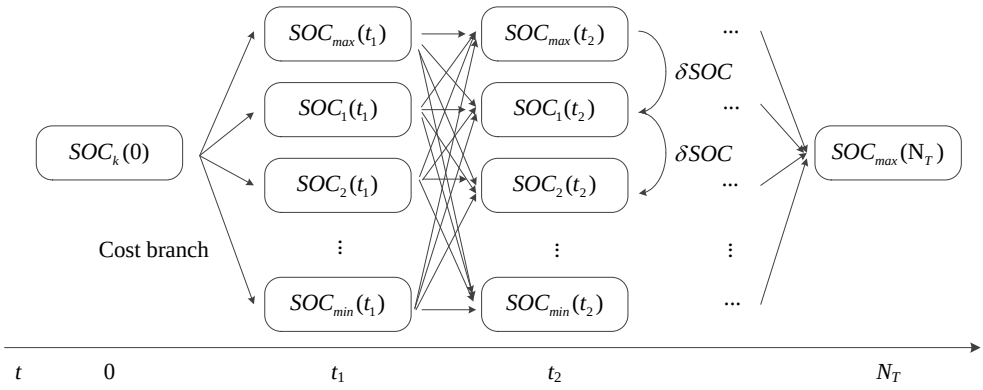

Figure 4.5 Optimization state transition route for ESS

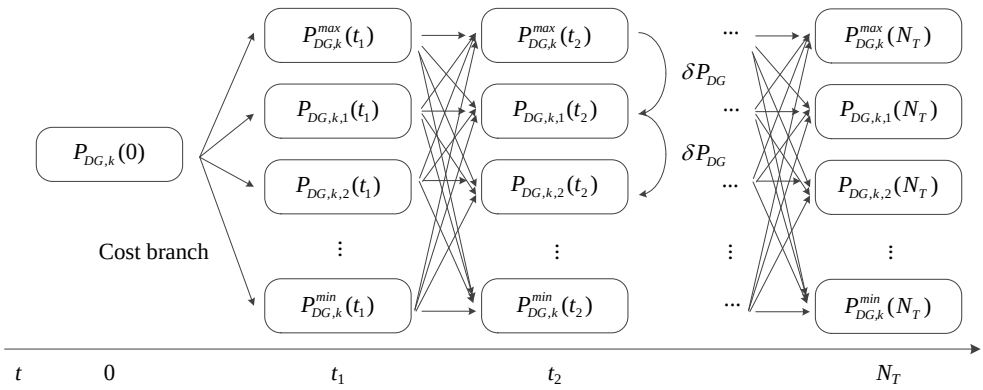

Figure 4.6 Optimization state transition route for non-storage DG

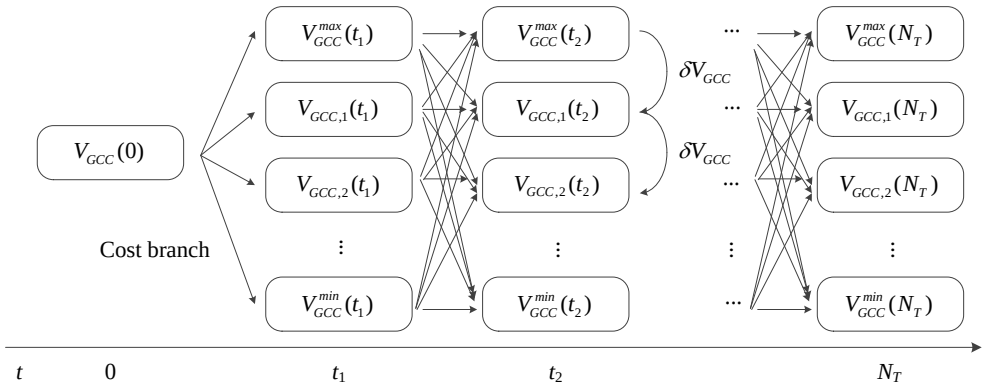

Figure 4.7 Optimization state transition route for GCC

In proposed control scheme, cooperative control of GCC and DG, or ESS, is carried out. Therefore, states at each time interval should be composed of each SOC state, DG power state, and GCC power state. Figure 4.8 illustrates such overall optimization state transition routes for the proposed cooperative control problem. Except initial and final state, there is a two-dimensional state at each time interval and each two-dimensional state includes $N_T \times N_K$ states. Feasible states, which are satisfying equality and inequality constraints, are chosen among these states and the optimization state transition route is calculated by DP algorithm.

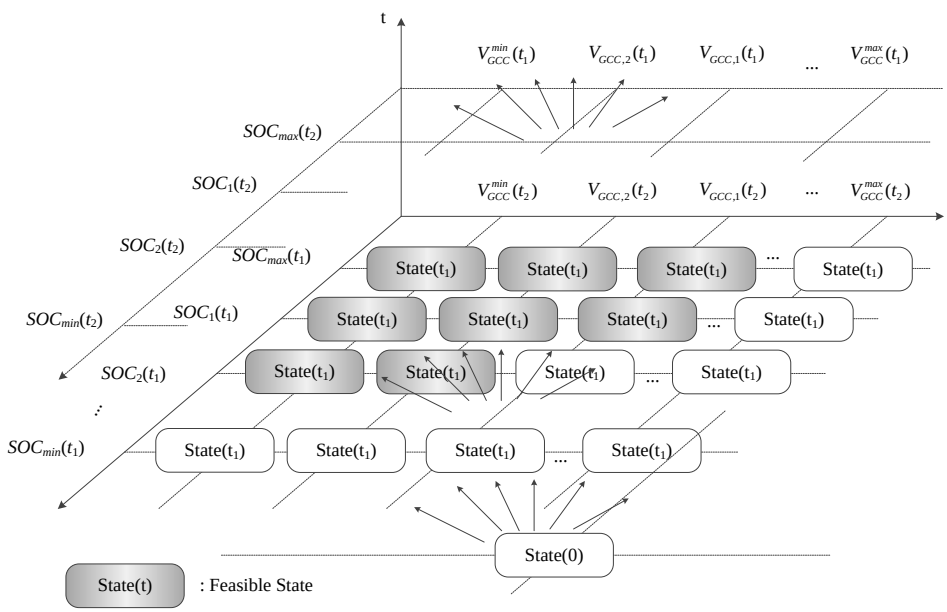

Figure 4.8 Overall optimization state transition route for DP modeling of proposed scheduling problem

After calculation of optimal state transition route, scheduled reference signal for the voltage control equipment is obtained. Figure 4.9 illustrates that how the scheduled reference signal is obtained from the set of optimal states. In this dissertation, scheduled reference signal of GCC has a form of reference voltage at its secondary side, which is equivalent to the slack bus at the DC distribution system side, of GCC. Therefore, slack bus voltage from power flow results should be saved when the optimal state transition route of delivering power by GCC is searched. Saved slack bus voltages at each time interval are equivalent to scheduled reference signal for GCC. Scheduled reference signal of non-ESS DG is equivalent to each state on optimal state transition route at each time interval, and additional calculation or process is not required. In case of ESS, output power is saved when the optimal state transition route of SOC is searches, and saved output power at each time interval is delivered by supervisory controller

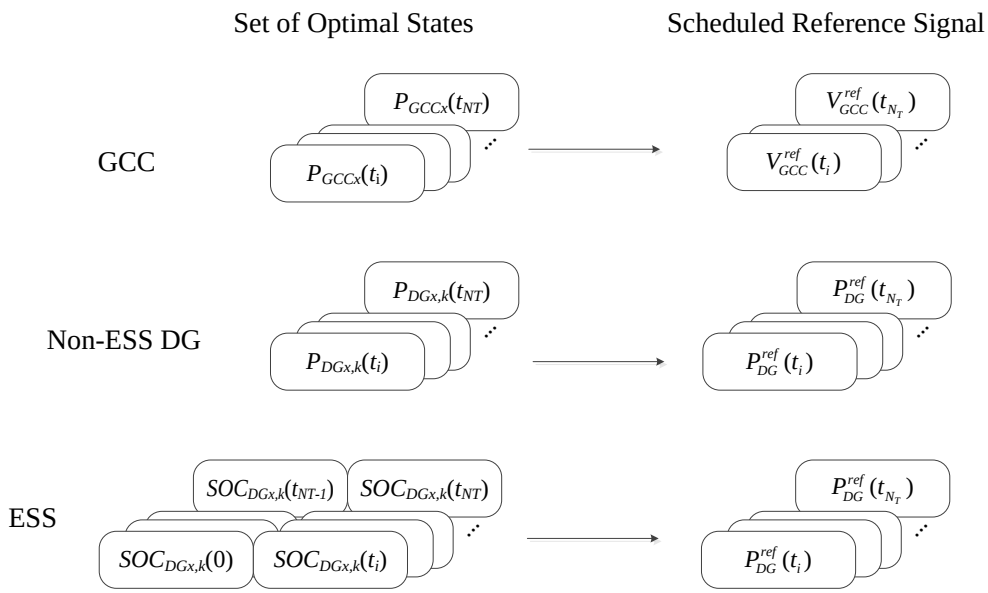

Figure 4.9 Arrangement of scheduled reference signal from set of optimal states

4.3. Local Control in the Proposed Voltage Control Scheme

4.3.1. Overview of local controller

The local controller generates actual references for the voltage control equipment based on a scheduled reference and measured data. Control purposes of the local controller are to reduce the whole system loss, which is including line loss and converter loss of DG and GCC, while maintain the bus voltages within suitable range.

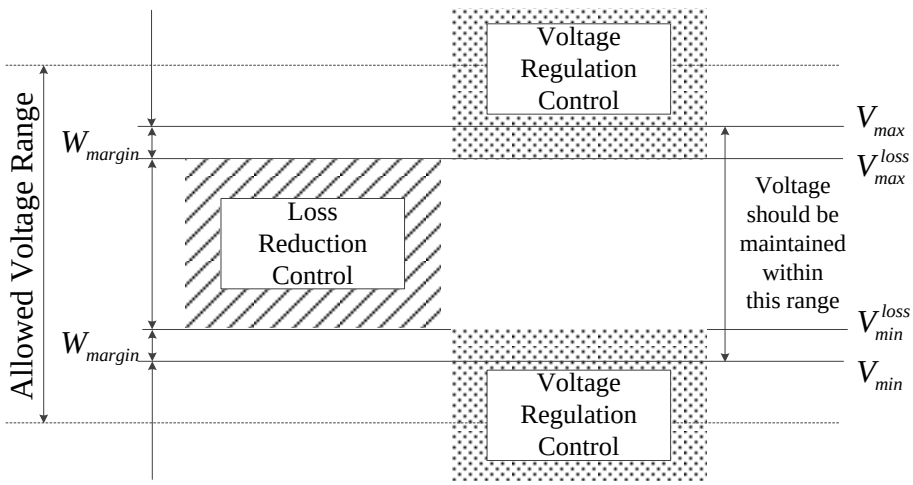

Figure 4.10 Control range of the local controller

Figure 4.10 presents control range of two main controllers. There is allowed voltage range and it is generally defined as grid code or distribution code. For example, IEC 60092-101 recommended to limit steady state DC voltage tolerance within 10% [17]. Maximum and minimum voltage limits are defined as shown in Figure 4.10 and width of these voltage limits is narrower than the allowed voltage range for the voltage reserve. The voltage regulation controller is always activated and maintains the bus voltage within these maximum and minimum voltage limits. Maximum and minimum voltage limit for loss reduction control are also defined and these limits are expressed as follows equations where W_{margin} is a marginal width for voltage regulation:

$$V_{max}^{loss} = V_{max} - W_{margin} \tag{4.18}$$

$$V_{min}^{loss} = V_{min} + W_{margin} \tag{4.19}$$

Loss reduction control is activated only when all of the bus voltages are maintained between maximum and minimum voltage limit for loss reduction control. If any bus voltage is reached these limits, loss reduction control is deactivated because this control affects the bus voltage and voltage violation can be occurred.

Figure 4.11 presents the overall flow of local control modules to achieve a proposed voltage control scheme. There are preprocessing modules and these calculate control signal for two main controllers. Two main control modules, loss reduction controller and voltage regulation controller, generate control signals to reduce the whole system loss and maintain the bus voltages, respectively.

Figure 4.12 presents control signals delivered to voltage control equipment. Each controller generates references for the voltage control equipment and the sum of these values and a scheduled reference from supervisory controller is delivered to the voltage control equipment. However, loss reduction control is not activated if type DER is an ESS. The energy supply capability of an ESS is limited by its SOC and capacity of the battery while general DG can supply electrical energy continuously. ESS should maintain its SOC adequately to deliver electrical energy and charging or discharging is essential for SOC management. This process induces additional converter internal losses and whole system loss during certain time intervals can increase. Consequently, performance of loss reduction can become worse if ESS participate in loss reduction control. This phenomenon is hard to predict and depending on loss characteristic of power converter and load consumptions in the DC distribution system. Therefore, only a scheduled reference and voltage regulation reference is applied to ESS in the proposed voltage control scheme.

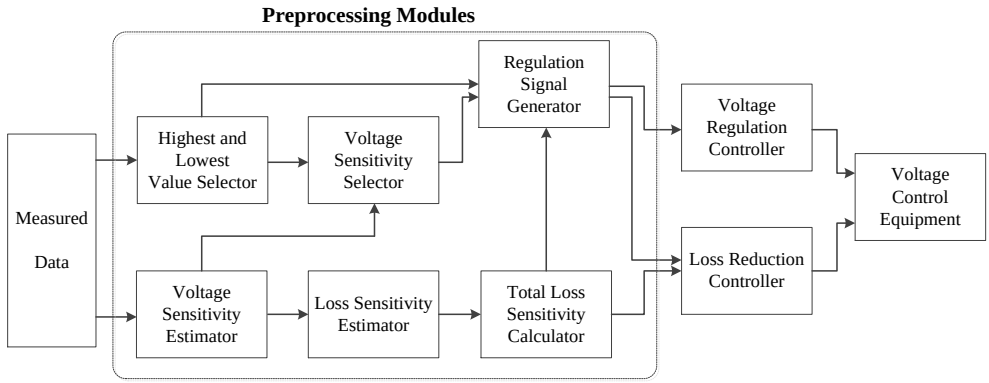

Figure 4.11 Overall flow of local control modules

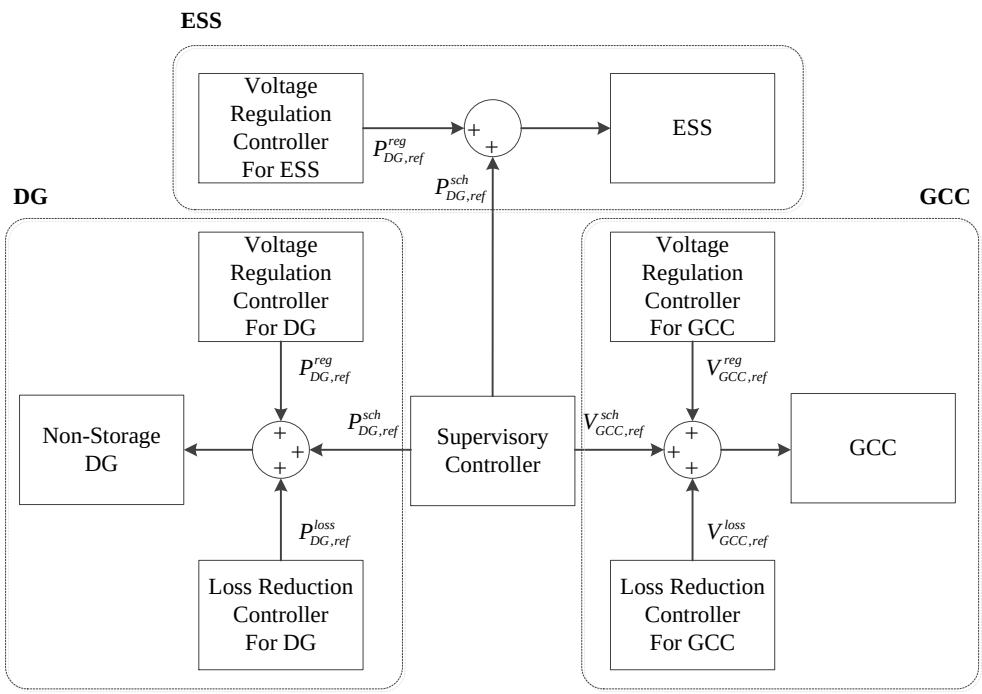

Figure 4.12 Control signals delivered to voltage control equipment

4.3.2. Proposed Loss Reduction Scheme

The purposes of this controller are to reduce the whole system loss, which is including line loss and converter loss of DG and GCC, in the radial DC distribution system. Based on flag signal from regulation signal generator module and total loss sensitivities, this module generates reference signals for the voltage control equipment to reduce total system loss.

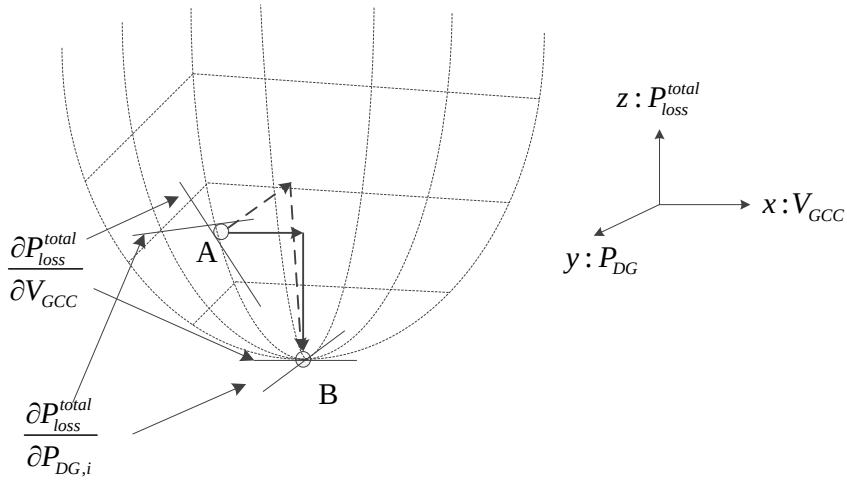

Figure 4.13 An example for loss reduction control scheme

Figure 4.13 illustrates an example to explain how to reduce loss when there are difference between actual load and generation and forecasting results. The figure shows a total loss curve as a function of the slack bus voltage, which is equivalent to voltage at the secondary side of GCC, and the output power of DG. This figure shows the trajectories of total system loss when actual load consumptions or output power of RES are different from forecasting load and generated power. The curve might be convex or sub-convex and it is affected by the network configuration and internal loss of the voltage control equipment. Point 'A' indicates the operating point by a scheduled reference signal delivered from supervisory controller. In this point, the total loss sensitivities with regard to the voltage control equipment are negative. In this case, loss reduction controller increases the reference of output voltage of GCC and DG output power, and then the operating point would be moved from point 'A' to 'B'. Conversely, controller decreases reference of the voltage control equipment if total loss sensitivity is positive and controller changes reference value until total loss sensitivities becomes zero. The new operating point by this control might be global optimum or not. However, this control can reduce the total system loss at the current status and controller can find the new global optimum if the optimized scheduler in the

supervisory controller renews scheduled reference reflecting the current system status and updated forecasting results.

4.3.3. Proposed Voltage Regulation Scheme

The purposes of this controller are to regulate the entire bus voltages when these are exceeding pre-defined voltage range. Proposed control scheme in this dissertation especially focuses on the voltage regulation in the long distance DC network and voltage can be maintained within suitable range even though the bus voltages exceed both maximum and minimum limit.

Three types of voltage violation can be classified as shown in Figure 4.14. In case of maximum or minimum voltage violation, the violation can be eliminated one voltage control equipment because voltage sensitivities with regard to control variables are always positive. For example, highest voltage should decrease to remove the maximum voltage violation, and it can be accomplished by decrease in output power of DG or output voltage of GCC. However, a lot of voltage control equipment which has different voltage sensitivity characteristic is required if both highest and lowest voltages exceed suitable voltage range. This is because both the highest and lowest bus voltage is affected by voltage control equipment. This phenomenon can be explained with an example shown in Figure 4.15. In this example, it is assumed that there are two DGs, which have similar voltage sensitivities on the highest and lowest voltage, and first DG regulates the highest bus voltage and second DG regulates the lowest bus voltage. If first DG decreases its output power to regulate the highest voltage, both highest and lowest bus voltages decrease. Then second DG increases its output power to increase the lowest bus voltage, and finally, the highest bus voltage increase and it might be out of suitable range.

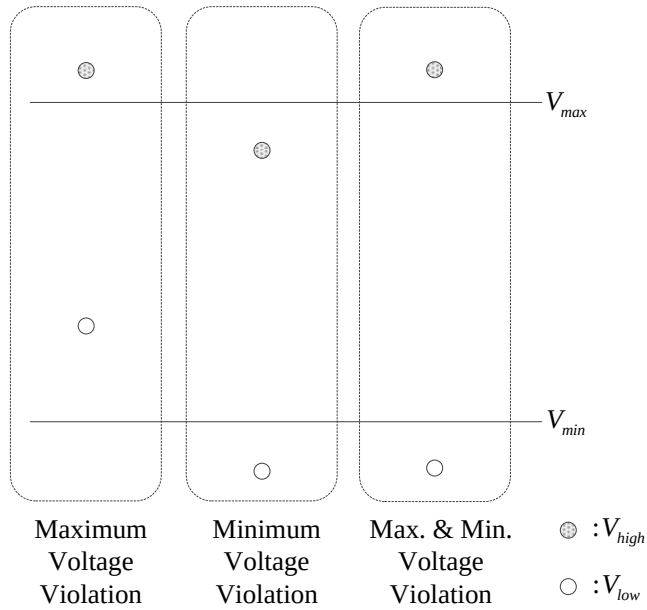

Figure 4.14 Three types of the voltage violation

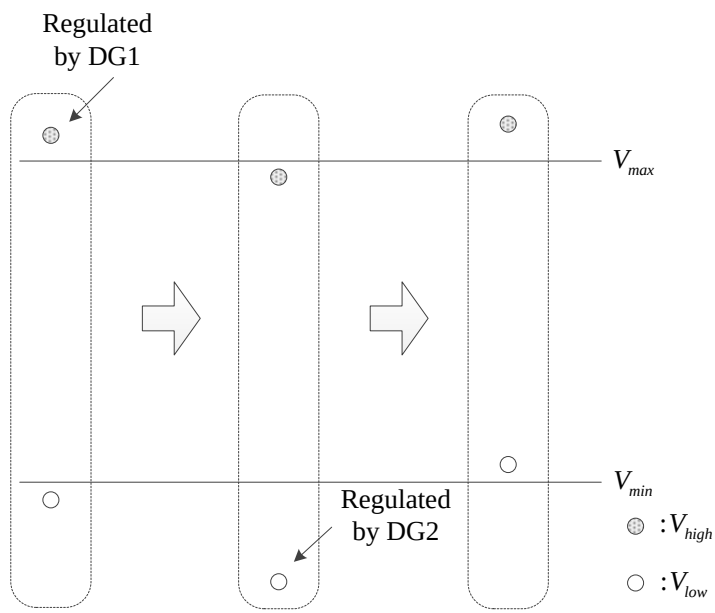

Figure 4.15 An example on the voltage regulation by two DGs in the maximum and minimum voltage violation condition

This kind of problem can be resolved by the proposed cooperative voltage control scheme. In proposed method, two kinds of voltage control equipment, which has different voltage sensitivity characteristics, are utilized and both

maximum and minimum voltage violation is removed by cooperative control. As shown in analytic analyses of voltage sensitivities, voltage sensitivities with regard to GCC output voltage is almost 1.0 and similar at all of the bus. Contrastively voltage sensitivities with regard to DG output power is different at each electrical distance between slack bus and each bus affects this sensitivity. Therefore, GCC and DG are appropriate for candidates of the cooperative voltage control equipment. Proposed voltage control scheme can be explained with an example shown in Figure 4.16.

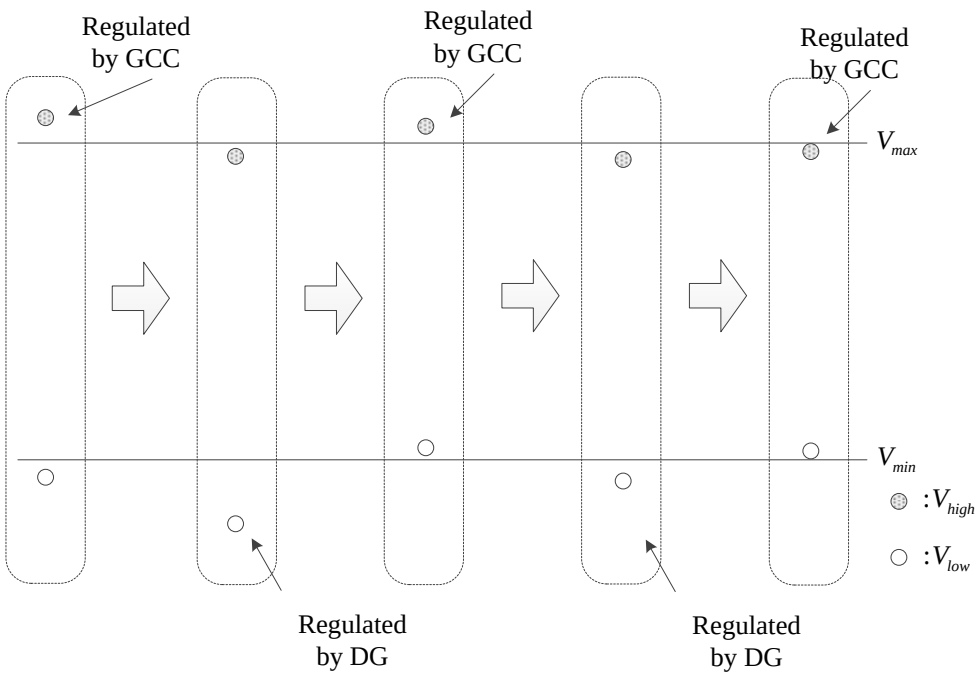

Figure 4.16 An example on the voltage regulation by GCC and DG to remove both maximum and minimum voltage violation

In proposed method, DG regulates the bus which voltage sensitivity is higher. Therefore, DG can regulate bus voltage with small variations of its output power. In other words, DG can have the better regulation capability by this control strategy. In this example, it is assumed that DG regulates the lowest bus voltage because voltage sensitivity on this bus is generally higher than other bus, and GCC regulates the highest bus voltage. In Figure 4.16, the highest bus voltage is

regulated by GCC and the variation of entire bus voltage due to the regulation is similar because voltage sensitivity with regard to GCC output voltage is similar at all of the bus. Then, DG regulates the lowest bus voltage and variation of the highest bus voltage is smaller than the lowest bus voltage due to different voltage sensitivity by DG. Finally, both highest and lowest bus voltage is maintained within suitable range by repeated process as mentioned before.

4.4. Local Controller: Preprocessing modules

In this section, preprocessing modules in the local controller are presented and these are utilized for both loss reduction and voltage regulation control modules.

4.4.1. Module 1: Voltage Sensitivity Estimator

This module generates estimated voltage sensitivities from measured bus voltages, bus injection power. There is one estimator for the slack bus voltage, and the number of estimators for the bus voltage is same as the number of DGs.

Figure 4.17 presents input and output variable of each estimator. The inputs of these estimators are set of the bus voltage, set of the bus injection power, and R-bus matrix. In addition, voltage sensitivity estimator for the bus injection power requires information on DG connected bus. The outputs are voltage sensitivities with regard to the slack bus voltage and the bus injection power at DG connected bus. Generally, calculation of power flow and Jacobian matrix is essential to calculate voltage sensitivity. However, the voltage sensitivity is calculated by proposed approximated voltage sensitivity equations (A.17) and (A.25) in proposed scheme and fast calculation is available without power flow calculation.

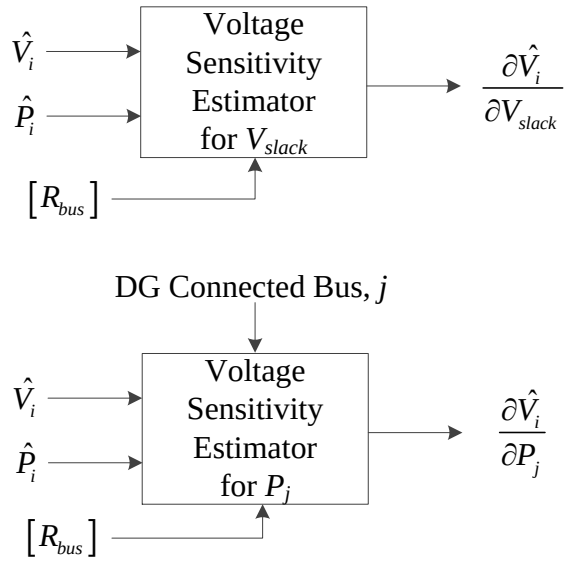

Figure 4.17 Voltage sensitivity estimator module

4.4.2. Module 2: Loss Sensitivity Estimator

This module generates various loss sensitivities from measured bus voltages, bus injection power, and internal loss model of the voltage control equipment. There are two kinds of loss sensitivity estimator which is presented in Figure 4.18 and Figure 4.19.

Line loss sensitivity estimators calculate approximate line loss sensitivities with regard to the slack bus voltage and the bus injection power. The inputs of these estimators are set of the bus voltage, set of the bus injection power, R-bus matrix, and voltage sensitivities calculated in the voltage sensitivity estimator module. The outputs are line loss sensitivity with regard to the slack bus voltage and a set of line loss sensitivity with regard to the bus injection power. These sensitivities are calculated quickly without power flow calculation by proposed approximate loss sensitivity expressions in (B.12) and (B.20).

Converter internal loss sensitivity estimators calculate the converter internal loss sensitivities with regard to the current output power of CC and DG. The Inputs of estimators are a set of coefficients of the quadratic converter loss equation in

(4.2) and. The outputs of estimators are converter internal loss sensitivities with regard to an output power of GCC and DG. These sensitivities are simply calculated linear equations because converter internal loss is modeled as quadratic equations. Therefore, sensitivities are calculated by equations shown below.

$$\frac{\partial P_{DG,k}^{loss}}{\partial P_{DG,k}} = 2a_k \left| P_{DG,k} \right| + b_k \tag{4.20}$$

$$\frac{\partial P_{GCC}^{loss}}{\partial P_{GCC}} = 2a_{GCC} \left| P_{GCC} \right| + b_{GCC} \tag{4.21}$$

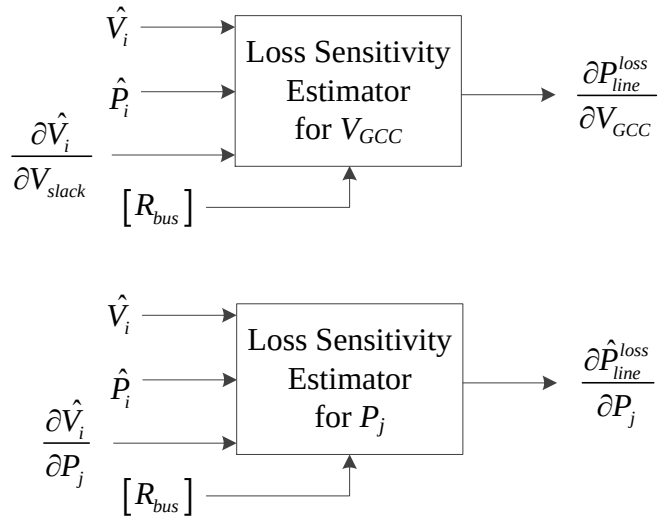

Figure 4.18 Line loss sensitivity estimator for the slack bus voltage and DG output power

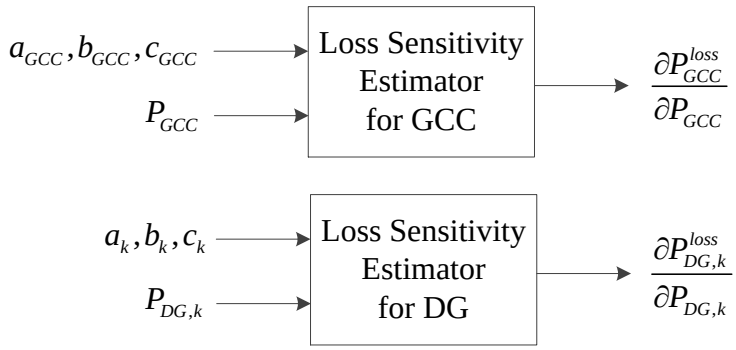

Figure 4.19 Converter internal loss sensitivity estimator for the GCC and DG output power

4.4.3. Module 3: Total Loss Sensitivity Calculator

The total loss sensitivity is sensitivity on whole system loss with regard to control variables and it represents actual loss sensitivity when control variables are changed. This module generates total loss sensitivities based on following relations.

Deviation total loss due to changes in reference of voltage control equipment is presented as follows:

$$\Delta P_{total}^{loss} = \Delta P_{line}^{loss} + \sum_{i=1}^{N_{DG}} \Delta P_{DG,i}^{loss} + \Delta P_{GCC}^{loss} \tag{4.22}$$

In (4.22), each term in the right hand side is presented as follows:

$$\Delta P_{line}^{loss} = \sum_{i=1}^{N_{DG}} \frac{\partial P_{line}^{loss}}{\partial P_{DG}} \Delta P_{DG} + \frac{\partial P_{line}^{loss}}{\partial V_{GCC}} \Delta V_{GCC} \tag{4.23}$$

$$\sum_{i=1}^{N_{DG}} \Delta P_{DG}^{loss} = \sum_{i=1}^{N_{DG}} \frac{\partial P_{DG,i}^{loss}}{\partial P_{DG,i}} \Delta P_{DG,i} \tag{4.24}$$

$$\Delta P_{GCC}^{loss} = \frac{\partial P_{GCC}^{loss}}{\partial P_{GCC}} \Delta P_{GCC} \tag{4.25}$$

In (4.23) and (4.24), deviation of each loss is expressed as a function of control variables, the output power of DG and output voltage of GCC. However, the output power of GCC in (4.25) is not control variable and this expression should be changed as a function of control variables to derive total loss sensitivity. The changes in GCC output power due to variation in DG output power is expressed as follows:

$$\Delta P_{GCC}^{by\,P_{DG}} = \sum_{i=1}^{N_{DG}} \left(\frac{\partial P_{line}^{loss}}{\partial P_{DG,i}} \Delta P_{DG,i} - \Delta P_{DG,i} \right) \tag{4.26}$$

In (4.26), line loss is changed due to a variation in DG output power. In addition, the GCC output power is changed reversely when the DG output power is varied because generation and load balance in the DC distribution system should be maintained. The changes in GCC output power due to variations in GCC output

voltage are presented as follows:

$$\Delta P_{GCC}^{byV_{GCC}} = \frac{\partial P_{line}^{loss}}{\partial V_{GCC}} \Delta V_{GCC} \tag{4.27}$$

In (4.27), variations in GCC output voltage does not influence load consumptions because it is assumed that there are CPLs in the distribution system. Therefore, changes in line loss are only affected and it is equivalent to changes in GCC output power. Therefore, deviation of GCC output power is arranged as follows using (4.26) and (4.27).

$$\Delta P_{GCC} = \sum_{i=1}^{N_{DG}} \left(\frac{\partial P_{line}^{loss}}{\partial P_{DG,o}} - 1 \right) \Delta P_{DG,o} + \frac{\partial P_{line}^{loss}}{\partial V_{GCC}} \Delta V_{GCC} \tag{4.28}$$

And deviation of GCC internal loss is arranged as follows:

$$\Delta P_{GCC}^{loss} = \left[\sum_{i=1}^{N_{DG}} \left(\frac{\partial P_{line}^{loss}}{\partial P_{DG,i}} - 1 \right) \Delta P_{DG,i} + \frac{\partial P_{line}^{loss}}{\partial V_{GCC}} \Delta V_{GCC} \right] \frac{\partial P_{GCC}^{loss}}{\partial P_{GCC}} \tag{4.29}$$

Deviation total loss due to changes in reference of voltage control equipment arranged as follows as a function of control variables.

$$\begin{aligned} \Delta P_{total}^{loss} = \sum_{i=1}^{N_{DG}} & \left[\left(\frac{\partial P_{line}^{loss}}{\partial P_{DG,i}} - 1 \right) \frac{\partial P_{GCC}^{loss}}{\partial P_{GCC}} + \frac{\partial P_{line}^{loss}}{\partial P_{DG,i}} + \frac{\partial P_{DG,i}^{loss}}{\partial P_{DG,i}} \right] \Delta P_{DG,i} \\ & + \left(\frac{\partial P_{GCC}^{loss}}{\partial P_{GCC}} + 1 \right) \frac{\partial P_{GCC}^{loss}}{\partial V_{GCC}} \Delta V_{GCC} \end{aligned} \tag{4.30}$$

From (4.30), deviation of total loss is arranged and total loss sensitivity with regard to DG output power and GCC output voltage is derived as follows:

$$\Delta P_{total}^{loss} = \sum_{i=1}^{N_{DG}} \frac{\partial P_{total}^{loss}}{\partial P_{DG,i}} \Delta P_{DG,i} + \frac{\partial P_{total}^{loss}}{\partial V_{GCC}} \Delta V_{GCC} \tag{4.31}$$

$$\frac{\partial P_{total}^{loss}}{\partial P_{DG,i}} = \left(\frac{\partial P_{line}^{loss}}{\partial P_{DG,i}} - 1 \right) \frac{\partial P_{GCC}^{loss}}{\partial P_{GCC}} + \frac{\partial P_{line}^{loss}}{\partial P_{DG,i}} + \frac{\partial P_{DG,i}^{loss}}{\partial P_{DG,i}} \tag{4.32}$$

$$\frac{\partial P_{total}^{loss}}{\partial V_{GCC}} = \left(\frac{\partial P_{GCC}^{loss}}{\partial P_{GCC}} + 1 \right) \frac{\partial P_{GCC}^{loss}}{\partial V_{GCC}} \tag{4.33}$$

Based on derive equations, total loss sensitivity calculators are presented as shown in Figure 4.20 and Figure 4.21. The input variables are obtained by loss sensitivity estimators and calculated total sensitivities are delivered to loss reduction controller.

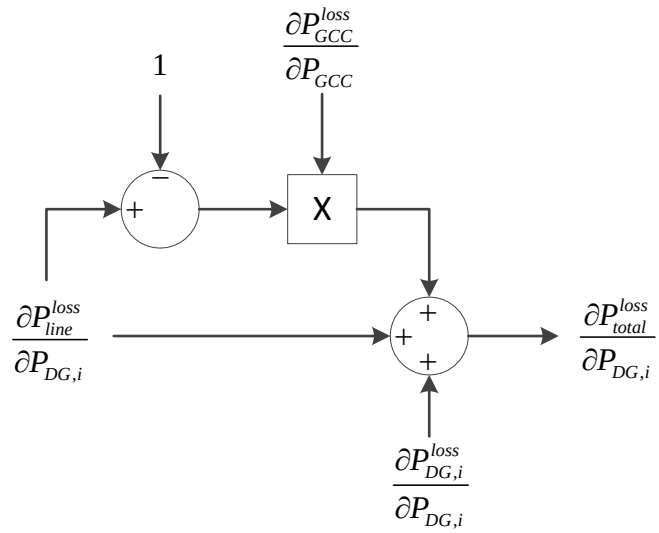

Figure 4.20 Calculation blocks for the total loss sensitivity with regard to the DG output power

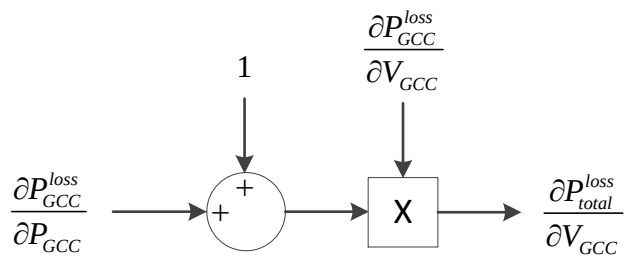

Figure 4.21 Calculation blocks for the total loss sensitivity with regard to the GCC output voltage

4.4.4. Module 4: Highest and Lowest Voltage Selector

From a set of measured bus voltage, this module determines highest and lowest voltages. The output variables are delivered to regulation signal generation

module.

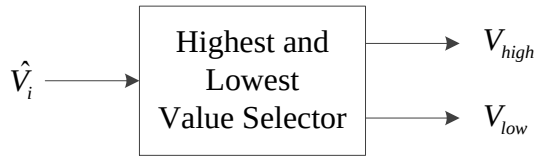

Figure 4.22 Highest and lowest voltage selector module

4.4.5. Module 5: Voltage Sensitivity Selector

From a set of measured bus voltage and voltage sensitivities calculated by voltage sensitivity estimator, this module chooses voltage sensitivities on highest and lowest voltage. The output variables are delivered to regulation signal generation module.

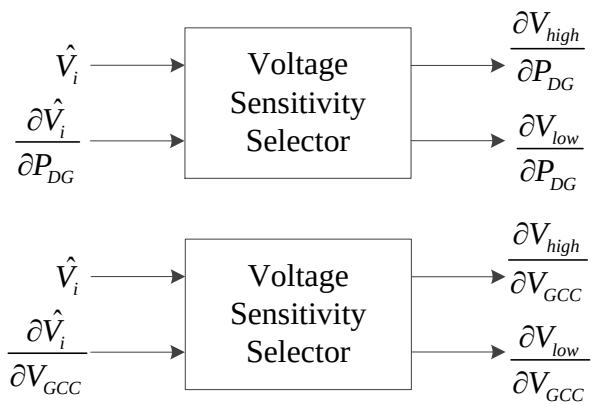

Figure 4.23 Voltage sensitivity selector module

4.4.6. Module 6: Regulation Signal Generator

This module generates regulation signals for loss reduction controller and voltage regulation controller. The input and output variables of this module are presented in Figure 4.24.

Figure 4.25 presents flow chart of regulation signal generator module and functions of each step are explained. In step 1, violations type is identified and each violation type is defined as Table 4.1

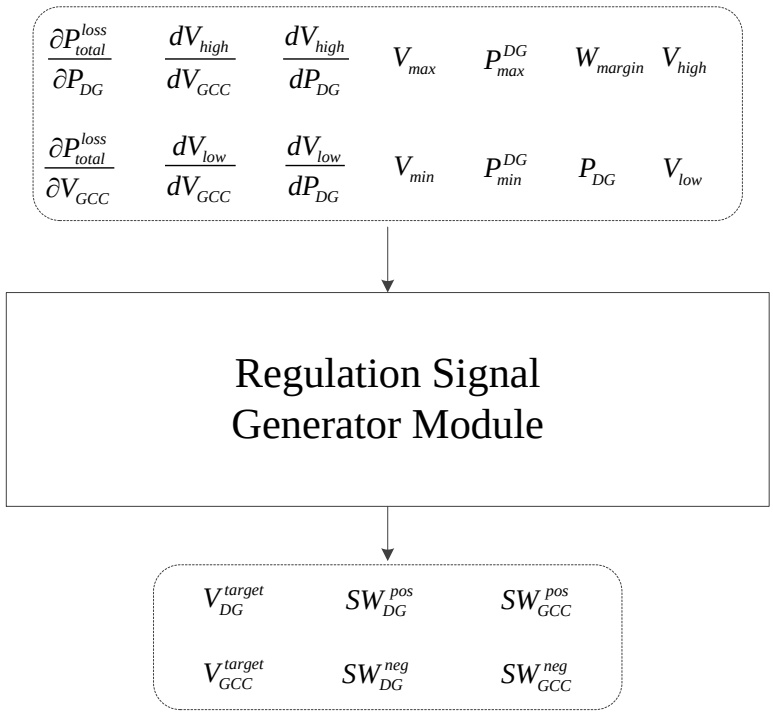

Figure 4.24 Regulation signal generator module

Table 4.1 Voltage violation type

Highest Voltage Condition	**Lowest Voltage Condition**	**Voltage Violation Type**
$V_{high} > V_{max}^{loss}$	$V_{low} < V_{min}^{loss}$	1, Max and min violation
$V_{high} > V_{max}^{loss}$	$V_{low} \geq V_{min}^{loss}$	2, Max violation
$V_{high} \leq V_{max}^{loss}$	$V_{low} < V_{min}^{loss}$	3, Min violation
$V_{high} \leq V_{max}^{loss}$	$V_{low} \geq V_{min}^{loss}$	4, No violation

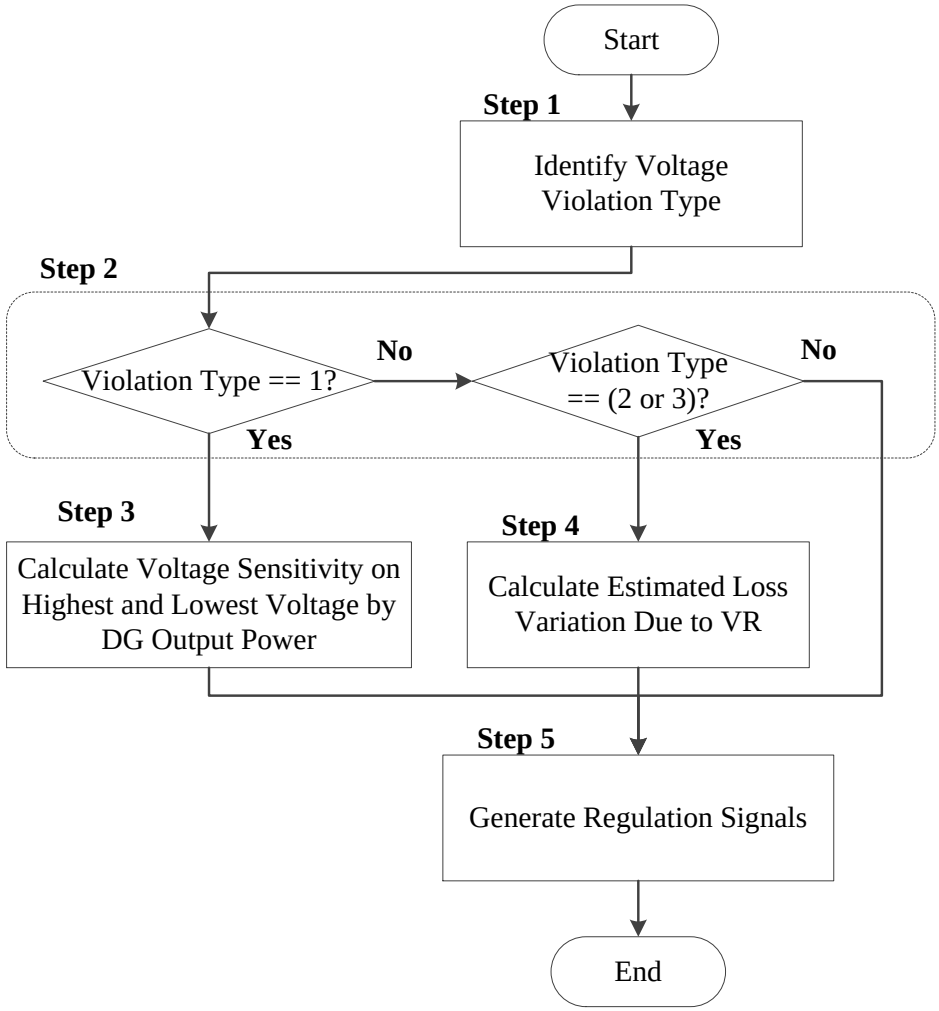

Figure 4.25 Regulation signal generator module

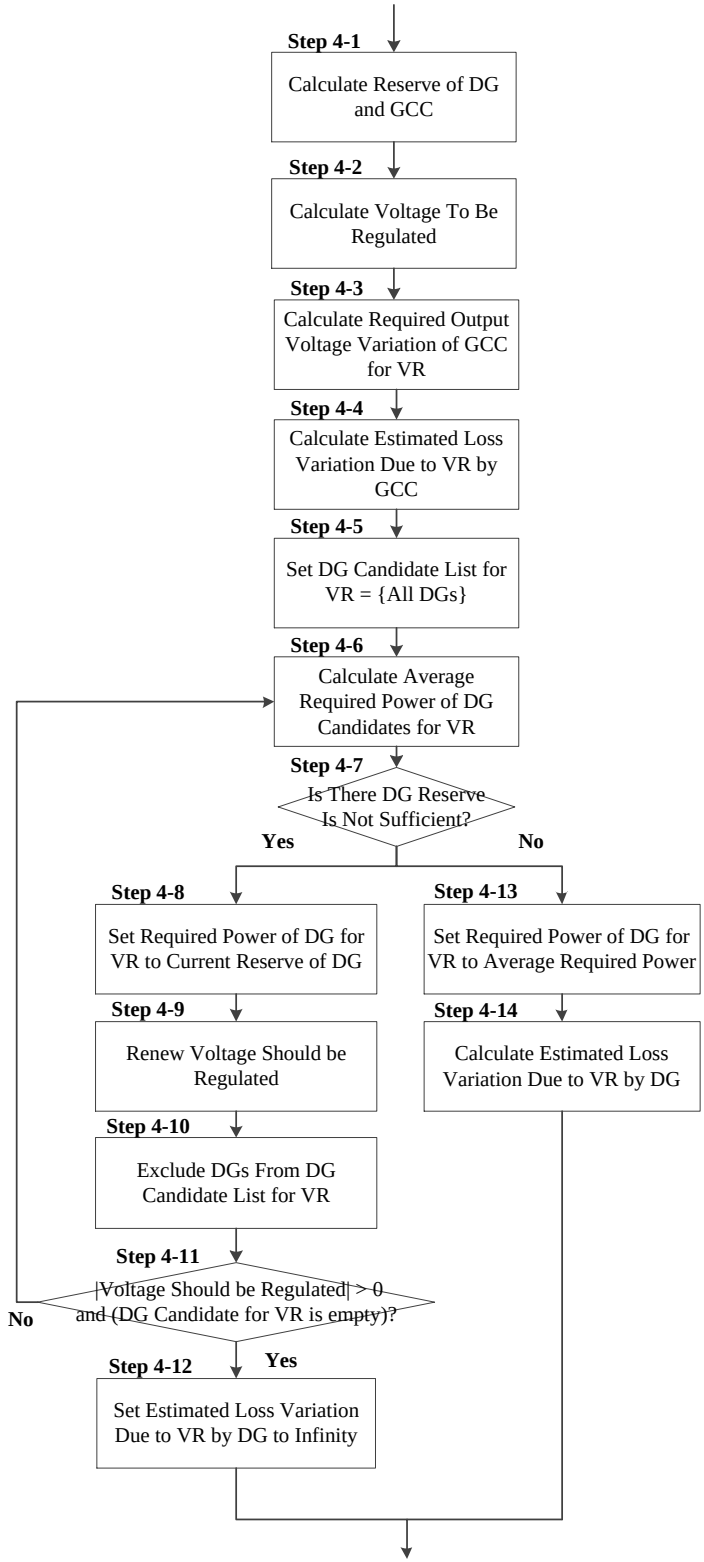

Figure 4.26. Specific algorithm in step 4 of regulation signal generator module

In step 2, implemented function is chosen depending on voltage violation type. Function in step 3 is implemented if both maximum and minimum voltage violation are occurred and step 4 is carried out if there is only one kind of voltage violation.

In step 3, both DGs and GCC participate in voltage regulation by proposed cooperative voltage regulation scheme. DGs regulate highest or lowest bus voltage depending on voltage sensitivity on DG output power. Equivalent voltage sensitivities on DG output power are expressed as follows if voltage regulation controllers of each DG have identical control characteristic.

$$\frac{\partial V_{high}}{\partial P_{DG}} = \sum_{i=1}^{N_{DG}} \frac{\partial V_{high}}{\partial P_{DG,i}} \tag{4.34}$$

$$\frac{\partial V_{low}}{\partial P_{DG}} = \sum_{i=1}^{N_{DG}} \frac{\partial V_{low}}{\partial P_{DG,i}} \tag{4.35}$$

If violation type is maximum voltage violation or minimum voltage violation, functions in step 4 are carried out. Specific functions in step 4 are presented in Figure 4.26. In step 4-1, reserve of DG and GCC is calculated as following equations.

$$P_{DG,upper}^{reserve} = P_{DG}^{max} - P_{DG} \tag{4.36}$$

$$P_{DG,lower}^{reserve} = P_{DG} - P_{DG}^{min} \tag{4.37}$$

$$P_{GCC,upper}^{reserve} = P_{GCC}^{max} - P_{GCC} \tag{4.38}$$

$$P_{GCC,lower}^{reserve} = P_{GCC} - P_{GCC}^{min} \tag{4.39}$$

In step 4-2, voltage to be regulated is calculated as (4.40) and (4.41). These values become zero if all of the bus voltages are within suitable range. If highest voltage exceeds the maximum voltage limit, this voltage should be decreased by regulation and voltage to be regulated is negative.

$$V_{high}^{reg} = V_{max} - V_{high} \quad if \;\; V_{high} > V_{max}$$
$$V_{high}^{reg} = 0 \qquad\quad if \;\; V_{high} \le V_{max} \tag{4.40}$$

$$V_{low}^{reg} = V_{min} - V_{low} \quad if \;\; V_{min} > V_{low}$$
$$V_{low}^{reg} = 0 \qquad\quad if \;\; V_{min} \le V_{low} \tag{4.41}$$

In step 4-3, required output voltage variation of GCC to regulate abnormal bus voltage is calculated and it is expressed as (4.42) and (4.43).

$$V_{GCC,high}^{reg} = V_{high}^{reg} / \frac{\partial V_{high}}{\partial V_{GCC}} \tag{4.42}$$

$$V_{GCC,low}^{reg} = V_{low}^{reg} / \frac{\partial V_{low}}{\partial V_{GCC}} \tag{4.43}$$

In step 4-4, estimated loss variation when voltage is regulated by GCC is calculated. It is linearized by proposed loss sensitivity and expressed as following equations.

$$\Delta P_{GCC,high}^{loss} = V_{GCC,high}^{reg} \frac{\partial P_{total}^{loss}}{\partial V_{GCC}} \tag{4.44}$$

$$\Delta P_{GCC,low}^{loss} = V_{GCC,low}^{reg} \frac{\partial P_{total}^{loss}}{\partial V_{GCC}} \tag{4.45}$$

From step 4-5 to 4-14, estimated loss variation when voltage regulated by a number of DGs is calculated. In step 4-5, a candidate list of DG for voltage regulation is initialized and all of DGs becomes candidate. In step 4-6, an average required power of DG candidates to regulate voltage is calculated by (4.46) and (4.47) if voltage regulation controllers of each DG have identical control characteristic.

$$P_{DG,high}^{reg} = V_{high}^{reg} / \left(\sum_{i=1}^{N_{DG}} \frac{\partial V_{high}}{\partial P_{DG,i}} \right) \quad for\ i\ which\ is\ a\ candidate\ for\ VR \tag{4.46}$$

$$P_{DG,low}^{reg} = V_{low}^{reg} / \left(\sum_{i=1}^{N_{DG}} \frac{\partial V_{low}}{\partial P_{DG,i}} \right) \quad for\ i\ which\ is\ a\ candidate\ for\ VR \tag{4.47}$$

In step 4-7, find DGs whose capacity reserve is not sufficient to participate in voltage regulation. If there are DGs which capacity reserve is smaller than

magnitude of an average required power for voltage regulation, required power of these DGs for voltage regulation is set to current reserve capacity of each DGs in step 4-8. In step 4-9, voltage to be regulated is renewed and voltage variation by DGs which reserve capacity is not sufficient is reflected as (4.48) and (4.49).

$$V_{high}^{reg} = V_{high}^{reg} + \sum_{i=1}^{N_{DG}} \frac{\partial V_{high}}{\partial P_{DG,i}} P_{DG,high,i}^{reg} \quad for\ i\ which\ reserve\ is\ not\ sufficient \tag{4.48}$$

$$V_{low}^{reg} = V_{low}^{reg} + \sum_{i=1}^{N_{DG}} \frac{\partial V_{high}}{\partial P_{DG,i}} P_{DG,low,i}^{reg} \quad for\ i\ which\ reserve\ is\ not\ sufficient \tag{4.49}$$

In step 4-10, these DGs are excluded from candidate list for voltage regulation. In step 4-11, function examines voltage regulation condition of DGs. If absolute value of voltage to be regulated is larger than zero and DG candidate list for voltage regulation is empty, voltage violation cannot be eliminated by DGs because reserve capacity of DGs is not enough to supply active power. In this case, estimated loss variation is set to infinity and it is a kind of a penalty value. If not, function in step 4-6 is carried out with renewed DG candidate list for voltage regulation. If all of DGs has enough capacity reserve to regulate violated voltage in step 4-7, required power of DGs in candidate list is set to average required power for voltage regulation in step 4-13. In step 4-14, estimated loss variation due to voltage regulation by DG is calculated as follows:

$$\Delta P_{DG,high}^{loss} = \sum_{i=1}^{N_{DG}} P_{DG,high,i}^{reg} \frac{\partial P_{total}^{loss}}{\partial P_{DG,i}} \tag{4.50}$$

$$\Delta P_{DG,low}^{loss} = \sum_{i=1}^{N_{DG}} P_{DG,low,i}^{reg} \frac{\partial P_{total}^{loss}}{\partial P_{DG,i}} \tag{4.51}$$

In step 5, voltage regulation signals are generated and seven modes are defined depending on the voltage violation type and estimated loss variations. Table 4.2 presents condition and output results of each mode. Detail explanations about controls in each mode are explained in later section.

Table 4.2 Mode and output result of regulation signal generator

Mode	Violation Type Condition	Sensitivity Condition	Output Variable
1	1	$\frac{\partial V_{high}}{\partial P_{DG}} > \frac{\partial V_{low}}{\partial P_{DG}}$	$V_{DG}^{target} = V_{high},\ V_{GCC}^{target} = V_{low},\ SW_{DG}^{pos} = 0$ $SW_{DG}^{neg} = 0, SW_{GCC}^{pos} = 0, SW_{GCC}^{neg} = 0$
2	1	$\frac{\partial V_{high}}{\partial P_{DG}} < \frac{\partial V_{low}}{\partial P_{DG}}$	$V_{DG}^{target} = V_{low},\ V_{high}^{target} = V_{high},\ SW_{DG}^{pos} = 0$ $SW_{DG}^{neg} = 0, SW_{GCC}^{pos} = 0\ ,\ SW_{GCC}^{neg} = 0$
3	2	$\Delta P_{DG,high}^{loss} < \Delta P_{GCC,high}^{loss}$	$V_{DG}^{target} = V_{high},\ V_{GCC}^{target} = 1,\ SW_{DG}^{pos} = 0$ $SW_{DG}^{neg} = 1, SW_{GCC}^{pos} = 1\ ,\ SW_{GCC}^{neg} = 1$
4	2	$\Delta P_{DG,high}^{loss} \geq \Delta P_{GCC,high}^{loss}$	$V_{DG}^{target} = 1,\ V_{high}^{target} = V_{high},\ SW_{DG}^{pos} = 1$ $SW_{DG}^{low} = 1, SW_{GCC}^{pos} = 0\ ,\ SW_{GCC}^{neg} = 1$
5	3	$\Delta P_{DG,low}^{loss} < \Delta P_{GCC,low}^{loss}$	$V_{DG}^{target} = V_{low},\ V_{GCC}^{target} = 1,\ SW_{DG}^{pos} = 1$ $SW_{DG}^{neg} = 0, SW_{GCC}^{pos} = 1\ ,\ SW_{GCC}^{neg} = 1$
6	3	$\Delta P_{DG,low}^{loss} \geq \Delta P_{GCC,low}^{loss}$	$V_{DG}^{target} = 1,\ V_{GCC}^{target} = V_{low},\ SW_{DG}^{pos} = 1$ $SW_{DG}^{neg} = 1, SW_{GCC}^{pos} = 1\ ,\ SW_{GCC}^{neg} = 0$
7	4	-	$V_{DG}^{target} = 1,\ V_{GCC}^{target} = 1,\ SW_{DG}^{pos} = 1$ $SW_{DG}^{neg} = 1, SW_{GCC}^{pos} = 1\ ,\ SW_{GCC}^{neg} = 1$

4.5. Local Controller Module 7: Loss Reduction Module

Based on loss reduction control scheme explained in Figure 4.13 and derived total loss sensitivities, loss reduction controller is composed as Figure 4.27 and Figure 4.28. The structures of these controllers are same and the only differences are input and output variable. The controller changes the reference of voltage control equipment until total loss sensitivity becomes zero to accomplish the proposed control scheme.

In part A, desired reference of total loss sensitivity is zero and it is subtracted by estimated total loss sensitivity. An error on reference sensitivity is delivered to part B.

In part B, control is depending on control mode and flag signal, which are

shown in Table 4.2, determined by regulation signal generator module. The error signal is divided into two parts, the positive and negative value part, and each part is activated by flag signal. If mode is 1 or 2, this is the case that violations occur on both the highest and lowest bus voltages. In this case, both DG and GCC should participate in the voltage regulation; the reason is explained in the voltage regulation module section. Therefore, the entire flag signal for loss reduction control is deactivated. In mode 3, there is a violation on highest bus voltage and DG has lower estimated loss variation to regulate voltage violation than GCC. Therefore, DG participates in voltage regulation to regulate the highest voltage, minimizing an increase in loss, and positive power flag signal of DG is deactivated. This is because voltage sensitivities with regard to control variables are always positive, and therefore, positive power reference in loss reduction controller of DG interrupts the voltage regulation control. In mode 4, GCC has a lower estimated loss variation than DG, and GCC participates in the voltage regulation. Similarly, positive voltage flag signal of GCC is deactivated to prevent the violation on the highest bus voltage. In mode 5 and 6, there is a violation on lowest bus voltage and the candidate for the voltage regulation is determined by estimated loss variation. In these cases, negative flag signal of the voltage regulation candidate is deactivated to prevent the violation on the lowest bus voltage. In mode 7, the entire bus voltages are maintained within suitable range and all flag signals for loss reduction control are activated.

In part C, an error of total sensitivity is delivered to integrator and it generates a reference signal of the voltage control equipment. In addition, the controllers include anti-windup controller to prevent integration wind-up and it is shown in part D.

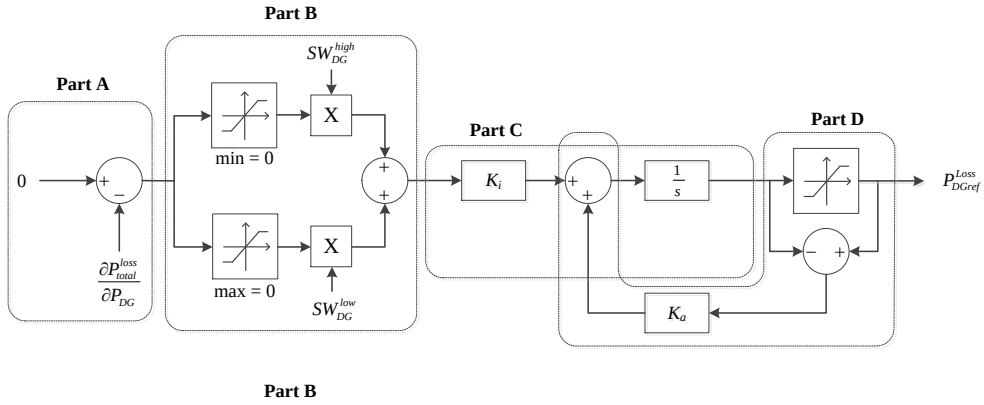

Figure 4.27 The loss reduction controller for the DG

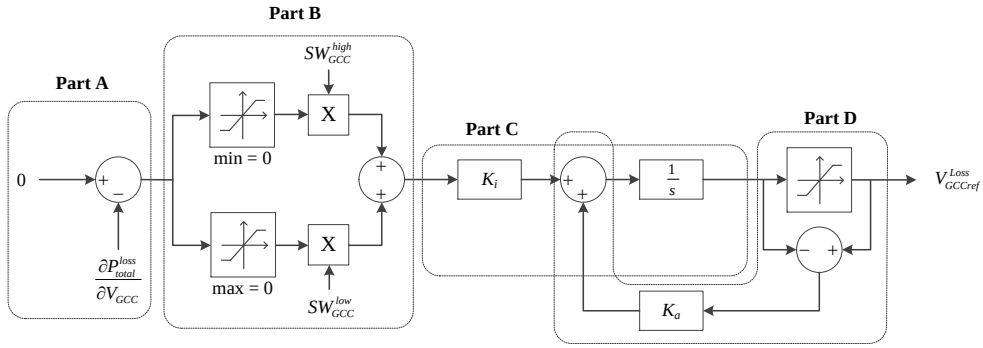

Figure 4.28 The loss reduction controller for the GCC

4.6. Local Controller Module 8: Voltage Regulation Control

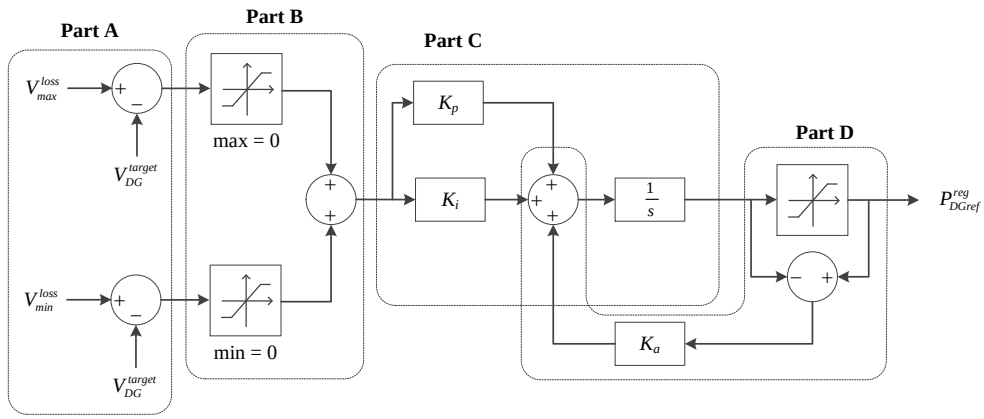

Figure 4.29 The voltage regulation controller for the DG

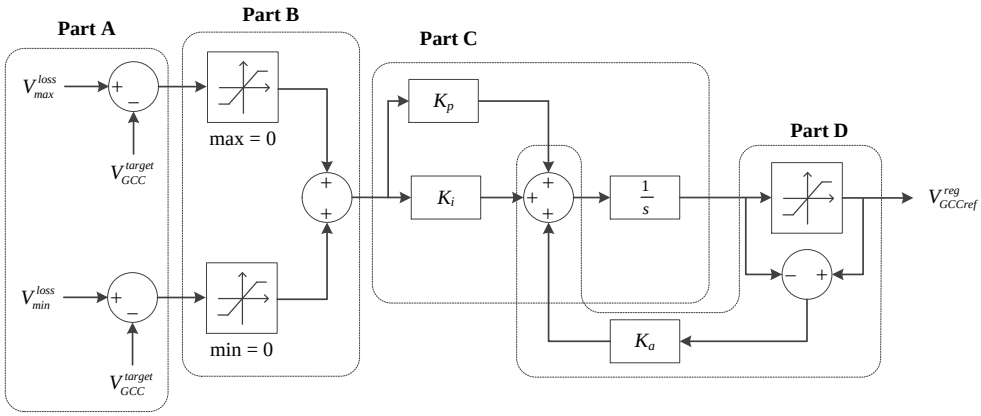

Figure 4.30 The voltage regulation controller for the GCC

To realize the proposed cooperative voltage control scheme, voltage regulation controllers are presented in Figure 4.29 and Figure 4.30. Controllers have same structure, and input / output variables and gain of controller are different. These controllers are activated by target voltage signal generated by regulation signal generator module. If both highest and lowest voltages exceed suitable voltage range, regulation mode, which is shown in Table 4.2, 1 or 2 is activated. In these modes, both DG and GCC should participate in the voltage regulation, and regulation targets of voltage control equipment are determined by the voltage sensitivity with regard to DG output power. For example, in mode 1, DG regulates the highest bus voltage because the voltage sensitivity on the highest bus voltage is larger than the lowest bus voltage, and target voltage of GCC is set to the lowest bus voltage. In mode 3 and 4, only the highest bus voltage exceed voltage limit and the candidate for the voltage regulation is determined by estimated loss variation due to the voltage regulation. In mode 3, DG becomes the candidate because estimated loss variation of DG is lower than GCC. Regulation target voltage of DG is set to the highest voltage and target voltage of GCC is set to 1.0, which is the median value of maximum and minimum voltage limits. Similarly, target voltage is determined in mode 5 and 6, and target voltage of DG and GCC is set to 1.0 in mode 7 because there is not voltage violation at any bus.

After the regulation target voltages are determined, these are compared with

the maximum and minimum voltage limits for loss reduction control in part A. In part A, result of upper and lower parts are value of the voltage should be changed for the voltage regulation on the highest and lower bus voltages, respectively. In part B, there are saturation blocks and only negative or positive value is passed, respectively, and result of part B becomes zero if the target voltage does not exceed any voltage limits. Therefore, output of part B becomes zero and does not affect the voltage regulation if the voltage control equipment does not participate in the regulation and the regulation target voltage is set to 1.0. In part C, regulation signal from part B is delivered to PI controller generate a reference for the voltage regulation. In addition, the PI controllers include anti-windup controller to prevent integration wind-up and it is shown in part D.

Chapter 5. Case Studies for Proposed Method

5.1. Test Model

Figure 5.1 presents the topology of the test distribution system model. The test system is 13-bus radial DC distribution system and including GCC, RES, and DG. The base voltage is 2 kV and the base power is 1 MW, and maximum and minimum voltage limit was 1.04 and 0.96 pu, respectively. There are two DGs at bus 6 and 11, which maximum output power of resources was 1 MW and 0.5 MW, respectively. Maximum power of PV generator at bus 8 was 0.6 MW. The DC distribution system is connected to the HVAC transmission system by GCC and the maximum output power of GCC was 4 MW.

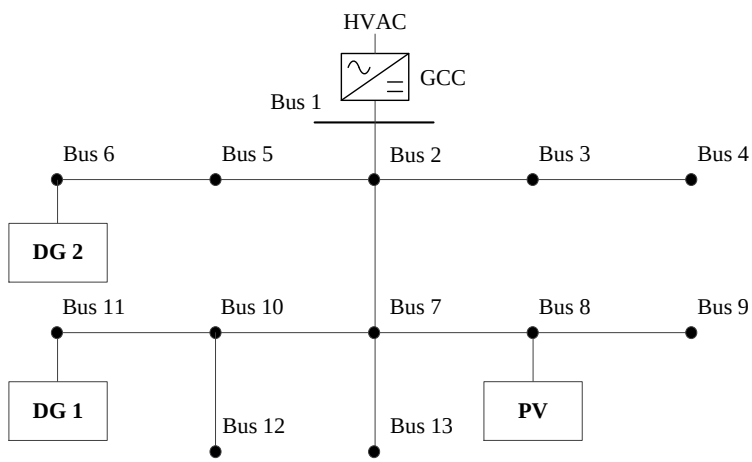

Figure 5.1 Topology for the test distribution system model

Table 5.1 presents the maximum current capacity maximum current capacity of the branches. Table 5.2 lists the generation forecasting results of PV generator, which are generated based weather forecasting in the Gasa-island, Korea. Table 5.3 lists the load pattern data in the test system. The load pattern is generated based on hourly load forecasting data presented by Korea power exchange (KPX) in 10, November, 2015 [63]. The Load has constant power consuming characteristic and

the peak load is 3 MW. Figure 5.2 and Figure 5.3 presents total load and forecasted PV generations for 24 hours, respectively. The efficient curves for a converter of DGs and GCC are presented in Figure 5.4 and the coefficients of converter internal loss of are modeled as shown in Table 5.4. Two DGs have identical internal loss coefficients. The communication delay between supervisory controller and local controller was reflected and this is modeled as an equation shown in (5.1), and it is assumed that the communication delay is 0.3 seconds.

$$x = \frac{1}{1+T_d} x_{measured} \tag{5.1}$$

Table 5.1 Branch data for the test system

From Bus	To Bus	Resistance (Ω)	Maximum Current (A)
1	2	0.02940	1318
2	3	0.03460	760
2	5	0.03951	655
2	7	0.01358	1091
3	4	0.02195	655
5	6	0.06120	726
7	8	0.01730	760
7	10	0.03512	655
7	13	0.04390	655
8	9	0.01730	760
10	11	0.03073	655
10	12	0.03951	655

Table 5.2 PV generation forecasting data for the test system

Time	**0**	**1**	**2**	**3**	**4**	**5**
Gen.(MW)	0	0	0	0	0	0.004723
Time	**6**	**7**	**8**	**9**	**10**	**11**
Gen.(MW)	0.083471	0.21563	0.344372	0.450237	0.525485	0.562556
Time	**12**	**13**	**14**	**15**	**16**	**17**
Gen.(MW)	0.551166	0.496102	0.405574	0.266373	0.127018	0.025672
Time	**18**	**19**	**20**	**21**	**22**	**23**
Gen.(MW)	0	0	0	0	0	0

Table 5.3 Hourly load pattern data for the test system

Ti-me	Bus No. and load in MW (There is no load at bus 1)												
	2	**3**	**4**	**5**	**6**	**7**	**8**	**9**	**10**	**11**	**12**	**13**	**Total Load**
0	0.311	0.224	0.250	0.242	0.164	0.242	0.194	0.319	0.199	0.151	0.155	0.151	2.602
1	0.192	0.223	0.216	0.190	0.202	0.212	0.212	0.225	0.192	0.220	0.200	0.200	2.483
2	0.192	0.186	0.220	0.204	0.220	0.192	0.204	0.214	0.200	0.218	0.182	0.198	2.425
3	0.197	0.209	0.183	0.205	0.213	0.189	0.223	0.193	0.193	0.183	0.219	0.199	2.406
4	0.216	0.216	0.181	0.196	0.185	0.212	0.212	0.210	0.194	0.218	0.216	0.196	2.450
5	0.205	0.201	0.230	0.217	0.217	0.226	0.209	0.205	0.199	0.190	0.207	0.230	2.536
6	0.206	0.219	0.243	0.199	0.239	0.206	0.221	0.235	0.228	0.221	0.230	0.208	2.656
7	0.218	0.218	0.228	0.216	0.264	0.228	0.226	0.233	0.264	0.242	0.226	0.223	2.785
8	0.242	0.220	0.264	0.250	0.242	0.269	0.257	0.242	0.247	0.255	0.232	0.232	2.954
9	0.247	0.236	0.272	0.239	0.236	0.244	0.244	0.272	0.236	0.249	0.275	0.241	2.992
10	0.248	0.258	0.253	0.258	0.226	0.258	0.228	0.258	0.263	0.238	0.238	0.245	2.969
11	0.258	0.238	0.238	0.223	0.223	0.236	0.251	0.273	0.266	0.238	0.251	0.238	2.935
12	0.221	0.228	0.241	0.214	0.244	0.244	0.221	0.203	0.205	0.239	0.239	0.237	2.737
13	0.260	0.248	0.256	0.224	0.222	0.219	0.258	0.231	0.241	0.234	0.260	0.241	2.896
14	0.263	0.258	0.225	0.220	0.256	0.256	0.227	0.246	0.261	0.261	0.232	0.249	2.954
15	0.231	0.221	0.258	0.258	0.244	0.261	0.268	0.244	0.268	0.244	0.231	0.221	2.949
16	0.227	0.234	0.270	0.244	0.227	0.270	0.249	0.259	0.242	0.237	0.259	0.270	2.988
17	0.261	0.226	0.226	0.258	0.266	0.268	0.251	0.271	0.236	0.239	0.229	0.256	2.986
18	0.233	0.256	0.251	0.231	0.258	0.236	0.276	0.238	0.251	0.276	0.243	0.253	3.000
19	0.234	0.256	0.254	0.256	0.259	0.268	0.222	0.224	0.246	0.227	0.261	0.220	2.927
20	0.223	0.250	0.221	0.221	0.247	0.262	0.233	0.264	0.218	0.238	0.240	0.254	2.870
21	0.249	0.255	0.246	0.249	0.216	0.214	0.244	0.239	0.211	0.214	0.228	0.249	2.813
22	0.205	0.248	0.214	0.237	0.243	0.205	0.237	0.250	0.243	0.250	0.237	0.221	2.789
23	0.244	0.251	0.205	0.230	0.242	0.233	0.233	0.244	0.208	0.214	0.246	0.244	2.795

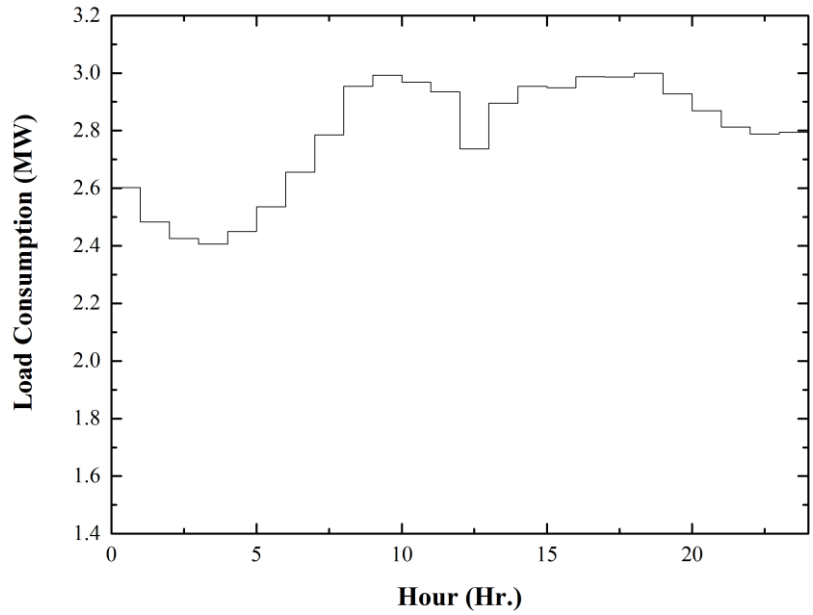

Figure 5.2 Daily total load consumption pattern for the test system

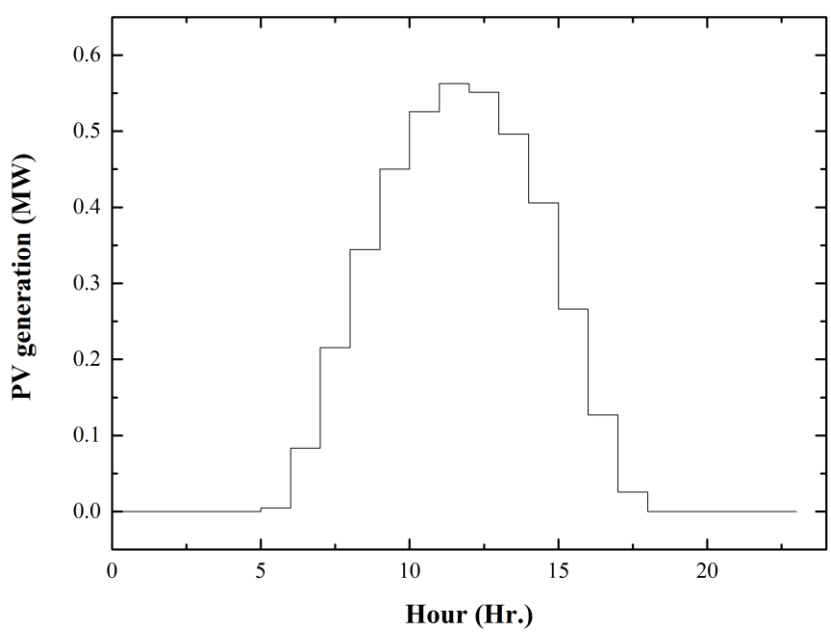

Figure 5.3 Forecasted PV generation power for a day for the test system

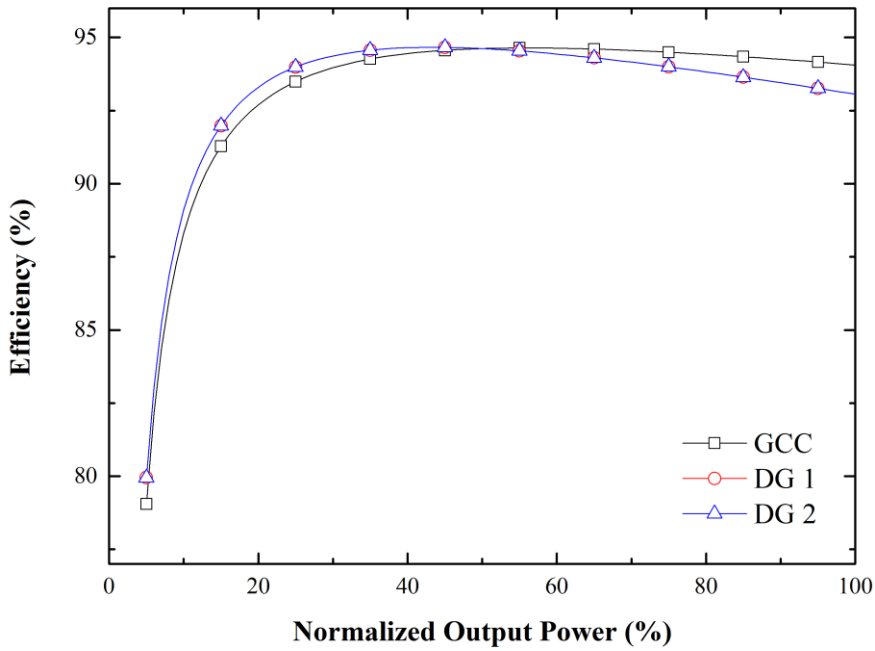

Figure 5.4 Efficiency curves of converters

Table 5.4 Coefficients of converter internal loss model

DG 1	a_k	b_k	c_k
	0.05	0.01	0.0094
DG 2	a_k	b_k	c_k
	0.05	0.01	0.0094
GCC	a_{GCC}	b_{GCC}	c_{GCC}
	0.03	0.02	0.0094

The optimal scheduling process is realized using MATLAB and the test system and control module is constructed in PSCAD/EMTDC system. In the test system, distribution line is modeled as RLC Pi-equivalent model. Converter average model is utilized. The converter of load and DG is modeled as a controllable current source and GCC is modeled as a controllable DC voltage source.

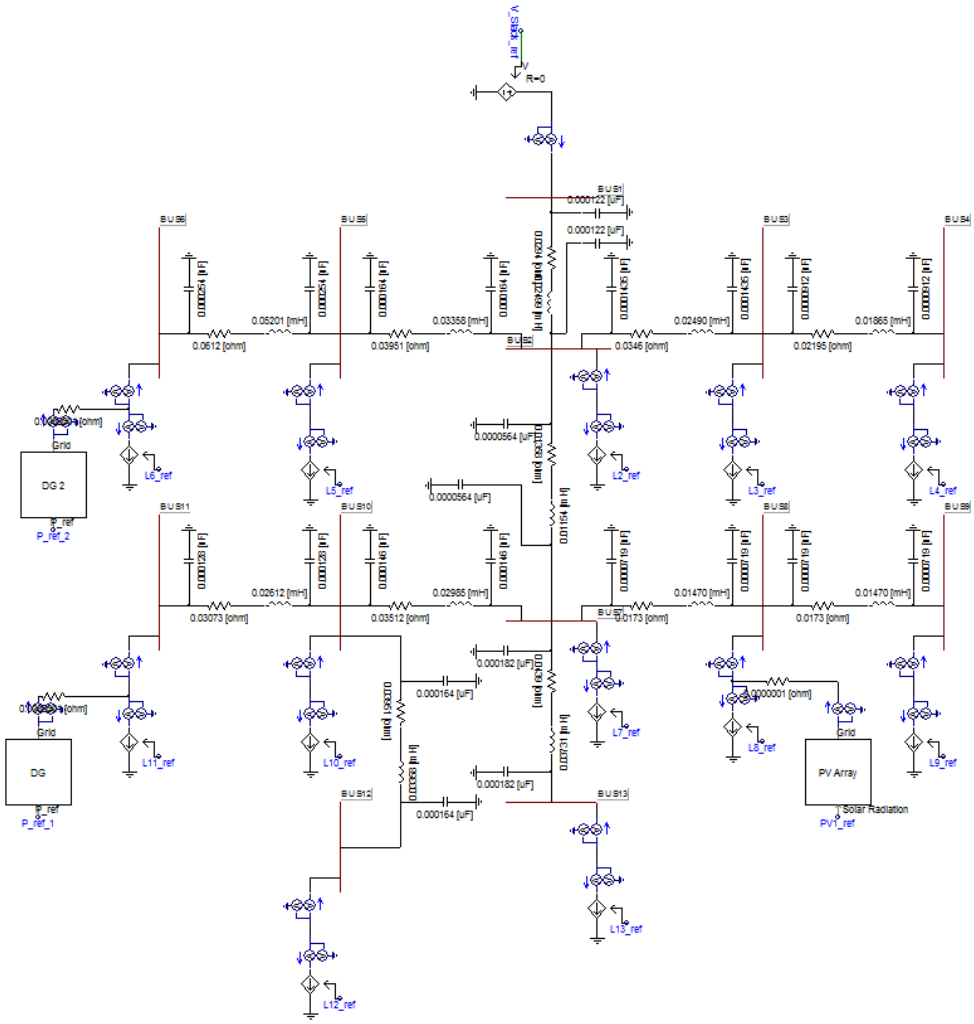

Figure 5.5.Test system for dynamic simulation constructed using PSCAD/EMTDC

5.2. Verification of Proposed Method

5.2.1. Case 1: when load and generation of RES are not varied

In this case, load and generation of RES is kept constantly during each time interval and it is identical to conditions in an optimal scheduling. The proposed method is verified in this case and results are compared with base case. It is assumed that load consumption and generation power of RES does not vary during each time interval in case 1. Four conditions are prepared for verification and each condition is presented in Table 5.5. In base condition, reference of GCC output

voltage is 1.0 pu and output power of DGs is 0 MW during entire time interval. It is assumed that optimal scheduled references are 1.0 pu for GCC and 0 MW for DGs if optimal scheduling is not implemented. Each condition is examined in test system constructed using PSCAD/EMTDC shown in Figure 5.5.

Table 5.5. Studied case conditions for verification of proposed method

Condition	Method	Optimal Scheduling	Real-time Control	Description
A	Base condition	X	X	Reference of GCC: 1.0 pu Reference of DGs: 0 MW
B	Proposed method	O	O	
C	Proposed method	O	X	An optimal scheduled result
D	Proposed method	X	O	It is assumed that optimal scheduled references are 1.0 pu for GCC and 0 MW for DGs

Figure 5.6 and Figure 5.7 present DG generation power and GCC delivering power in case 1. Generation power of each DG was determined by proposed method and it is indicated that generation power and GCC delivering power in case 1-B and 1-D were similar to result of an optimal scheduling, which is presented in case 1-C. There was only small deviation due to an error of approximate sensitivity equation. Figure 5.8 to Figure 5.10 present line loss, conversion loss, and total loss in case 1 during 24 hours. In case 1-B, 1-C, and 1-D, each loss was almost identical and it emphasizes that proposed cooperative control scheme can reduce total loss in the radial DC distribution system effectively. In addition, there was not any voltage violation for entire time interval.

Simulation results for case 1 are summarized in Table 5.6. It shows that total loss can be reduced effectively by proposed cooperative voltage control scheme. Generation power of DGs and terminal voltage of GCC was increased to minimize the total loss in the DC distribution system. Therefore, bus voltages in the DC distribution system were boosted and line loss was decreased. Conversion loss in DGs was increased due to generation power of DGs. However, there were larger

amount of decrease in conversion loss in GCC because required delivering power by GCC was decreased. As a result, 1.444 MWh of total loss, which is 25.717% of total loss in case 1-A, was decreased by proposed method during a day and it is equivalent to 2.159% of total load consumption during a day.

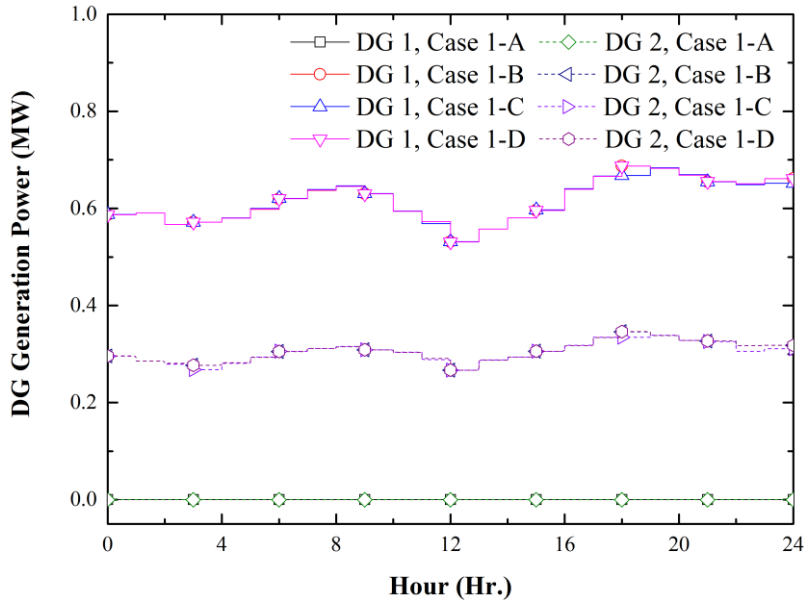

Figure 5.6. DG generation power in case 1

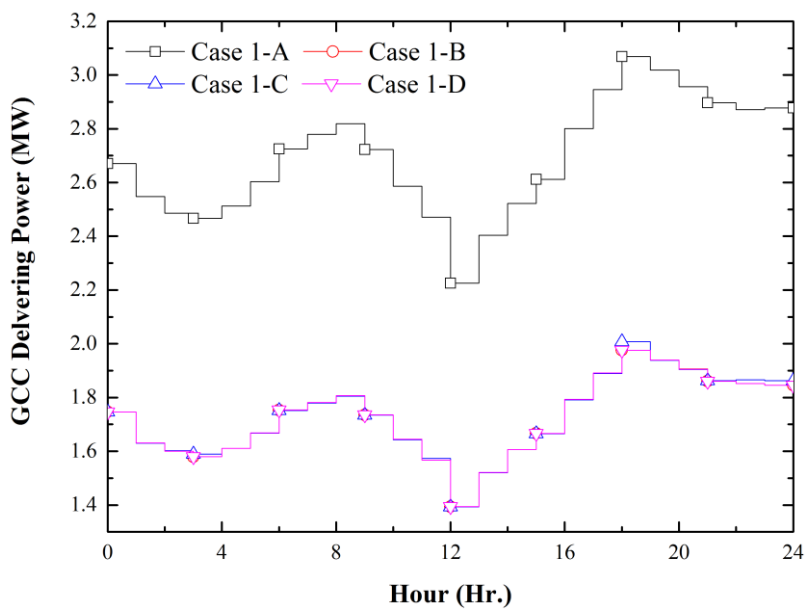

Figure 5.7. GCC delivering power in case 1

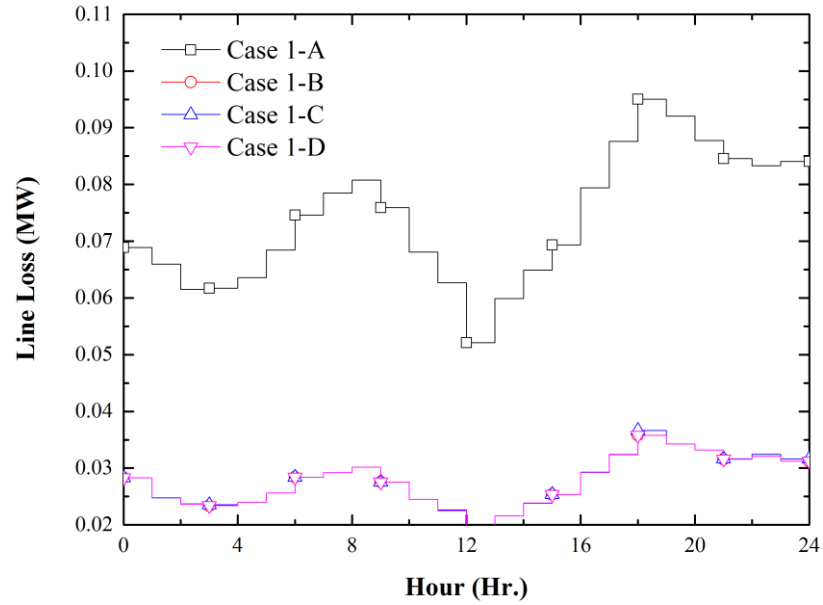

Figure 5.8. Line loss in case 1

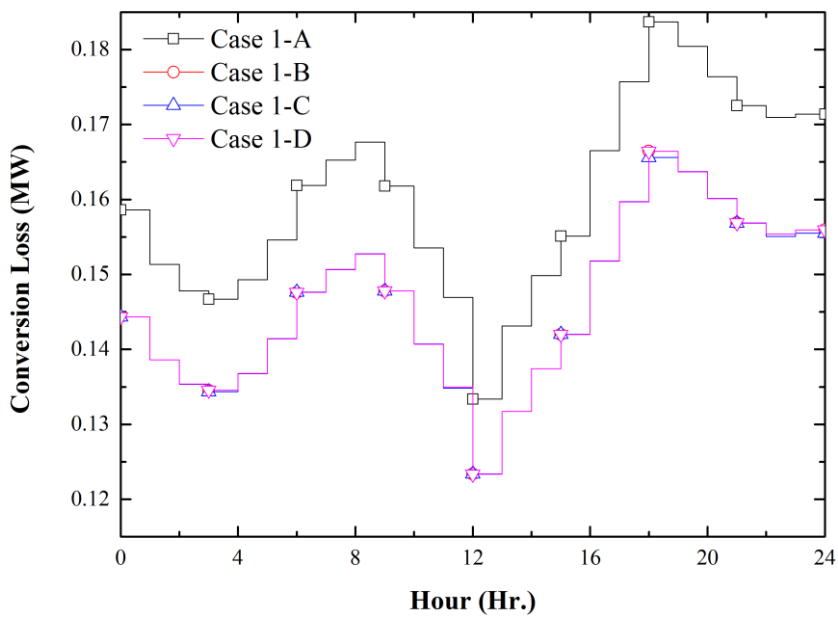

Figure 5.9. Conversion loss in case 1

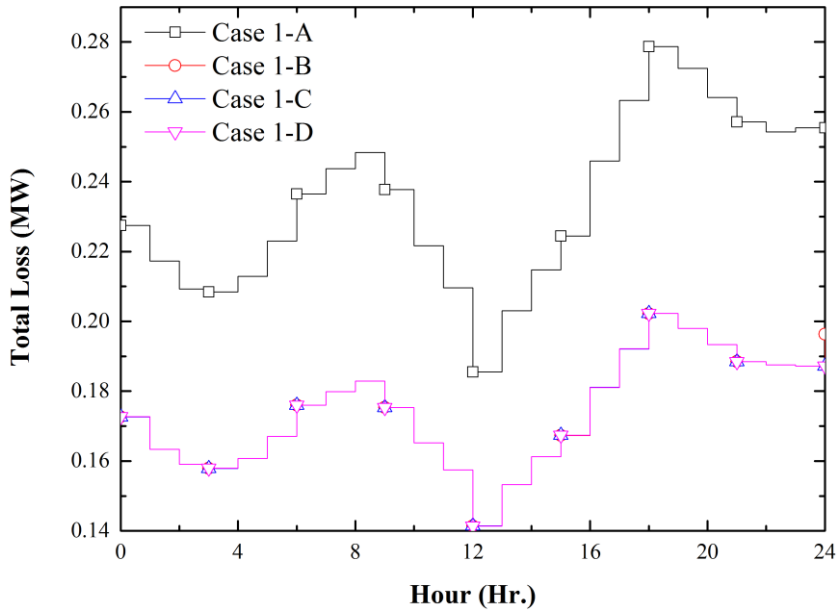

Figure 5.10. Total loss in case 1

Table 5.6. Summary of result for case 1

Case	1 - A	1 - B	1 - C	1 - D
Line Loss (MWh)	1.771	0.661	0.663	0.661
Conversion Loss in DGs (MWh)	0.338	1.241	1.237	1.241
Conversion Loss in GCC (MWh)	3.506	2.269	2.272	2.269
Total Loss (MWh)	5.615	4.171	4.171	4.171
Total Loss / Load (%)	8.396	6.237	6.237	6.237
Voltage Violation	X	X	X	X

Table 5.7. Simulation result: converter output power in case 1-B

Hour	DG 1 Generation Power (MWh)	DG 2 Generation Power (MWh)	GCC Delivering Power (MWh)
0	0.587	0.296	1.747
1	0.590	0.286	1.631
2	0.567	0.281	1.601
3	0.572	0.277	1.580
4	0.580	0.282	1.611
5	0.599	0.294	1.669
6	0.620	0.305	1.754
7	0.637	0.312	1.781
8	0.645	0.315	1.807
9	0.630	0.309	1.735
10	0.594	0.303	1.645
11	0.573	0.291	1.567
12	0.531	0.267	1.394
13	0.557	0.287	1.521
14	0.580	0.294	1.607
15	0.596	0.306	1.666
16	0.639	0.317	1.793
17	0.666	0.334	1.891
18	0.687	0.346	1.976
19	0.683	0.338	1.940
20	0.668	0.328	1.906
21	0.655	0.327	1.861
22	0.651	0.318	1.852
23	0.661	0.318	1.846
Sum	14.771	7.331	41.378

Table 5.8. Simulation result: converter output power in case 1-C

Hour	DG 1 Generation Power (MWh)	DG 2 Generation Power (MWh)	GCC Delivering Power (MWh)
0	0.588	0.296	1.746
1	0.591	0.286	1.630
2	0.567	0.279	1.603
3	0.572	0.268	1.589
4	0.581	0.281	1.611
5	0.600	0.294	1.667
6	0.621	0.306	1.752
7	0.639	0.312	1.780
8	0.647	0.316	1.805
9	0.631	0.309	1.735
10	0.595	0.304	1.643
11	0.569	0.289	1.573
12	0.532	0.267	1.393
13	0.558	0.288	1.520
14	0.581	0.294	1.606
15	0.597	0.306	1.665
16	0.641	0.318	1.791
17	0.667	0.335	1.889
18	0.668	0.335	2.007
19	0.684	0.339	1.938
20	0.670	0.328	1.904
21	0.655	0.326	1.863
22	0.649	0.306	1.866
23	0.652	0.311	1.863
Sum	14.751	7.291	41.440

Table 5.9. Simulation result: converter output power in case 1-D

Hour	DG 1 Generation Power (MWh)	DG 2 Generation Power (MWh)	GCC Delivering Power (MWh)
0	0.587	0.296	1.747
1	0.590	0.286	1.631
2	0.567	0.281	1.601
3	0.572	0.277	1.580
4	0.580	0.282	1.611
5	0.599	0.294	1.669
6	0.620	0.305	1.753
7	0.637	0.312	1.781
8	0.645	0.315	1.807
9	0.630	0.309	1.735
10	0.594	0.303	1.645
11	0.573	0.291	1.567
12	0.531	0.267	1.394
13	0.558	0.287	1.521
14	0.580	0.294	1.607
15	0.596	0.306	1.666
16	0.639	0.317	1.793
17	0.666	0.334	1.891
18	0.687	0.346	1.976
19	0.683	0.338	1.940
20	0.668	0.328	1.906
21	0.655	0.327	1.861
22	0.651	0.318	1.852
23	0.662	0.318	1.845
Sum	14.771	7.332	41.377

Table 5.10. Simulation result: loss in case 1-A

Hour	Line Loss (MWh)	Conversion Loss (MWh)	Total Loss (MWh)	Voltage Violation
0	6.889×10^{-2}	1.586×10^{-1}	2.275×10^{-1}	X
1	6.597×10^{-2}	1.513×10^{-1}	2.173×10^{-1}	X
2	6.151×10^{-2}	1.478×10^{-1}	2.093×10^{-1}	X
3	6.172×10^{-2}	1.467×10^{-1}	2.084×10^{-1}	X
4	6.359×10^{-2}	1.493×10^{-1}	2.129×10^{-1}	X
5	6.843×10^{-2}	1.546×10^{-1}	2.230×10^{-1}	X
6	7.463×10^{-2}	1.619×10^{-1}	2.365×10^{-1}	X
7	7.848×10^{-2}	1.652×10^{-1}	2.437×10^{-1}	X
8	8.075×10^{-2}	1.676×10^{-1}	2.484×10^{-1}	X
9	7.593×10^{-2}	1.618×10^{-1}	2.377×10^{-1}	X
10	6.811×10^{-2}	1.536×10^{-1}	2.217×10^{-1}	X
11	6.268×10^{-2}	1.469×10^{-1}	2.096×10^{-1}	X
12	5.212×10^{-2}	1.334×10^{-1}	1.855×10^{-1}	X
13	5.988×10^{-2}	1.431×10^{-1}	2.030×10^{-1}	X
14	6.490×10^{-2}	1.498×10^{-1}	2.147×10^{-1}	X
15	6.933×10^{-2}	1.551×10^{-1}	2.244×10^{-1}	X
16	7.940×10^{-2}	1.665×10^{-1}	2.459×10^{-1}	X
17	8.757×10^{-2}	1.757×10^{-1}	2.633×10^{-1}	X
18	9.501×10^{-2}	1.837×10^{-1}	2.787×10^{-1}	X
19	9.206×10^{-2}	1.804×10^{-1}	2.725×10^{-1}	X
20	8.773×10^{-2}	1.764×10^{-1}	2.641×10^{-1}	X
21	8.455×10^{-2}	1.725×10^{-1}	2.571×10^{-1}	X
22	8.329×10^{-2}	1.710×10^{-1}	2.543×10^{-1}	X
23	8.408×10^{-2}	1.714×10^{-1}	2.555×10^{-1}	X
Sum	1.771	3.844	5.615	-

Table 5.11. Simulation result: loss in case 1-B

Hour	Line Loss (MWh)	Conversion Loss (MWh)	Total Loss (MWh)	Voltage Violation
0	2.832×10^{-2}	1.443×10^{-1}	1.727×10^{-1}	X
1	2.479×10^{-2}	1.386×10^{-1}	1.634×10^{-1}	X
2	2.367×10^{-2}	1.354×10^{-1}	1.590×10^{-1}	X
3	2.339×10^{-2}	1.345×10^{-1}	1.579×10^{-1}	X
4	2.399×10^{-2}	1.368×10^{-1}	1.608×10^{-1}	X
5	2.564×10^{-2}	1.414×10^{-1}	1.670×10^{-1}	X
6	2.842×10^{-2}	1.476×10^{-1}	1.760×10^{-1}	X
7	2.922×10^{-2}	1.506×10^{-1}	1.799×10^{-1}	X
8	3.018×10^{-2}	1.527×10^{-1}	1.829×10^{-1}	X
9	2.755×10^{-2}	1.478×10^{-1}	1.753×10^{-1}	X
10	2.452×10^{-2}	1.407×10^{-1}	1.652×10^{-1}	X
11	2.250×10^{-2}	1.350×10^{-1}	1.575×10^{-1}	X
12	1.805×10^{-2}	1.234×10^{-1}	1.414×10^{-1}	X
13	2.156×10^{-2}	1.317×10^{-1}	1.533×10^{-1}	X
14	2.384×10^{-2}	1.374×10^{-1}	1.613×10^{-1}	X
15	2.537×10^{-2}	1.420×10^{-1}	1.674×10^{-1}	X
16	2.930×10^{-2}	1.518×10^{-1}	1.811×10^{-1}	X
17	3.244×10^{-2}	1.597×10^{-1}	1.921×10^{-1}	X
18	3.580×10^{-2}	1.664×10^{-1}	2.022×10^{-1}	X
19	3.426×10^{-2}	1.637×10^{-1}	1.979×10^{-1}	X
20	3.323×10^{-2}	1.601×10^{-1}	1.933×10^{-1}	X
21	3.158×10^{-2}	1.569×10^{-1}	1.885×10^{-1}	X
22	3.211×10^{-2}	1.554×10^{-1}	1.875×10^{-1}	X
23	3.122×10^{-2}	1.559×10^{-1}	1.872×10^{-1}	X
Sum	6.610×10^{-1}	3.510	4.171	-

Table 5.12. Simulation result: loss in case 1-C

Hour	Line Loss (MWh)	Conversion Loss (MWh)	Total Loss (MWh)	Voltage Violation
0	2.830×10^{-2}	1.444×10^{-1}	1.727×10^{-1}	X
1	2.478×10^{-2}	1.386×10^{-1}	1.634×10^{-1}	X
2	2.370×10^{-2}	1.353×10^{-1}	1.590×10^{-1}	X
3	2.357×10^{-2}	1.343×10^{-1}	1.579×10^{-1}	X
4	2.399×10^{-2}	1.368×10^{-1}	1.608×10^{-1}	X
5	2.563×10^{-2}	1.414×10^{-1}	1.671×10^{-1}	X
6	2.838×10^{-2}	1.476×10^{-1}	1.760×10^{-1}	X
7	2.919×10^{-2}	1.507×10^{-1}	1.799×10^{-1}	X
8	3.015×10^{-2}	1.528×10^{-1}	1.829×10^{-1}	X
9	2.754×10^{-2}	1.478×10^{-1}	1.753×10^{-1}	X
10	2.450×10^{-2}	1.407×10^{-1}	1.652×10^{-1}	X
11	2.264×10^{-2}	1.348×10^{-1}	1.575×10^{-1}	X
12	1.805×10^{-2}	1.234×10^{-1}	1.414×10^{-1}	X
13	2.156×10^{-2}	1.317×10^{-1}	1.533×10^{-1}	X
14	2.383×10^{-2}	1.374×10^{-1}	1.613×10^{-1}	X
15	2.537×10^{-2}	1.420×10^{-1}	1.674×10^{-1}	X
16	2.928×10^{-2}	1.518×10^{-1}	1.811×10^{-1}	X
17	3.240×10^{-2}	1.597×10^{-1}	1.921×10^{-1}	X
18	3.666×10^{-2}	1.656×10^{-1}	2.023×10^{-1}	X
19	3.425×10^{-2}	1.637×10^{-1}	1.980×10^{-1}	X
20	3.320×10^{-2}	1.602×10^{-1}	1.933×10^{-1}	X
21	3.162×10^{-2}	1.568×10^{-1}	1.885×10^{-1}	X
22	3.243×10^{-2}	1.551×10^{-1}	1.875×10^{-1}	X
23	3.164×10^{-2}	1.555×10^{-1}	1.872×10^{-1}	X
Sum	6.627×10^{-1}	3.508	4.171	-

Table 5.13. Simulation result: loss in case 1-D

Hour	Line Loss (MWh)	Conversion Loss (MWh)	Total Loss (MWh)	Voltage Violation
0	2.832×10^{-2}	1.443×10^{-1}	1.727×10^{-1}	X
1	2.480×10^{-2}	1.386×10^{-1}	1.634×10^{-1}	X
2	2.367×10^{-2}	1.354×10^{-1}	1.590×10^{-1}	X
3	2.340×10^{-2}	1.345×10^{-1}	1.579×10^{-1}	X
4	2.399×10^{-2}	1.368×10^{-1}	1.608×10^{-1}	X
5	2.565×10^{-2}	1.414×10^{-1}	1.671×10^{-1}	X
6	2.843×10^{-2}	1.476×10^{-1}	1.760×10^{-1}	X
7	2.923×10^{-2}	1.506×10^{-1}	1.799×10^{-1}	X
8	3.019×10^{-2}	1.527×10^{-1}	1.829×10^{-1}	X
9	2.756×10^{-2}	1.478×10^{-1}	1.754×10^{-1}	X
10	2.452×10^{-2}	1.407×10^{-1}	1.652×10^{-1}	X
11	2.251×10^{-2}	1.350×10^{-1}	1.575×10^{-1}	X
12	1.805×10^{-2}	1.234×10^{-1}	1.414×10^{-1}	X
13	2.156×10^{-2}	1.317×10^{-1}	1.533×10^{-1}	X
14	2.384×10^{-2}	1.374×10^{-1}	1.613×10^{-1}	X
15	2.538×10^{-2}	1.420×10^{-1}	1.674×10^{-1}	X
16	2.931×10^{-2}	1.518×10^{-1}	1.811×10^{-1}	X
17	3.246×10^{-2}	1.597×10^{-1}	1.921×10^{-1}	X
18	3.582×10^{-2}	1.664×10^{-1}	2.023×10^{-1}	X
19	3.428×10^{-2}	1.637×10^{-1}	1.980×10^{-1}	X
20	3.324×10^{-2}	1.601×10^{-1}	1.934×10^{-1}	X
21	3.160×10^{-2}	1.569×10^{-1}	1.885×10^{-1}	X
22	3.213×10^{-2}	1.554×10^{-1}	1.875×10^{-1}	X
23	3.123×10^{-2}	1.559×10^{-1}	1.872×10^{-1}	X
Sum	6.612×10^{-1}	3.510	4.171	-

5.2.2. Case 2: when load and generation of RES are varied

In case 2, load and RES generation pattern are modified to reflect actual operating condition of a DC distribution system during a day. It is assumed that average load consumption and PV generation power is changed along average pattern data shown in Figure 5.2 and Figure 5.3. Modified average patterns are presented in Figure 5.11 and Figure 5.12. In addition, unexpected variations in load consumption and PV generation are considered. Load consumption power is varied within $\pm 15\%$ range of average load consumption every 60 seconds. Partially cloudy weather is considered and there is random variation in PV generation power every 60 seconds, which is varied 0 to -30% range of average PV generation power. Figure 5.13 and Figure 5.14 displays actual pattern data between 14:00 and 15:00 in PSCAD simulation. Condition in case 2 is identical to those in case 1 presented in Table 5.5.

Figure 5.15 and Figure 5.16 displays actual DG generation power and GCC delivering power in case 2. There was a difference between an optimal scheduled result and actual converter terminal power in case 2-B and 2-D, which is the case that proposed cooperative control scheme is activated, because there were variations in load consumption and generation of RES. Figure 5.17 to Figure 5.19 presents each loss during a day in case 2.

The result of case 2 is summarized in Table 5.14. About 25.861% of total loss was decreased by proposed method. In case 2-B and 2-C, difference of total loss is only 0.002 MWh and it is 0.003% of total load during a day. Result of case 2-B and 2-D emphasizes that cooperative voltage control scheme can reduce total loss effectively while regulating bus voltages without an optimal scheduling process. In addition, it is indicated that voltage violation occurred when proposed control scheme is not utilized. In case 2-A, lower voltage violation occurred between 18:00 and 19:00 because large load consumption and decreased PV generation make bus voltages lower. In addition, in case 2-C, there were upper voltage violations during

a day when only optimal scheduled reference is utilized.

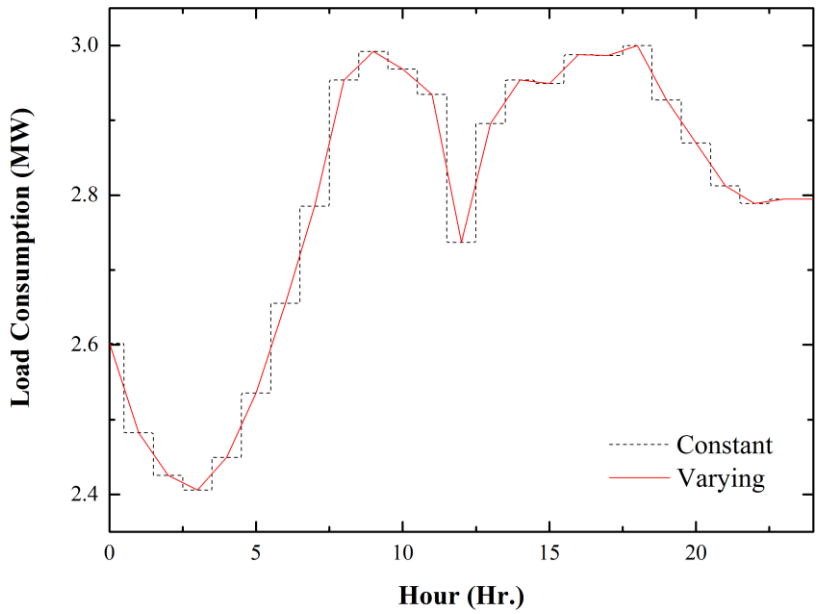

Figure 5.11. Average load consumption in case 2

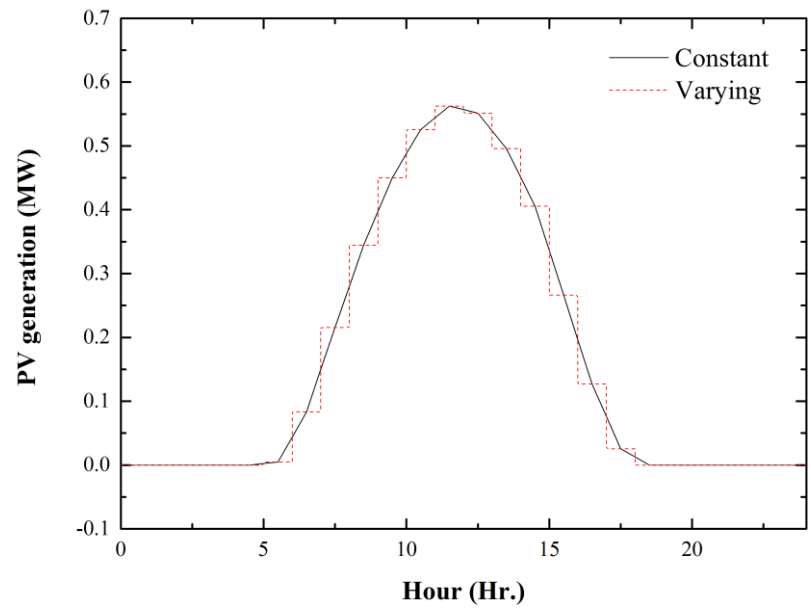

Figure 5.12. Average PV generation power in case 2

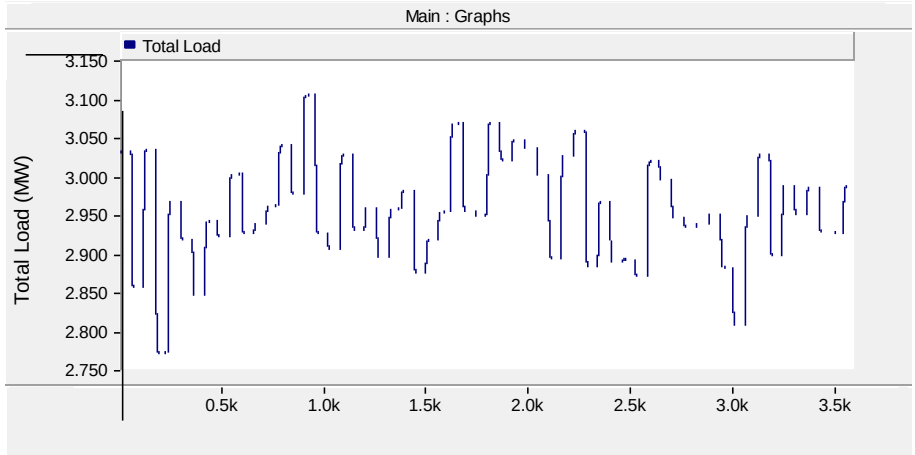

Figure 5.13. Total load power between 14:00 and 15:00

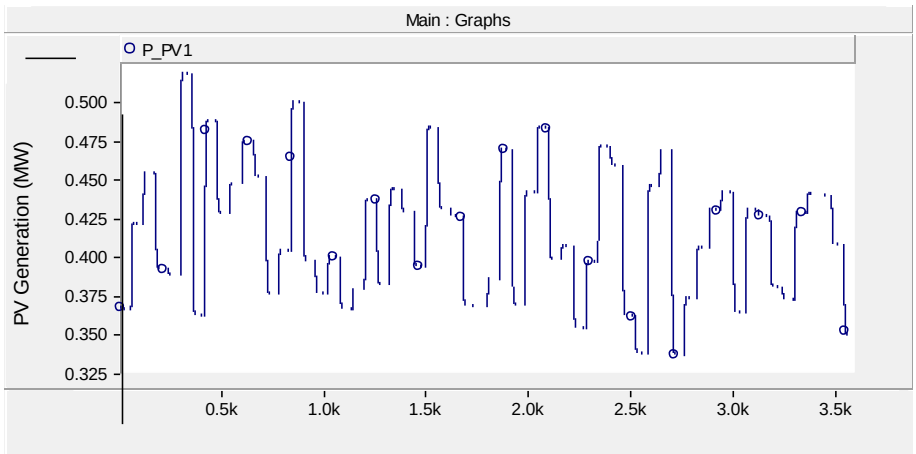

Figure 5.14. PV generation power between 14:00 and 15:00

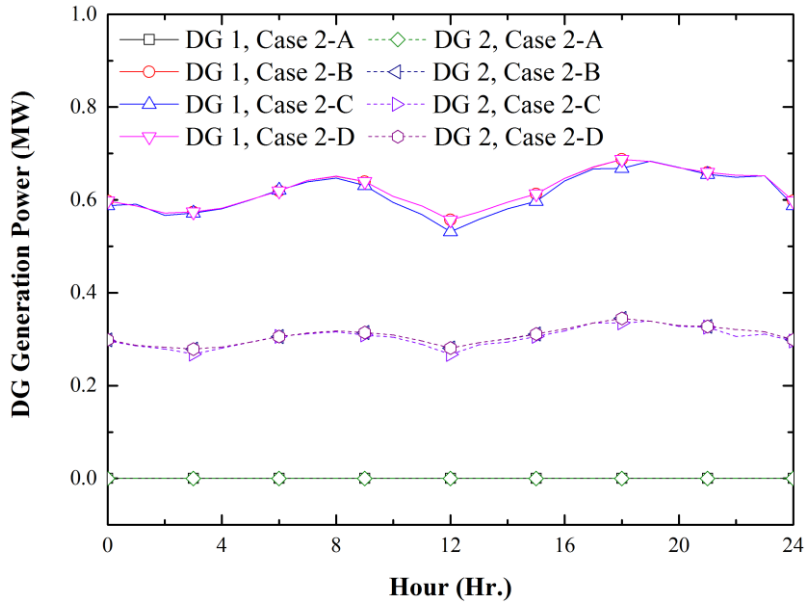

Figure 5.15. DG generation power in case 2

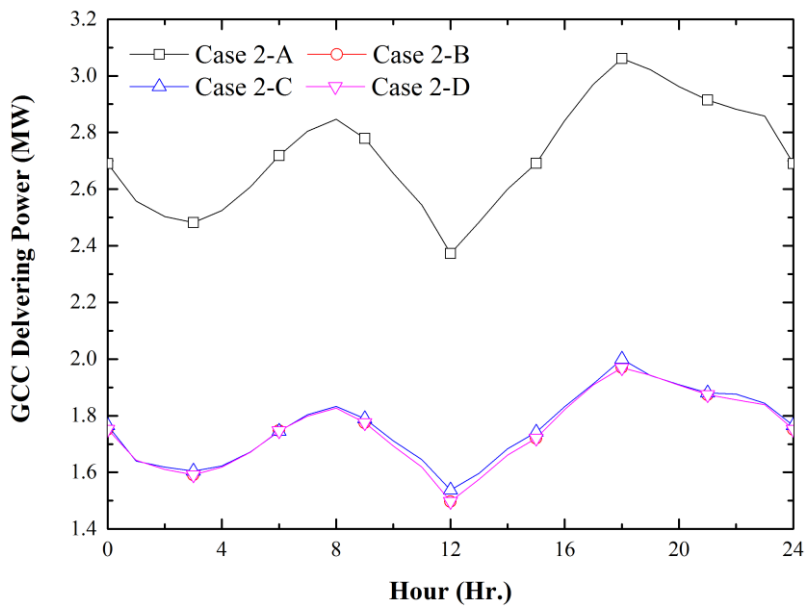

Figure 5.16. GCC delivering power in case 2

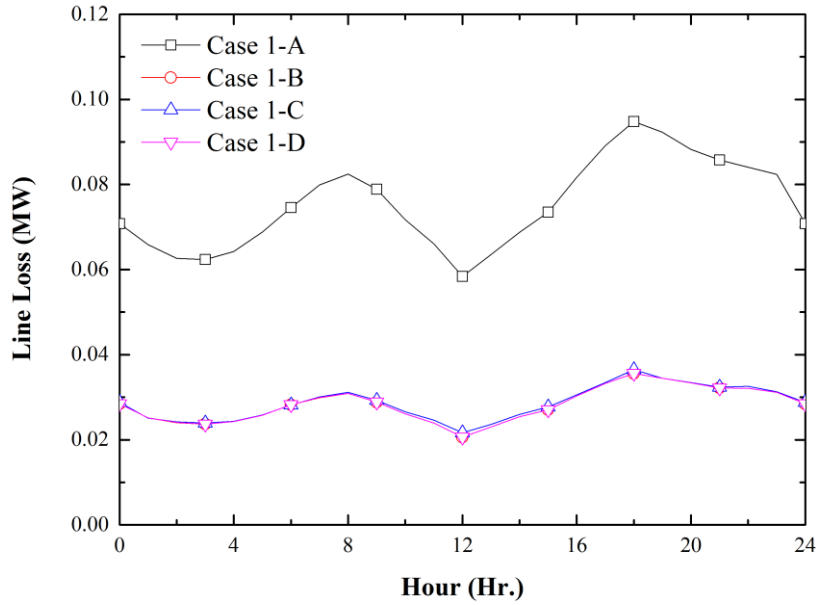

Figure 5.17. Line loss in case 2

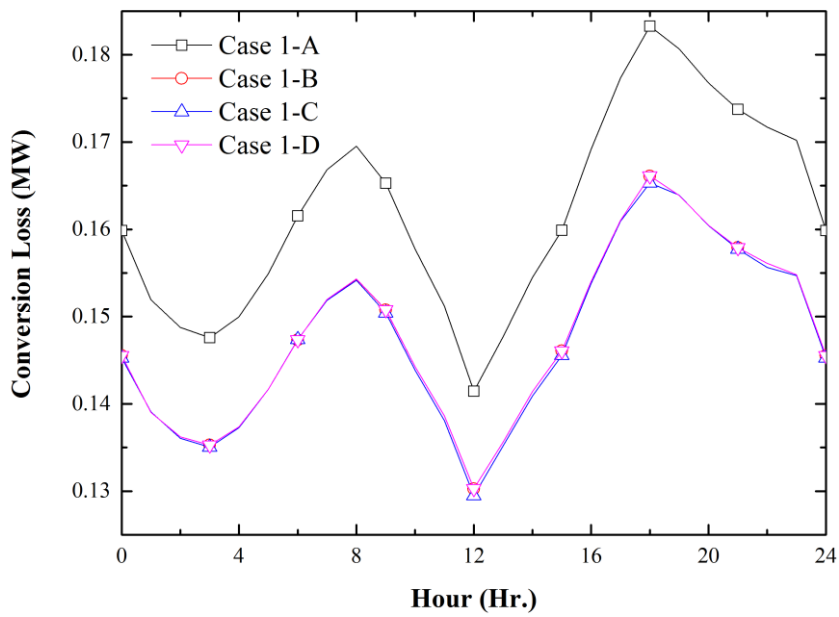

Figure 5.18. Conversion loss in case 2

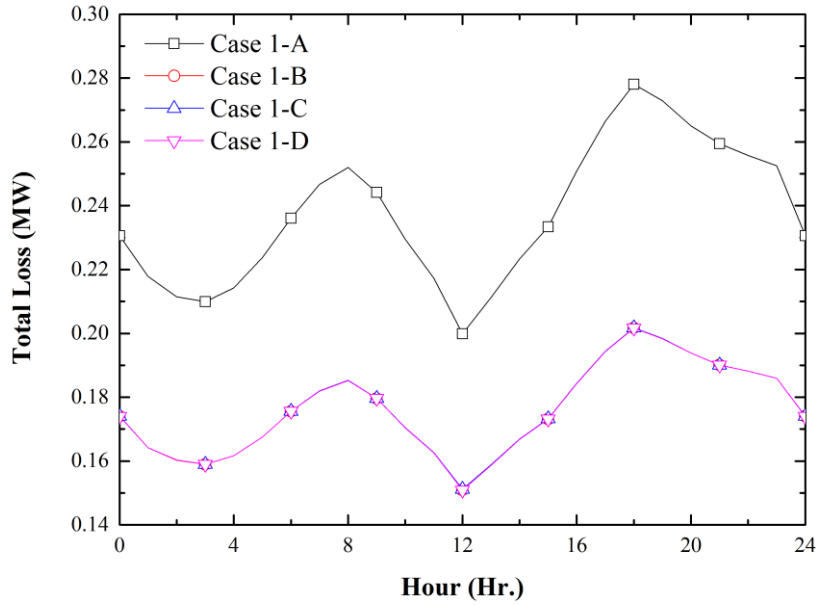

Figure 5.19. Total loss in case 2

Table 5.14. Summary of result for case 2

Case	2 - A	2 - B	2 - C	2 - D
Line Loss (MWh)	1.811	0.678	0.686	0.678
Conversion Loss in DGs (MWh)	0.338	1.257	1.237	1.257
Conversion Loss in GCC (MWh)	3.553	2.293	2.307	2.293
Total Loss (MWh)	5.702	4.228	4.230	4.228
Total Loss / Load (%)	8.507	6.307	6.310	6.308
Voltage Violation	O (Lower)	X	O (Upper)	X

Table 5.15. Simulation result: converter output power in case 2-B

Hour	DG 1 Generation Power (MWh)	DG 2 Generation Power (MWh)	GCC Delivering Power (MWh)
0	0.598	0.299	1.752
1	0.587	0.287	1.643
2	0.572	0.283	1.610
3	0.574	0.279	1.591
4	0.582	0.283	1.618
5	0.600	0.293	1.672
6	0.619	0.306	1.747
7	0.642	0.313	1.799
8	0.651	0.318	1.827
9	0.640	0.314	1.775
10	0.607	0.309	1.694
11	0.587	0.296	1.619
12	0.557	0.281	1.497
13	0.574	0.292	1.575
14	0.595	0.301	1.661
15	0.613	0.311	1.720
16	0.646	0.322	1.822
17	0.671	0.335	1.909
18	0.687	0.345	1.970
19	0.683	0.339	1.943
20	0.670	0.329	1.908
21	0.659	0.328	1.874
22	0.653	0.321	1.856
23	0.652	0.316	1.839
Sum	14.921	7.399	41.921

Table 5.16. Simulation result: converter output power in case 2-C

Hour	DG 1 Generation Power (MWh)	DG 2 Generation Power (MWh)	GCC Delivering Power (MWh)
0	0.588	0.296	1.765
1	0.591	0.286	1.640
2	0.567	0.279	1.619
3	0.572	0.268	1.604
4	0.581	0.281	1.622
5	0.600	0.294	1.672
6	0.621	0.306	1.745
7	0.639	0.312	1.804
8	0.647	0.316	1.833
9	0.631	0.309	1.790
10	0.595	0.304	1.712
11	0.569	0.289	1.645
12	0.532	0.267	1.537
13	0.558	0.288	1.597
14	0.581	0.294	1.683
15	0.597	0.306	1.742
16	0.641	0.318	1.832
17	0.667	0.335	1.913
18	0.668	0.335	2.000
19	0.684	0.339	1.942
20	0.670	0.328	1.909
21	0.655	0.326	1.880
22	0.649	0.306	1.877
23	0.652	0.311	1.844
Sum	14.751	7.291	42.207

Table 5.17. Simulation result: converter output power in case 2-D

Hour	DG 1 Generation Power (MWh)	DG 2 Generation Power (MWh)	GCC Delivering Power (MWh)
0	0.598	0.299	1.752
1	0.587	0.287	1.643
2	0.572	0.283	1.610
3	0.574	0.279	1.591
4	0.582	0.283	1.618
5	0.600	0.293	1.672
6	0.619	0.306	1.747
7	0.642	0.313	1.799
8	0.651	0.318	1.827
9	0.640	0.314	1.775
10	0.607	0.309	1.694
11	0.587	0.296	1.619
12	0.557	0.281	1.497
13	0.574	0.292	1.575
14	0.595	0.301	1.661
15	0.613	0.311	1.720
16	0.646	0.322	1.822
17	0.671	0.335	1.909
18	0.687	0.345	1.970
19	0.683	0.339	1.943
20	0.670	0.329	1.908
21	0.659	0.328	1.874
22	0.654	0.321	1.856
23	0.652	0.316	1.839
Sum	14.921	7.399	41.920

Table 5.18. Simulation result: loss in case 2-A

Hour	Line Loss (MWh)	Conversion Loss (MWh)	Total Loss (MWh)	Voltage Violation
0	7.075×10^{-2}	1.599×10^{-1}	2.306×10^{-1}	X
1	6.589×10^{-2}	1.519×10^{-1}	2.178×10^{-1}	X
2	6.265×10^{-2}	1.488×10^{-1}	2.114×10^{-1}	X
3	6.236×10^{-2}	1.476×10^{-1}	2.099×10^{-1}	X
4	6.426×10^{-2}	1.500×10^{-1}	2.142×10^{-1}	X
5	6.881×10^{-2}	1.549×10^{-1}	2.238×10^{-1}	X
6	7.454×10^{-2}	1.615×10^{-1}	2.361×10^{-1}	X
7	7.988×10^{-2}	1.668×10^{-1}	2.467×10^{-1}	X
8	8.248×10^{-2}	1.695×10^{-1}	2.520×10^{-1}	X
9	7.886×10^{-2}	1.653×10^{-1}	2.441×10^{-1}	X
10	7.173×10^{-2}	1.578×10^{-1}	2.295×10^{-1}	X
11	6.610×10^{-2}	1.512×10^{-1}	2.173×10^{-1}	X
12	5.840×10^{-2}	1.415×10^{-1}	1.999×10^{-1}	X
13	6.354×10^{-2}	1.477×10^{-1}	2.112×10^{-1}	X
14	6.878×10^{-2}	1.545×10^{-1}	2.233×10^{-1}	X
15	7.351×10^{-2}	1.599×10^{-1}	2.334×10^{-1}	X
16	8.166×10^{-2}	1.692×10^{-1}	2.508×10^{-1}	X
17	8.914×10^{-2}	1.774×10^{-1}	2.665×10^{-1}	X
18	9.476×10^{-2}	1.833×10^{-1}	2.780×10^{-1}	O(Lower)
19	9.226×10^{-2}	1.807×10^{-1}	2.730×10^{-1}	X
20	8.826×10^{-2}	1.768×10^{-1}	2.650×10^{-1}	X
21	8.572×10^{-2}	1.737×10^{-1}	2.595×10^{-1}	X
22	8.407×10^{-2}	1.717×10^{-1}	2.558×10^{-1}	X
23	8.239×10^{-2}	1.702×10^{-1}	2.526×10^{-1}	X
Sum	1.811	3.892	5.702	-

Table 5.19. Simulation result: loss in case 2-B

Hour	Line Loss (MWh)	Conversion Loss (MWh)	Total Loss (MWh)	Voltage Violation
0	2.845×10^{-2}	1.455×10^{-1}	1.740×10^{-1}	X
1	2.513×10^{-2}	1.390×10^{-1}	1.642×10^{-1}	X
2	2.404×10^{-2}	1.362×10^{-1}	1.603×10^{-1}	X
3	2.368×10^{-2}	1.353×10^{-1}	1.590×10^{-1}	X
4	2.427×10^{-2}	1.374×10^{-1}	1.616×10^{-1}	X
5	2.578×10^{-2}	1.417×10^{-1}	1.675×10^{-1}	X
6	2.822×10^{-2}	1.473×10^{-1}	1.756×10^{-1}	X
7	2.990×10^{-2}	1.520×10^{-1}	1.819×10^{-1}	X
8	3.088×10^{-2}	1.543×10^{-1}	1.852×10^{-1}	X
9	2.884×10^{-2}	1.508×10^{-1}	1.796×10^{-1}	X
10	2.608×10^{-2}	1.443×10^{-1}	1.704×10^{-1}	X
11	2.393×10^{-2}	1.386×10^{-1}	1.626×10^{-1}	X
12	2.061×10^{-2}	1.303×10^{-1}	1.509×10^{-1}	X
13	2.299×10^{-2}	1.356×10^{-1}	1.586×10^{-1}	X
14	2.539×10^{-2}	1.414×10^{-1}	1.668×10^{-1}	X
15	2.707×10^{-2}	1.461×10^{-1}	1.731×10^{-1}	X
16	3.025×10^{-2}	1.540×10^{-1}	1.843×10^{-1}	X
17	3.326×10^{-2}	1.610×10^{-1}	1.943×10^{-1}	X
18	3.559×10^{-2}	1.661×10^{-1}	2.017×10^{-1}	X
19	3.444×10^{-2}	1.639×10^{-1}	1.983×10^{-1}	X
20	3.336×10^{-2}	1.605×10^{-1}	1.938×10^{-1}	X
21	3.218×10^{-2}	1.579×10^{-1}	1.901×10^{-1}	X
22	3.207×10^{-2}	1.561×10^{-1}	1.882×10^{-1}	X
23	3.114×10^{-2}	1.548×10^{-1}	1.859×10^{-1}	X
Sum	0.678	3.550	4.228	-

Table 5.20. Simulation result: loss in case 2-C

Hour	Line Loss (MWh)	Conversion Loss (MWh)	Total Loss (MWh)	Voltage Violation
0	2.879×10^{-2}	1.453×10^{-1}	1.741×10^{-1}	O(Upper)
1	2.510×10^{-2}	1.391×10^{-1}	1.642×10^{-1}	O(Upper)
2	2.425×10^{-2}	1.361×10^{-1}	1.603×10^{-1}	O(Upper)
3	2.397×10^{-2}	1.350×10^{-1}	1.590×10^{-1}	O(Upper)
4	2.437×10^{-2}	1.373×10^{-1}	1.617×10^{-1}	O(Upper)
5	2.584×10^{-2}	1.417×10^{-1}	1.675×10^{-1}	O(Upper)
6	2.821×10^{-2}	1.474×10^{-1}	1.756×10^{-1}	O(Upper)
7	3.008×10^{-2}	1.519×10^{-1}	1.819×10^{-1}	O(Upper)
8	3.113×10^{-2}	1.542×10^{-1}	1.853×10^{-1}	O(Upper)
9	2.927×10^{-2}	1.504×10^{-1}	1.797×10^{-1}	O(Upper)
10	2.660×10^{-2}	1.439×10^{-1}	1.705×10^{-1}	O(Upper)
11	2.462×10^{-2}	1.381×10^{-1}	1.627×10^{-1}	O(Upper)
12	2.163×10^{-2}	1.295×10^{-1}	1.511×10^{-1}	O(Upper)
13	2.360×10^{-2}	1.352×10^{-1}	1.588×10^{-1}	O(Upper)
14	2.599×10^{-2}	1.409×10^{-1}	1.669×10^{-1}	O(Upper)
15	2.770×10^{-2}	1.456×10^{-1}	1.733×10^{-1}	O(Upper)
16	3.058×10^{-2}	1.538×10^{-1}	1.844×10^{-1}	O(Upper)
17	3.343×10^{-2}	1.609×10^{-1}	1.944×10^{-1}	O(Upper)
18	3.646×10^{-2}	1.653×10^{-1}	2.018×10^{-1}	O(Upper)
19	3.447×10^{-2}	1.639×10^{-1}	1.984×10^{-1}	O(Upper)
20	3.343×10^{-2}	1.604×10^{-1}	1.939×10^{-1}	O(Upper)
21	3.238×10^{-2}	1.577×10^{-1}	1.901×10^{-1}	O(Upper)
22	3.259×10^{-2}	1.556×10^{-1}	1.882×10^{-1}	O(Upper)
23	3.127×10^{-2}	1.547×10^{-1}	1.860×10^{-1}	O(Upper)
Sum	0.686	3.544	4.230	-

Table 5.21. Simulation result: loss in case 2-D

Hour	Line Loss (MWh)	Conversion Loss (MWh)	Total Loss (MWh)	Voltage Violation
0	2.846×10^{-2}	1.455×10^{-1}	1.740×10^{-1}	X
1	2.514×10^{-2}	1.390×10^{-1}	1.642×10^{-1}	X
2	2.405×10^{-2}	1.362×10^{-1}	1.603×10^{-1}	X
3	2.369×10^{-2}	1.353×10^{-1}	1.590×10^{-1}	X
4	2.427×10^{-2}	1.374×10^{-1}	1.616×10^{-1}	X
5	2.579×10^{-2}	1.417×10^{-1}	1.675×10^{-1}	X
6	2.823×10^{-2}	1.473×10^{-1}	1.756×10^{-1}	X
7	2.991×10^{-2}	1.520×10^{-1}	1.819×10^{-1}	X
8	3.089×10^{-2}	1.543×10^{-1}	1.852×10^{-1}	X
9	2.885×10^{-2}	1.508×10^{-1}	1.796×10^{-1}	X
10	2.608×10^{-2}	1.443×10^{-1}	1.704×10^{-1}	X
11	2.394×10^{-2}	1.386×10^{-1}	1.626×10^{-1}	X
12	2.062×10^{-2}	1.303×10^{-1}	1.509×10^{-1}	X
13	2.299×10^{-2}	1.356×10^{-1}	1.586×10^{-1}	X
14	2.540×10^{-2}	1.414×10^{-1}	1.668×10^{-1}	X
15	2.707×10^{-2}	1.461×10^{-1}	1.731×10^{-1}	X
16	3.025×10^{-2}	1.540×10^{-1}	1.843×10^{-1}	X
17	3.327×10^{-2}	1.610×10^{-1}	1.943×10^{-1}	X
18	3.560×10^{-2}	1.661×10^{-1}	2.017×10^{-1}	X
19	3.446×10^{-2}	1.639×10^{-1}	1.984×10^{-1}	X
20	3.337×10^{-2}	1.605×10^{-1}	1.938×10^{-1}	X
21	3.219×10^{-2}	1.579×10^{-1}	1.901×10^{-1}	X
22	3.207×10^{-2}	1.561×10^{-1}	1.882×10^{-1}	X
23	3.115×10^{-2}	1.548×10^{-1}	1.860×10^{-1}	X
Sum	0.678	3.550	4.228	-

Simulation result of Case 2-B and 2-C are compared are displayed in Figure 5.20 to Figure 5.26 to analyze the result in case 2 and results shows response between 14:00 and 15:00. Average total load was 2.953 MW and average PV generation power was 0.496 at this time interval. However net load consumption in DC distribution system, which means the value subtracted PV generation power from actual load, was decreased at 65 seconds and 180 seconds. It causes an increase in bus voltage and Figure 5.21 shows that upper voltage violation was occurred in case 2-C. Figure 5.22 (a) shows entire bus voltage was increased within its limit to reduce total loss by proposed method. At this moment in 2-B, GCC became a candidate for voltage regulation and DGs participate in loss reduction control only. Therefore, reference of GCC was limited by proposed method to regulate highest bus voltage and references of DGs were determined to minimize total loss. Consequently, total loss sensitivities of DGs were kept to zero as shown in Figure 5.26 whereas GCC had negative total loss sensitivity. Total loss in case 2-B was slight smaller than case 2-C while entire bus voltage is kept within suitable range.

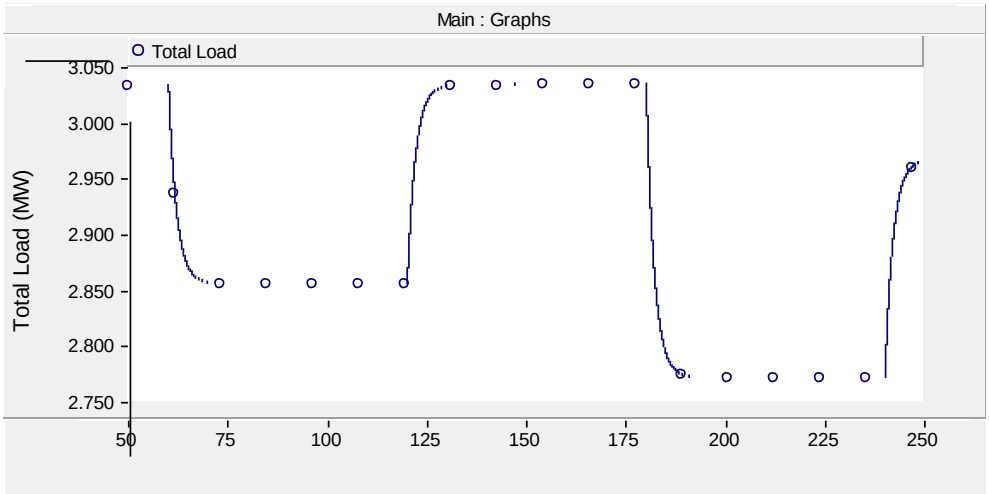

(a) Total load consumption

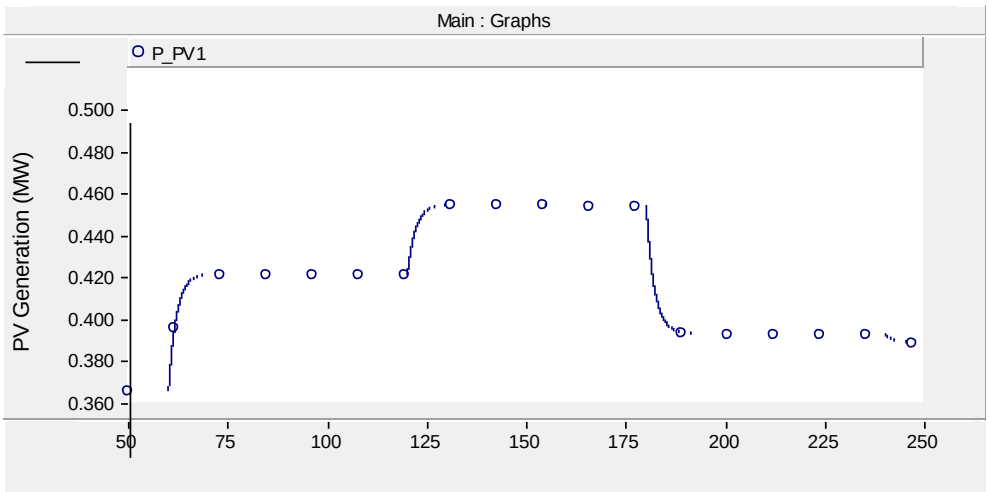

(b) PV generation power

Figure 5.20. Actual load and PV generation power between 14:00 and 15:00

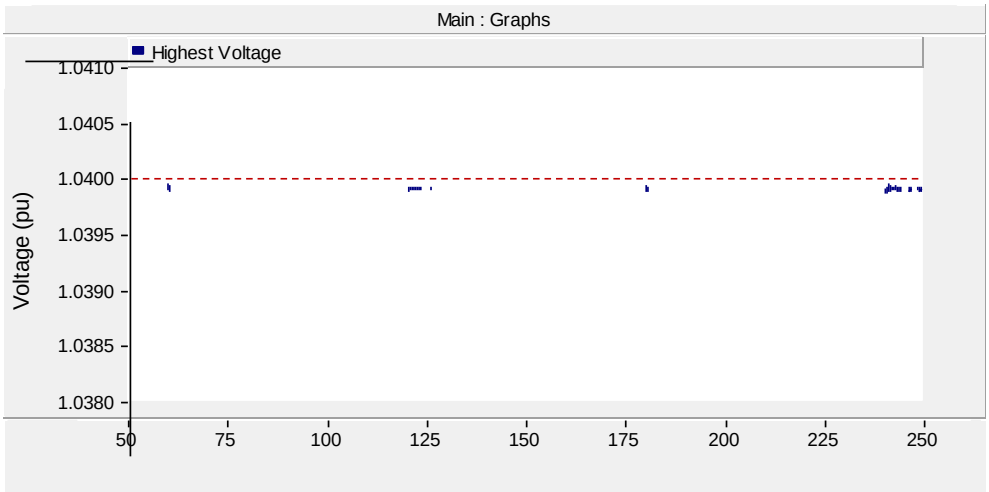

(a) Case 2-B

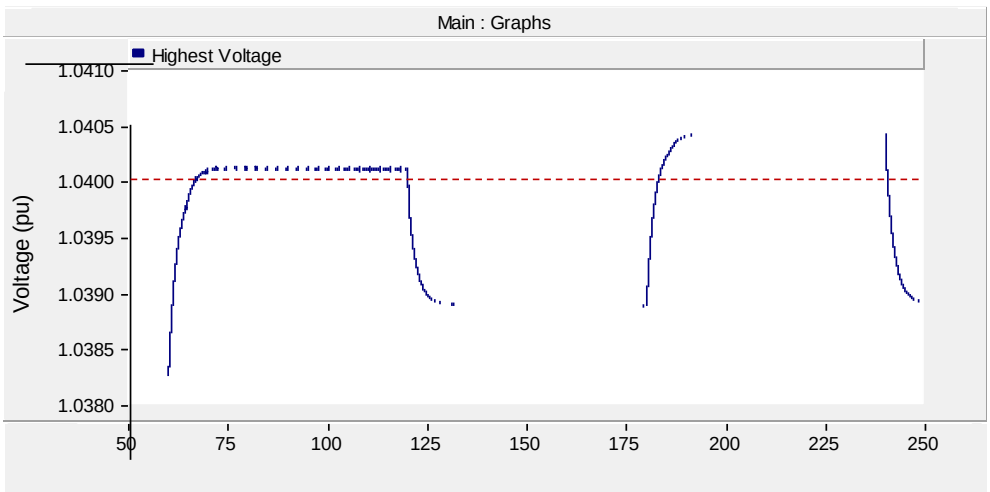

(b) Case 2-C

Figure 5.21. Simulation results: highest bus voltage in case 2

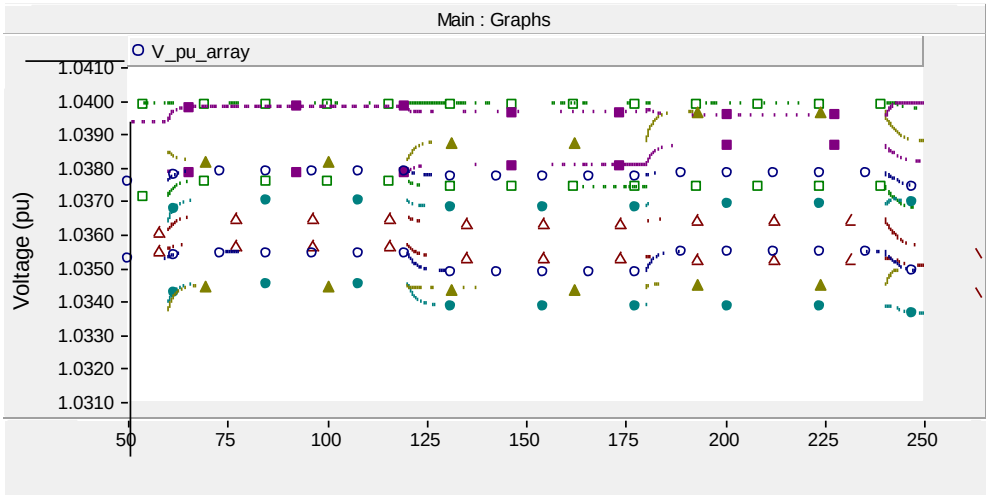

(a) Case 2-B

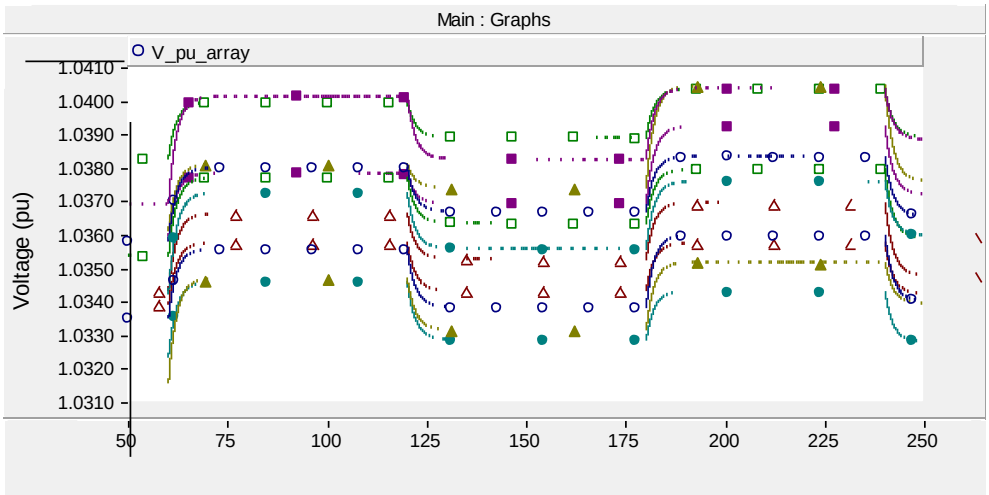

(b) Case 2-C

Figure 5.22. Simulation results: bus voltages in case 2

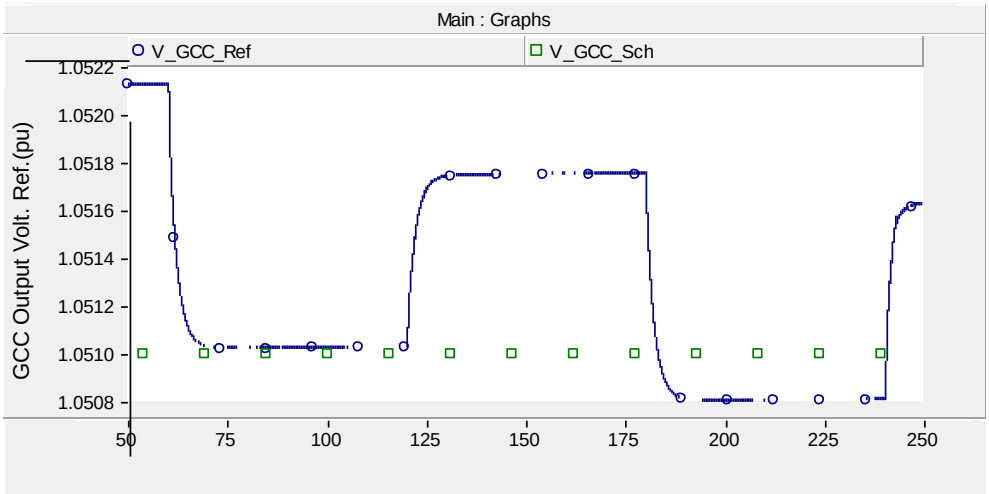

(a) Case 2-B

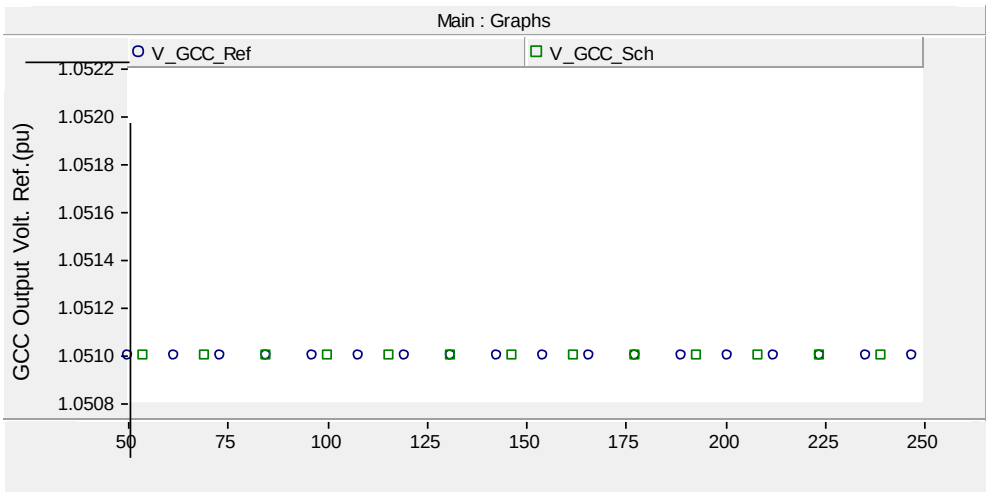

(a) Case 2-C

Figure 5.23. Simulation results: GCC output voltage reference

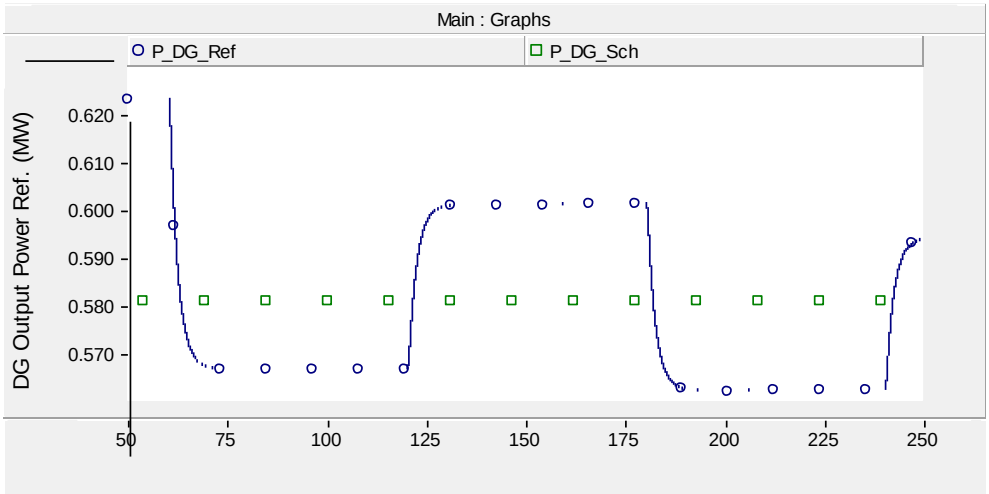

(a) Case 2-B

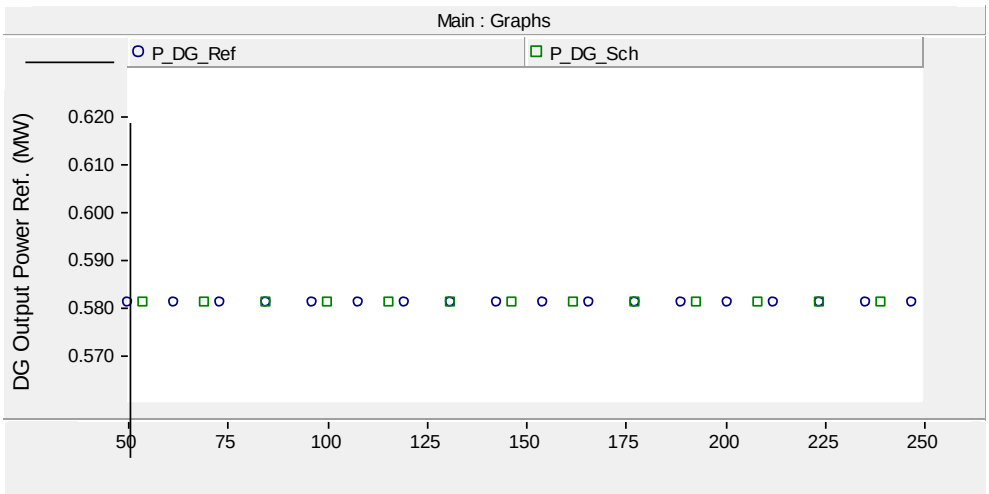

(b) Case 2-C

Figure 5.24. Simulation results: output power reference of DG 1

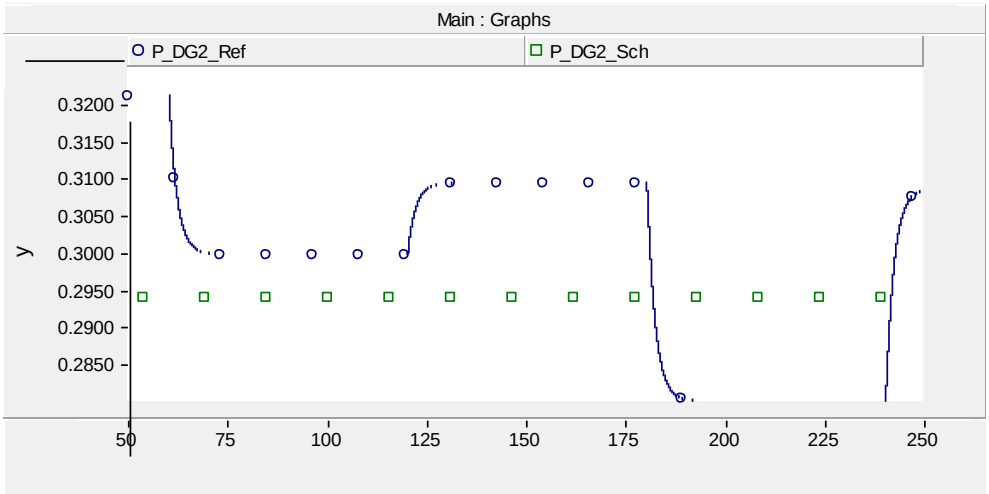

(a) Case 2-B

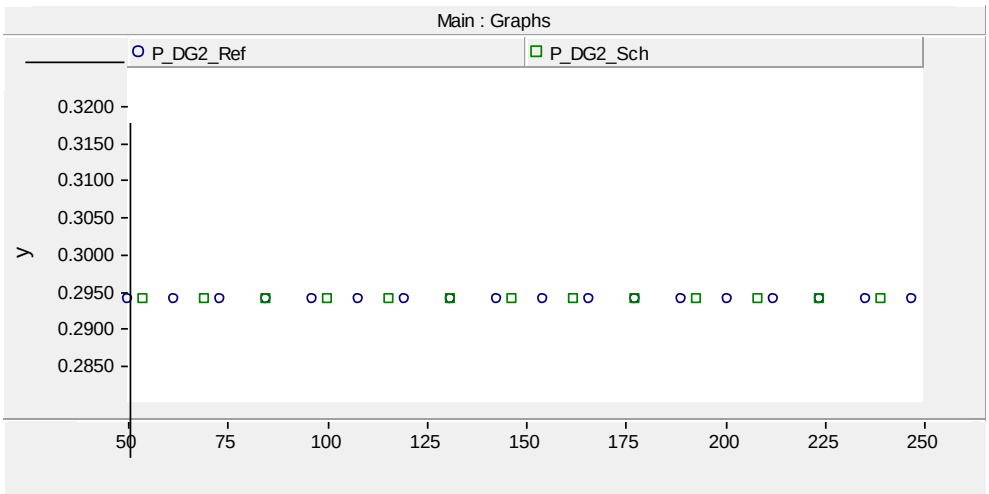

(b) Case 2-C

Figure 5.25. Simulation results: output power reference of DG 2

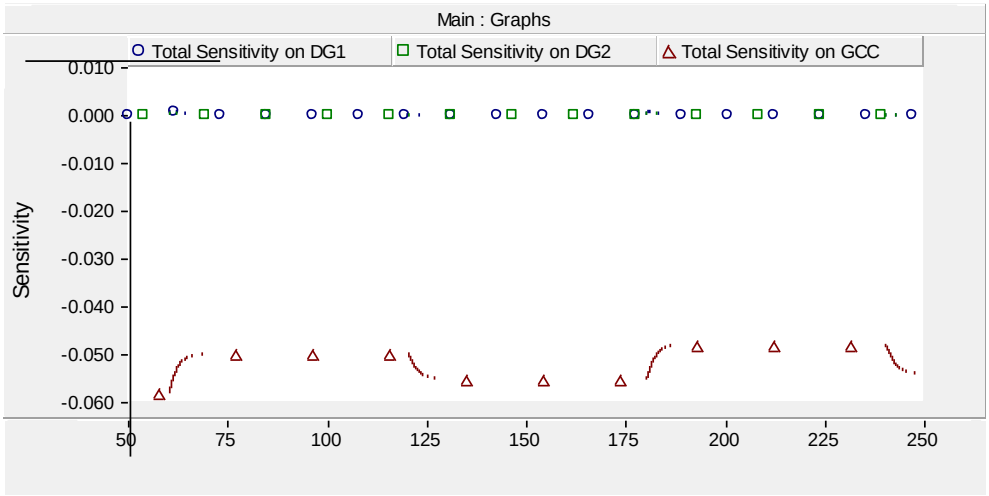

(a) Case 2-B

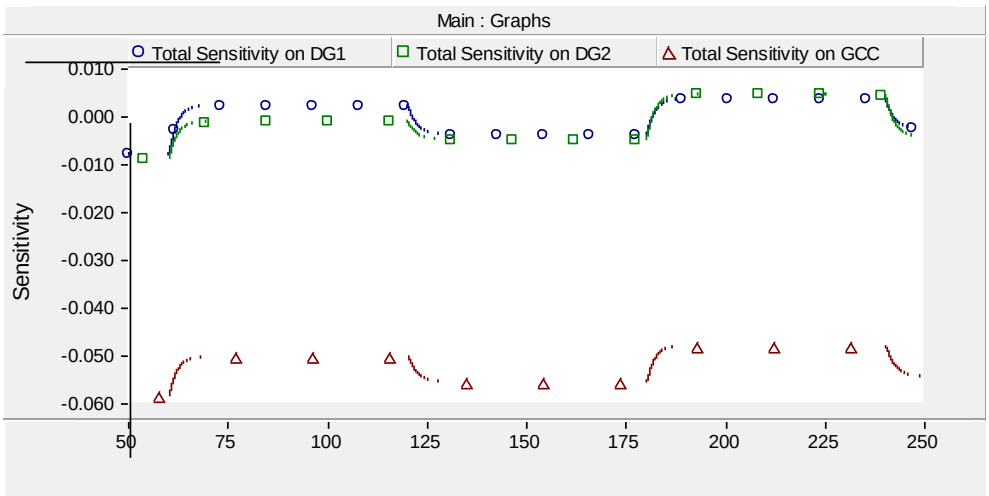

(b) Case 2-C

Figure 5.26. Simulation results: loss sensitivities in case 2

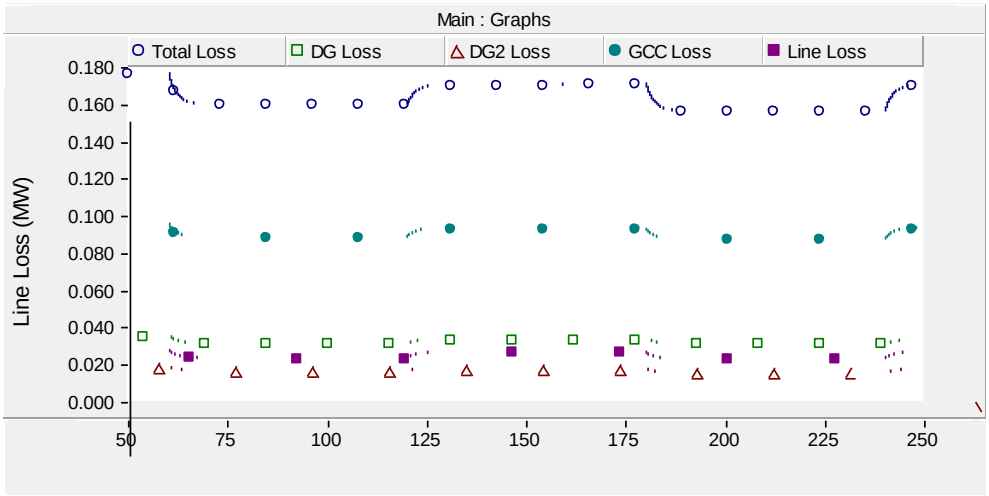

(a) Case 2-B

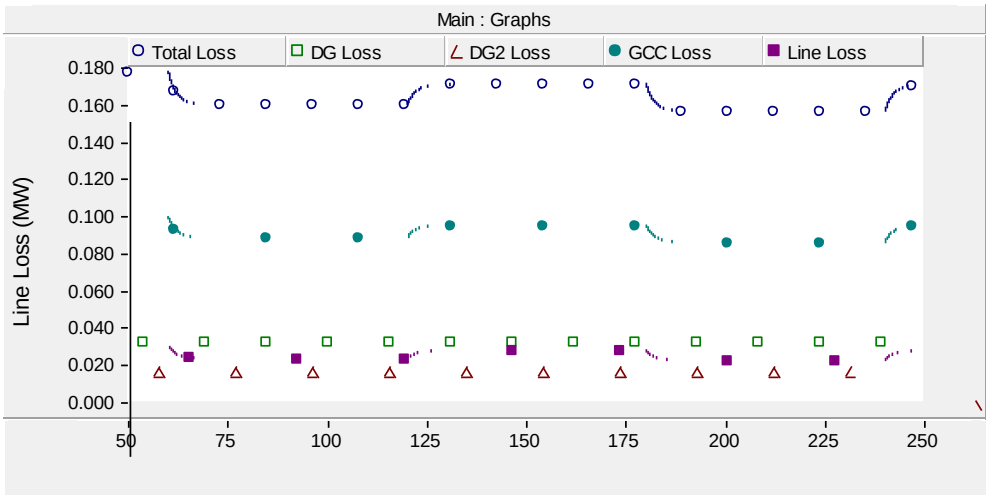

(b) Case 2-C

Figure 5.27. Simulation results: each loss in case 2

5.3. Comparison with Other Researches on Voltage Control Considering Loss Reduction

In case 1 and 2, effectiveness of proposed cooperative voltage control scheme is verified. In case 3, these results are compared with other researches on loss reduction in [40] and [41]. Proposed OPF strategy, scheduling methods, and controllers are realized in the same test system presented above. Methodologies of these studies are investigated before verification of the proposed method.

5.3.1. Dynamic consensus algorithm based distributed global efficiency optimization of a droop controlled DC microgrid [40]

The purpose of this study is to reduce conversion loss of DGs and scheduling and control methods are presented. The adaptive virtual resistance method is applied and virtual resistance for conversion loss minimization is determined by scheduling considering objective function and constraints shown below.

$$objective\ function: Min\{P_{TL}\} \tag{5.2}$$

$$decision\ variable: \{R_{d\_1}, R_{d\_2}, \cdots, R_{d\_N_{oC}}\} \tag{5.3}$$

$$s.t.: \begin{Bmatrix} 0.25 \le \{R_{d\_1}, R_{d\_2}, \cdots, R_{d\_N_{oC}}\} \le 5 \\ \{i_{o\_1,} i_{o\_2,} \cdots, i_{d\_N_{oC}}\} \le I_{MAX} \end{Bmatrix} \tag{5.4}$$

The conversion efficiency is modeled as a function of terminal current of converter using MATLAB curve fitting tool and conversion loss is expressed as a function of terminal voltage, terminal current and efficiency.

$$\eta(i) = 0.975 \cdot e^{-2\times10^{-3}\cdot i} - 0.1257 \cdot e^{-0.3\cdot i} \tag{5.5}$$

$$P_{TL} = \sum_{m=1}^{N} V_{DC} \cdot i_{o\_m} \cdot \frac{1-\eta_m}{\eta_m} \tag{5.6}$$

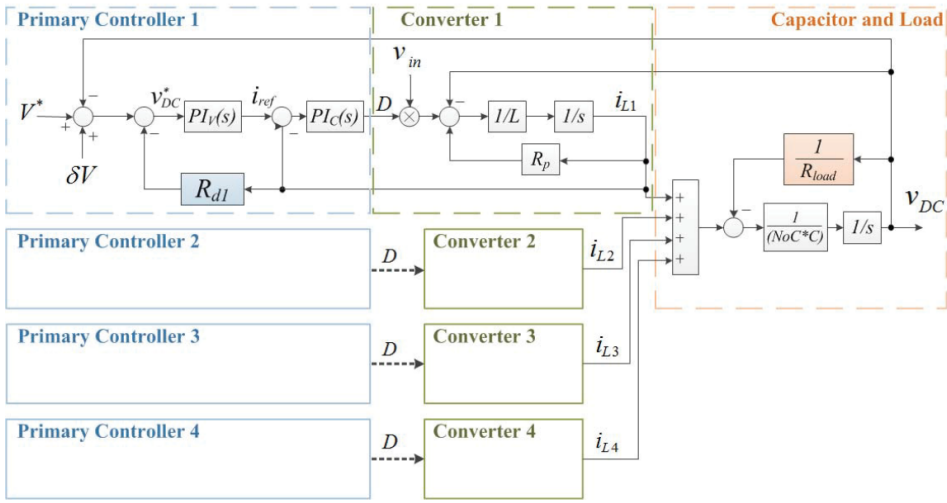

Figure 5.28. Controller based on adaptive virtual resistance method

Figure 5.28 presents proposed controller in this study. Controller utilizes current-voltage droop control and including virtual resistance, which is determined in the scheduling process, in a proportional current feedback loop.

5.3.2. Line Loss Optimization Based OPF Strategy by Hierarchical Control for DC Microgrid [41]

This study focused on reducing line loss in the DC microgrid when there are a number of power converters. OPF strategy is proposed for line loss minimization and terminal reference voltage of each DG is decided by OPF. The optimal condition for line loss minimization is presented as below from analysis of line loss.

$$u_1^* = u_2^* = \cdots = u_N^* \tag{5.7}$$

The optimal condition describes terminal voltages of converter should be identical. However, actual operation might be not in accordance with optimal condition if the terminal output power of converter is limited by its maximum capacity. In this case, the study explains that it should be minimized that difference between an average terminal reference voltage of the converter, which power is not reached to limit, and terminal reference voltage of the converter, which power is reached to limit. This condition is described as following equation.

$$\left\{ \begin{array}{l} \min \left| \dfrac{\sum_{j=2}^{N} u_j^*}{N-1} - u_1^* \right| = \sigma \\ u_2^* = u_3^* = \cdots = u_N^* \end{array} \right\} \tag{5.8}$$

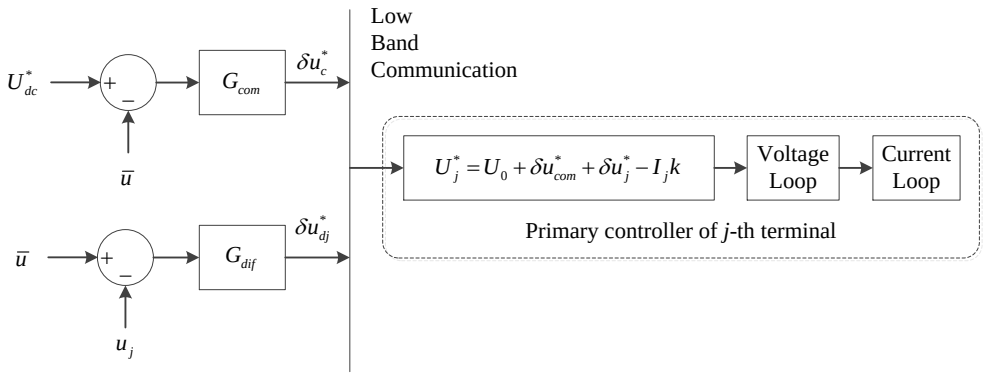

Figure 5.29. Hierarchical control block

Figure 5.29 illustrates a hierarchical control block proposed in this study and it consists of primary and secondary control part. Secondary control is done by centralized controller. Voltage references to meet the line loss minimization condition are generated in secondary control and information is delivered to primary controller. In primary control, a decentralized control is implemented based on droop control and terminal voltage reference is generated based on reference generated in secondary control.

5.3.3. Case 3: Comparison with other researches when load and generation of RES are varied

Table 5.22 summarized detail conditions for case study 3 and three cases are prepared to verify proposed operation scheme. In control method in [40], DC voltage reference was kept to a constant value and method to decide reference terminal voltage is not suggested. Therefore, the arbitrary reference value, which not occur voltage violation, is chosen. As a result, there was not any voltage violation in steady state for all cases.

Table 5.22. Conditions for case study 3

Case	Method	Scheduling	Control	Description
3-A	Proposed method	O	O	$V_{max}^{loss} = 1.0399\,pu$ and $V_{min}^{loss} = 0.9601\,pu$
3-B	Research in [40]	O	O	References: GCC output voltage is 1.04 pu and output voltage of two DGs is 1.03 pu
3-C	Research in [41]	O	O	-

Figure 5.30 to Figure 5.32 are comparing each loss in case 3. Line loss was smallest in case 3-C because terminal voltage reference of converter to minimize line loss was determined by method in [41]. Figure 5.31 shows that conversion loss in case 3-C was larger than other cases and conversion loss in case 3-A and 3-B were similar each other. In proposed method, control object is to reduce both line loss and conversion loss in the DC distribution system. Therefore, reduced conversion might be smaller than case 3-B if only conversion loss is minimized well in case 3-B. However, research in [40] suggested the method to calculate virtual resistance only to minimize conversion loss and did not consider voltage reference of each converter in optimal condition. Consequently, optimized control variable to minimize conversion loss cannot be determined in case 3-B. Figure 5.32 presents that total loss was smallest in 3-A and results are summarized in Table 5.23. It presents that proposed method is more effective than compared researches to reduce loss in the DC distribution system.

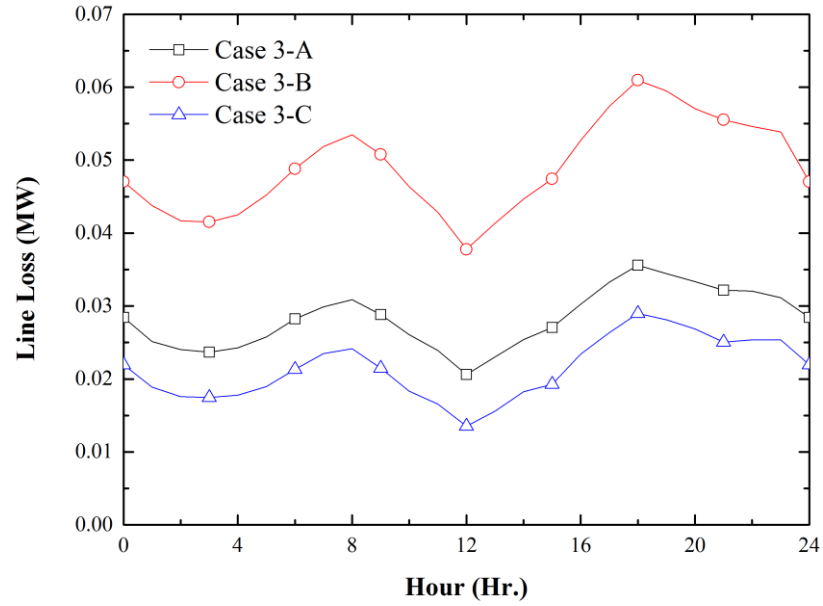

Figure 5.30. Simulation result: line loss in case 3

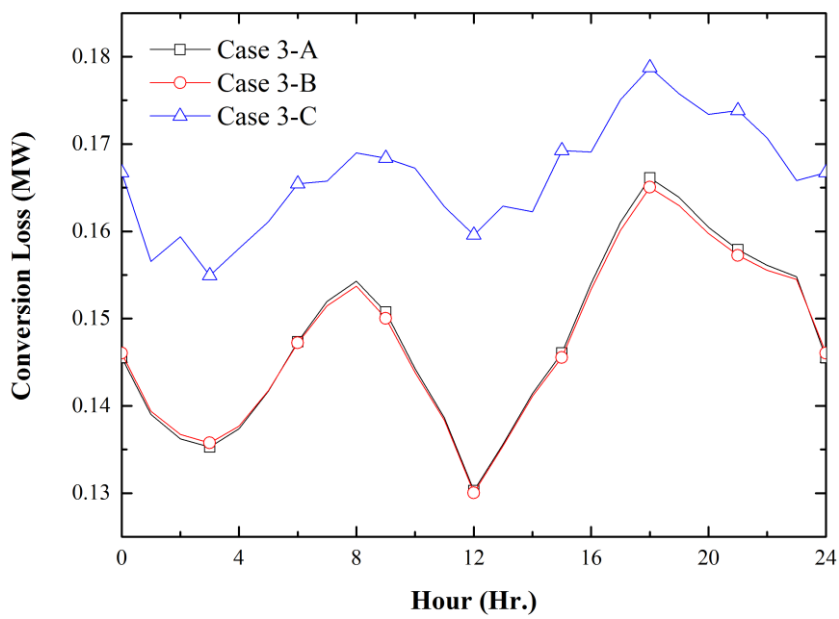

Figure 5.31. Simulation result: conversion loss in case 3

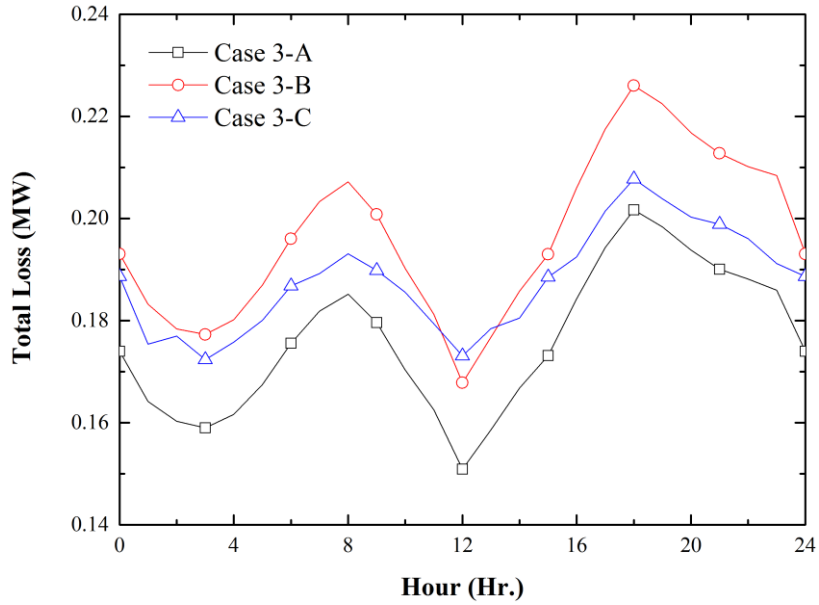

Figure 5.32. Simulation result: total loss in case 3

Table 5.23. Summary of result for case 3

Case	3 - A	3 - B	3 - C
Line Loss (MWh)	0.678	1.179	0.514
Conversion Loss in DGs (MWh)	1.257	0.530	2.135
Conversion Loss in GCC (MWh)	2.293	3.013	1.856
Total Loss (MWh)	4.228	4.721	4.506
Total Loss / Load (%)	6.307	7.044	6.722
Voltage Violation	X	X	X

5.3.4. Case 4: Cost evaluation

Based on result of case study 3, energy supply cost and loss cost are evaluated to verify the operation cost reduction effect. Base case and three cases in case study 3 are chosen for cost evaluation. Energy supply cost consists of cost of drawing energy from transmission system and generation power of DGs. Loss cost includes cost of conversion loss and line loss. It is assumed that generation cost of DGs is calculated by the cost function of generated power and other cost is calculated by

system marginal price (SMP). PV is not owned by DNO and PV owner receive generation cost directly from market operator. The hourly SMP pattern is applied to calculate cost and it is actual SMP in 10, November, 2015 reported by KPX [64].

Table 5.24. Hourly SMP in 10, November, 2015

Hour	0	1	2	3	4	5
SMP (KRW/kWh)	95.83	93.26	93.65	91.26	90.98	92.33
Hour	6	7	8	9	10	11
SMP (KRW/kWh)	92.57	94.15	95.9	96.38	96.37	96.36
Hour	12	13	14	15	16	17
SMP (KRW/kWh)	96.36	95.19	96.84	96.84	116.52	116.52
Hour	18	19	20	21	22	23
SMP (KRW/kWh)	116.52	97.5	97.5	96.81	95.89	95.83

It is assumed that a DG is thermal power generator consuming oil. Unit generation cost of thermal power generator consuming oil in November, 2015, which is reported by KPX, was 130.32 KRW/kWh. The generation cost functions of DGs are designed as below and unit price becomes 130.32 KRW/kWh at the rated generation power of DGs.

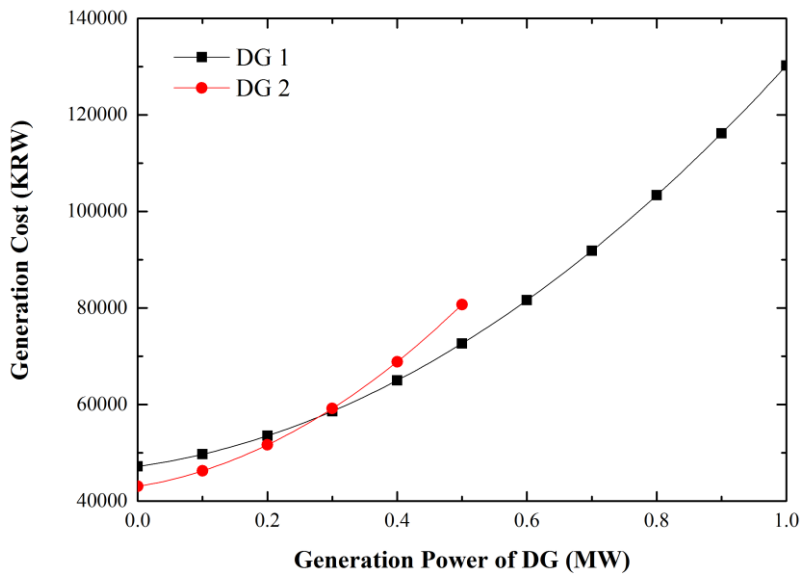

Figure 5.33. Generation cost function of DG

$$f(P_{DG,1}) = 64171.3 \times P_{DG,1}^2 + 18873.91 \times P_{DG,1} + 47184.78 \quad (5.9)$$

$$f(P_{DG,2}) = 107628 \times P_{DG,2}^2 + 21525.6 \times P_{DG,2} + 43051.2 \quad (5.10)$$

Table 5.25. Comparison of cost for case study 3

Case	Loss Cost	DG Generation Cost	Energy Supply Cost	Total Cost	Decreased Cost on Base Case (%)
Base case	₩559,926	₩2,165,664	₩6,412,591	₩9,138,181	-
Case 3-A	₩414,898	₩3,450,593	₩4,112,191	₩7,977,683	12.7 %
Case 3-B	₩463,349	₩2,463,927	₩5,501,031	₩8,428,308	7.8 %
Case 3-C	₩441,739	₩4,575,234	₩3,113,588	₩8,130,561	11.0 %

Table 5.25 compares the each cost in case study 3. The results emphasize that total cost was minimum when proposed operation scheme was applied. Loss cost in case 3-B and 3-C were not minimum because this case did not consider both reduction of line and conversion loss.

In case 3-B, DG generation power is quite smaller than case 3-A and 3-B to reduce conversion loss of DG. Therefore, drawing energy from transmission system was increased. There was a considerable DG generation cost while DG generation power was quite small due to fixed cost of DG generation. As a result, the operation scheme in case 3-B was not effective in reducing cost.

In case 3-C, there was a lot of DG generation power and it caused huge generation cost of DG because unit generation price of DG is more expensive than SMP. Therefore, sum of generation cost and energy supply cost in this case was quite larger than other cases. Consequently, operation scheme in case 3-C did not reduce total cost than proposed cooperative operation scheme in this dissertation.

Chapter 6. Conclusions and Future Extensions

6.1. Conclusions

This dissertation presented a new cooperative control method considering line loss and conversion losses in the radial DC distribution system. Formulation of approximate voltage sensitivities and loss sensitivities are presented and these formulations were basis of a proposed cooperative control scheme.

Specific topics and technical issues on this dissertation were reviewed. Issues on voltage stability, voltage control, loss reduction, voltage sensitivity, and loss sensitivity is investigated and drawback of conventional researches was analyzed. Loads are generally fed through an AC/DC or DC/DC converter in the DC distribution system, which have CPL behavior if converter at load side maintains consuming power constant. In this case, negative incremental resistance appears in the DC distribution system, and voltage instability can be occurred depending on the operation point of the system. Therefore IEC 60092-101 recommended that maintain the voltage within 10% tolerance limit. To prevent voltage instability problem, studies on voltage control method were presented. Various studies on voltage control were presented using master / slave concept, PI and droop based control concept, adaptive droop control concept, fuzzy control concept, and DBS based concept. Common characteristics and drawback of conventional studies were reviewed. This dissertation investigated loss reduction issue in the DC distribution system and drawbacks of conventional researches were discussed. Limits of conventional sensitivity analysis studies were described and necessity of a novel form of sensitivity expression was discussed

This dissertation proposed a novel formulation of the voltage sensitivity and loss sensitivity in the radial DC distribution system. From a new form of voltage equation expressed as a function of the slack bus voltage and voltage drop over the

conductor, formulations of sensitivities were derived based on linear approximation and reasonable assumptions are suggested for these formulations. To verify an accuracy of the proposed sensitivity expressions, sensitivities calculated by approximate expression are compared with actual sensitivities calculated by a series of power flow results. Maximum error of proposed voltage sensitivity expression with regard to the slack bus voltage and bus injection power did not exceed 1%. Maximum error of proposed line loss sensitivity with regard to the slack bus voltage and bus injection power did not exceed 1.5% and 0.25%, respectively. These results emphasized that proposed sensitivity formulations have good accuracy. Based on the formulation of the voltage sensitivity, the relation between electrical quantities and the voltage sensitivity is analyzed. The electrical length between the slack bus and target bus is a major factor affecting voltage sensitivity with regard to the bus injection power. Therefore, voltage sensitivity with regard to bus injection power is different at each bus, whereas voltage sensitivity with regard to the slack bus voltage is similar at entire bus and has value about 1.0.

Cooperative voltage control scheme for GCC and DG in the radial DC distribution system is proposed based on the formulation and analyses of sensitivities. A structure of the proposed method was described and candidates for a communication system to realize this structure are introduced. Formulations for optimal scheduling using DP, which are including objective function, constraints for bus voltage, output power of DG, and SOC of ESS, were presented to reduce total losses in the DC distribution system. An outline of a local controller was described and it is presented that how the proposed control scheme regulate the bus voltages considering reduction of total loss in the DC distribution system. Local controller consists of 8 modules and detail design and function of each module were explained. Sensitivity estimator modules calculated approximate sensitivities based on proposed formulations of sensitivities. Total loss sensitivity calculator module generated actual total loss sensitivity with regard to the voltage control

equipment based on estimated voltage and loss sensitivity. Regulation signal generator module determined references of the voltage control equipment based on outputs of proposed modules. The control mode was determined considering voltage violation, voltage sensitivity, loss sensitivity, and estimated variation in total loss due to voltage regulation. Reference signals for voltage controller were generated depending on the control mode determined in this module. Proposed loss reduction strategy based on estimated loss sensitivity was introduced and controller was designed to realize this strategy. Examples for voltage violation were illustrated and solution for solving this voltage problem based on voltage sensitivity analysis was presented. Voltage regulation controller was designed to realize presented voltage regulation strategy.

Case studies were presented to verify performance of the proposed method. Total loss by proposed method was almost similar to the result of an optimal scheduling when there are not variation in generation and load. Case study considering a varying load and generation during a day was also presented. In this case, voltage problem occurred when only scheduled reference is utilized. However, voltage violation was removed by proposed method and, even though, the total loss was also decreased. Consequently, proposed method presented better results for voltage regulation and loss reduction when scheduled references were not utilized. Case studies to compare the proposed method with conventional method were presented. All of these results proven that proposed method is more effective to regulate the bus voltage and reduce total losses in the radial DC distribution system. In addition, cost evaluation was investigated and proposed operation scheme was helpful to reduce operation cost in DC distribution system.

6.2. Future Extensions

Since the methodology developed in this dissertation focuses on the operation in the radial DC distribution system, I will extend proposed method to apply to the operation in more general DC power network.

Moreover, the following subjects, in continuation of this study, are suggested for the future works:

- This dissertation focused the operation in the radial DC distribution system. The control scheme in various topology DC power network is necessary to extend the proposed method to general DC power network environment.

- This dissertation was not discussed an issue on communication failure and this is an important issue in actual operation of power system. Control strategy for temporary communication failure will be developed. Additional analysis and development on sensitivity might be also required to improve the proposed method.

- A number of series-connected converter and DERs are required if the scale and distance of the DC distribution system are increased. In this case, interactions between voltage control equipment are more complex and proposed method should be modified.

- This dissertation focused on total loss reduction concerning efficient operation in the radial DC distribution system. The main object of loss reduction is to minimize operating cost of DNO and it is important from economic concern. However, proposed method in this dissertation does not considered operating cost directly although it is shown that proposed method is helpful for cost reduction. Therefore, author will study operating and control scheme for operating cost reduction. Power market environment will be reflected and operating scheme will be constructed considering electricity price

Appendix A. Formulation and Analysis for Approximated Expression for Voltage Sensitivity in the Radial DC Distribution System

A.1 Approximate Expression for the Voltage Sensitivity in a Radial DC Distribution System

A.1.1 Derivative of the General Voltage Equation

The voltage sensitivity in a DC distribution system indicates the voltage deviation in response to small variations in the electrical quantities at an arbitrary bus. Therefore, the relationship between the voltage and the electrical quantities at an arbitrary bus should be investigated in the general voltage equation to derive voltage sensitivity. It follows that the voltage equation should include variables to be controlled and the injected power at the bus and the slack bus voltage is considered controllable variables. For example, the voltage equation can be expressed as follows for the system shown in Figure 3.1:

$$V_i = V_i(P, V_{slack}) \tag{A.1}$$

Using the general voltage equation in (3.6), the real power at bus *i* is shown, whereas the real powers at other buses are not given directly. It follows that this equation cannot yield information on the direct relationship between voltage deviations and the real power deviation at an arbitrary bus. Moreover, the general voltage equation with a conventional power flow analysis is unsuitable for an analytical description of voltage sensitivity. Therefore, the set of equations in (3.2) should be replaced with equations that describe the voltage drop between the slack bus and the load bus to acquire a general voltage equation in the form of (A.1); *i.e.*,

$$
\begin{aligned}
V_2 &= V_1 + r_{12}\left(\frac{P_2}{V_2} + \frac{P_3}{V_3} + \cdots + \frac{P_6}{V_6}\right) \\
V_3 &= V_1 + r_{12}\left(\frac{P_2}{V_2} + \frac{P_3}{V_3} + \cdots + \frac{P_6}{V_6}\right) + r_{23}\left(\frac{P_3}{V_3} + \frac{P_4}{V_4}\right) \\
V_4 &= V_1 + r_{12}\left(\frac{P_2}{V_2} + \frac{P_3}{V_3} + \cdots + \frac{P_6}{V_6}\right) + r_{23}\left(\frac{P_3}{V_3} + \frac{P_4}{V_4}\right) + r_{34}\left(\frac{P_4}{V_4}\right) \\
V_5 &= V_1 + r_{12}\left(\frac{P_2}{V_2} + \frac{P_3}{V_3} + \cdots + \frac{P_6}{V_6}\right) + r_{25}\left(\frac{P_5}{V_5} + \frac{P_6}{V_6}\right) \\
V_6 &= V_1 + r_{12}\left(\frac{P_2}{V_2} + \frac{P_3}{V_3} + \cdots + \frac{P_6}{V_6}\right) + r_{25}\left(\frac{P_5}{V_5} + \frac{P_6}{V_6}\right) + r_{56}\left(\frac{P_6}{V_6}\right)
\end{aligned}
\tag{A.2}
$$

In Equation (A.2), each term except V_1 on the right-hand side of the equation describes a line voltage drop at each conductor segment. For ease of manipulation, this set of equations is arranged as follows:

$$
V_i = V_{slack} + \sum_{k=1}^{n} R_{ik} \frac{P_k}{V_k} \tag{A.3}
$$

The R-Bus matrix can be redefined as follows:

$$
R = \begin{bmatrix}
R_{11} & R_{12} & \cdots & R_{1n} \\
R_{21} & R_{22} & \cdots & R_{2n} \\
\vdots & \vdots & \ddots & \vdots \\
R_{n1} & R_{n2} & \cdots & R_{nn}
\end{bmatrix} \tag{A.4}
$$

and the R-Bus matrix for the system shown in Figure 3.1is as follows:

$$
R = \begin{bmatrix}
0 & 0 & 0 & 0 & 0 & 0 \\
0 & r_{12} & r_{12} & r_{12} & r_{12} & r_{12} \\
0 & r_{12} & r_{12}+r_{23} & r_{12}+r_{23} & r_{12} & r_{12} \\
0 & r_{12} & r_{12}+r_{23} & r_{12}+r_{23}+r_{34} & r_{12} & r_{12} \\
0 & r_{12} & r_{12} & r_{12} & r_{12}+r_{25} & r_{12}+r_{25} \\
0 & r_{12} & r_{12} & r_{12} & r_{12}+r_{25} & r_{12}+r_{25}+r_{56}
\end{bmatrix} \tag{A.5}
$$

each element of the R-Bus matrix R_{ij} is defined as the sum of the elements in the intersection of groups $\{R_i\}$ and $\{R_j\}$, where group $\{R_i\}$ is the set of line resistances located on the shortest path between the slack bus of the radial DC distribution system and bus *i*.

A.1.2 Formulation of an Approximate Expression for Voltage Sensitivity with Respect to Real Bus Power

The main purpose of this work is to obtain an approximate expression for voltage sensitivity. To formulate this, it is assumed that the voltage variation at bus *i* (the target bus) can be used to describe the variation in real power at bus *j* (the controlled bus).

A simple method to determine the voltage sensitivity is to use partial differentiation. However, in Equation (A.3), the bus voltage is expressed as a function of the bus voltage at all buses in the DC distribution system, which is too complex for a partial differentiation approach. To address this, some assumptions are made and linearization is employed.

If the real power at bus *j* were varied slightly, only small changes would be expected to occur in the bus voltages (except for the slack bus). Therefore, the deviation in the bus voltage and real power can be linearized because the voltage sensitivity deals with small variations in these parameters, allowing (A.3) to be re-written as:

$$V_i + \Delta V_i = V_{slack} + R_{ij}\frac{P_j + \Delta P_j}{V_j + \Delta V_j} + \sum_{k=1,k\neq j}^{n} R_{ik}\frac{P_k}{V_k + \Delta V_k} \tag{A.6}$$

where *i* is the index of the target bus for which voltage sensitivity is investigated and *j* is the index of the bus for which the real bus power is varied. The voltage deviation at the slack bus is neglected because it is assumed that voltage at the slack bus is controlled continuously by GCC. To relate the deviation of the electrical quantities, the voltage deviation at bus *i* can be described by subtracting (A.3) from (A.6); *i.e.*,

$$\Delta V_i = R_{ij}\frac{V_j\Delta P_j - P_j\Delta V_j}{V_j^2 + V_j\Delta V_j} - \sum_{k=1,k\neq j}^{n} R_{ik}\frac{P_k\Delta V_k}{V_k^2 + V_k\Delta V_k} \tag{A.7}$$

For stable operation of a DC distribution system, the voltage should be maintained within an appropriate range, which is typically near to the rated voltage.

IEEE Standard 1709™-2010 uses the voltage tolerance standard in IEC 60092-101, and specifies steady-state (*i.e.*, continuous) DC voltage tolerance limits of 10% [17]. Therefore, voltage deviations due to small variations in the real bus power can be expected to be smaller than the bus voltage, and Equation (A.7) can be approximated to Equation (A.9) via the assumption shown in Equation (A.8).

$$V_k^2 + V_k \Delta V_k = V_k (V_k + \Delta V_k) \cong V_k^2 \tag{A.8}$$

$$\Delta V_i \approx R_{ij} \frac{V_j \Delta P_j - P_j \Delta V_j}{V_j^2} - \sum_{k=1, k \neq j}^{n} R_{ik} \frac{P_k \Delta V_k}{V_k^2} \tag{A.9}$$

In this case, if the voltage becomes significantly smaller than the rated voltage, voltage deviation is increased when the real bus power varies because the current flow and voltage drop over the conductors significantly increase. In this case the assumptions in (A.8) may not hold.

Using (A.9), the relationship between ΔV_i and ΔP_j can be expressed as follows:

$$\left(1 + \frac{R_{ii} P_i}{V_i^2}\right) \Delta V_i \approx R_{ij} \frac{\Delta P_j}{V_j} - \sum_{k=1, k \neq i}^{n} R_{ik} \frac{P_k \Delta V_k}{V_k^2} \tag{A.10}$$

and the voltage deviation at bus *i* in response to deviations in the real power at bus *j* (which is equivalent to the voltage sensitivity) is given by

$$\frac{\Delta V_i}{\Delta P_j} \approx \frac{V_i^2}{V_i^2 + R_{ii} P_i} \left(\frac{R_{ij}}{V_j} - \sum_{k=1, k \neq i}^{n} \frac{R_{ik} P_k}{V_k^2} \frac{\Delta V_k}{\Delta P_j} \right) \tag{A.11}$$

where the voltage sensitivity at bus *i* depends on the voltage sensitivity of the other buses. For this reason, it is not straightforward to describe the voltage sensitivity analytically. To address this problem, the following recursive substitution is carried out:

$$\frac{\Delta V_i}{\Delta P_j} \approx \frac{V_i^2}{\left(V_i^2 + R_{ii}P_i\right)V_j}\Big(R_{ij} - \sum_{k=1,k\neq i}^{n} \frac{R_{ik}P_k}{V_k^2 + R_{kk}P_k} R_{kj}$$
$$+ \sum_{k=1,k\neq i}^{n} \frac{R_{ik}P_k}{V_k^2 + R_{kk}P_k} \sum_{k'=1,k'\neq k}^{n} \frac{R_{ik'}P_{k'}}{V_{k'}^2 + R_{k'k'}P_{k'}} R_{k'j} \tag{A.12}$$
$$- \sum_{k=1,k\neq i}^{n} \frac{R_{ik}P_k}{V_k^2 + R_{kk}P_k} \sum_{k'=1,k'\neq k}^{n} \frac{R_{ik'}P_{k'}}{V_{k'}^2 + R_{k'k'}P_{k'}} \sum_{k''=1,k''\neq k'}^{n} \frac{R_{ik''}P_{k''}}{V_{k''}^2 + R_{k''k''}P_{k''}} R_{k''j} + \cdots\Big)$$

$$V_k^2 + R_{kk}P_k = V_k\left(V_k + R_{kk}\frac{P_k}{V_k}\right) \tag{A.13}$$

$$V_{Drop,k} = R_{kk}\frac{P_k}{V_k} \tag{A.14}$$

$$R_{kk} \geq R_{kj} \tag{A.15}$$

The left-hand term in Equation (A.13), which is the denominator of each term in (A.12), is equivalent to the right-hand term in (A.13). The term in (A.14) describes the voltage drop between the slack bus and bus *k*, which is induced by the real power at bus *k*'. This voltage drop is generally smaller than the bus voltage because the bus voltage should be maintained within the voltage tolerance limits. It follows that (A.14) is significantly smaller than the bus voltage at bus *k*, and therefore (A.14) can be neglected. Furthermore, the relationship in (A.15) is established because of the definition of the R-Bus matrix, which leads to the following expression:

$$0 < \left|\frac{R_{ik}P_k}{V_k^2 + R_{kk}P_k}\right| \leq \left|\frac{R_{kk}P_k}{V_k^2 + R_{kk}P_k}\right| << 1 \tag{A.16}$$

where the backward term (except the first two terms in (A.12) is neglected because the first two terms in the right-hand side of (A.12) dominate. These considerations lead to the following approximate expression for the relationship of the voltage sensitivity at bus *i* to the real power at bus *j*:

$$\frac{\Delta V_i}{\Delta P_j} \approx \frac{V_i^2}{\left(V_i^2 + R_{ii}P_i\right)V_j}\left(R_{ij} - \sum_{k=1,k\neq i}^{n} \frac{R_{ik}R_{kj}P_k}{V_k^2 + R_{kk}P_k}\right) \tag{A.17}$$

The proposed formulation has variables that include the bus voltage at all buses, the real power at all buses except bus *j*, and the elements of the R-Bus matrix, which are a combination of line resistances. The expression is somewhat complex, which makes it difficult to analyze clearly how each variable affects the voltage sensitivity. The details of the analysis will be described later.

A.1.3 Formulation of an Approximate Expression for Voltage Sensitivity with Respect to the Slack Bus Voltage

In Figure 3.1, the slack bus is the secondary terminal of the AC/DC or DC/DC converter. The output voltage of the converter (*i.e.*, the slack bus voltage) can be controlled by the GCC depending on the control strategy of the distribution network operator (DNO) [54]. In this case, the slack bus voltage is considered as a controlled variable that reflects variations in the bus voltage in the DC distribution system, and an analysis of voltage sensitivity to slack bus voltage should be useful for establishing a voltage control strategy.

To formulate an approximate expression for voltage sensitivity to slack bus voltage, the voltage at bus *i* is investigated in response to changes in the slack bus voltage, V_{slack}. The bus voltage can be expressed in a linearized form, as discussed in the previous section, when there is a small deviation in the slack bus voltage. The linearized equation can be represented as follows:

$$V_i + \Delta V_i = V_{slack} + \Delta V_{slack} + \sum_{k=1}^{n} R_{ik} \frac{P_k}{V_k + \Delta V_k} \tag{A.18}$$

To find the relationship between deviations in V_{slack} and bus voltages, the voltage deviation at bus *i* can be found by subtracting (A.3) from (A.18); *i.e.*,

$$\Delta V_i = \Delta V_{slack} - \sum_{k=1}^{n} R_{ik} \frac{P_k \Delta V_k}{V_k^2 + V_k \Delta V_k} \tag{A.19}$$

This expression can be approximated as follows using the assumption in (A.8):

$$\Delta V_i \approx \Delta V_{slack} - \sum_{k=1}^{n} R_{ik} \frac{P_k \Delta V_k}{V_k^2} \tag{A.20}$$

The following relationship relates V_{slack} to the voltage at other buses:

$$\left(1 + R_{ii} \frac{P_i}{V_i^2}\right) \Delta V_i \approx \Delta V_{slack} - \sum_{k=1, k \neq i}^{n} R_{ik} \frac{P_k \Delta V_k}{V_k^2} \tag{A.21}$$

and the voltage deviation at bus *i* in response to changes in V_{slack} is given by

$$\frac{\Delta V_i}{\Delta V_{slack}} \approx \frac{V_i^2}{V_i^2 + R_{ii} P_i} \left(1 - \sum_{k=1, k \neq i}^{n} R_{ik} \frac{P_k}{V_k^2} \frac{\Delta V_k}{\Delta V_{slack}}\right) \tag{A.22}$$

This expression is dependent on the voltage sensitivity of other buses to V_{slack}, which allows us to develop an approximate expression for voltage sensitivity as a function of the injected power at the buses. The following expression relates bus voltages to V_{slack}, and is arrived at via recursive substitution:

$$\frac{\Delta V_i}{\Delta V_{slack}} \approx \frac{V_i^2}{V_i^2 + R_{ii} P_i} \left[1 - \sum_{k=1, k \neq i}^{n} R_{ik} \frac{P_k}{V_k^2} \left\{ \frac{V_k^2}{V_k^2 + R_{kk} P_k} \left(1 - \sum_{k'=1, k' \neq k}^{n} R_{ik'} \frac{P_{k'}}{V_{k'}^2} \frac{\Delta V_{k'}}{\Delta V_{slack}}\right)\right\}\right] \tag{A.23}$$

and

$$\frac{\Delta V_i}{\Delta V_{slack}} \approx \frac{V_i^2}{V_i^2 + R_{ii} P_i} \left[1 - \sum_{k=1, k \neq i}^{n} \frac{R_{ik} P_k}{V_k^2 + R_{kk} P_k} + \sum_{k=1, k \neq i}^{n} \frac{R_{ik} P_k}{V_k^2 + R_{kk} P_k} \sum_{k'=1, k' \neq k}^{n} R_{ik'} \frac{R_{ik'} P_{k'}}{V_{k'}^2 + R_{k'k'} P_{k'}} - \cdots\right] \tag{A.24}$$

The above expression has a similar form to the voltage sensitivity equation in response to changes in the injected power at buses given in (A.12) and (A.16), and was established using the assumptions in (A.13) to (A.15). Therefore, the backward terms on the right-hand side of (A.24) can be neglected because the earlier terms dominate. These considerations lead to the following approximate expression for voltage sensitivity in response to variations in slack bus voltage:

$$\frac{\Delta V_i}{\Delta V_{slack}} \approx \frac{V_i^2}{V_i^2 + R_{ii} P_i} \left(1 - \sum_{k=1, k \neq i}^{n} \frac{R_{ik} P_k}{V_k^2 + R_{kk} P_k}\right) \tag{A.25}$$

A.2 Verification of the Approximate Voltage Sensitivity Equation

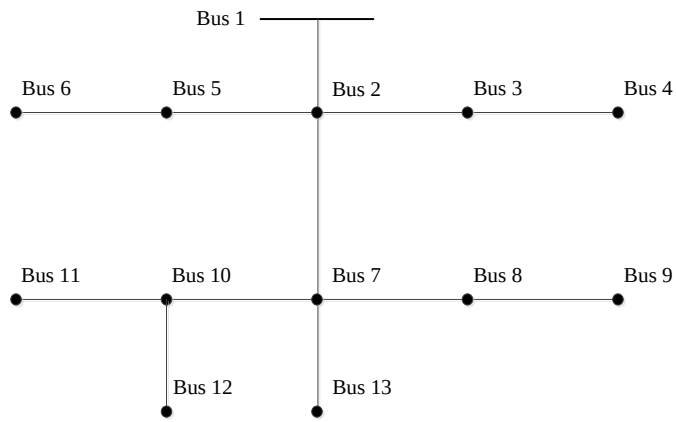

Figure A.1 Diagram of a radial DC distribution system

To verify the proposed approximate expression for voltage sensitivity, case studies are carried out to compare voltage sensitivities derived using the proposed equation with values derived using exact calculations. Figure A.1 shows the 13-bus radial medium-voltage DC (MVDC) distribution test system. The base voltage was 2 kV and the base power was 1 MW; the system was constructed for case studies based on the IEEE 13-node test feeder system. Bus 1 was the slack bus, and was connected to the secondary terminal of the AC/DC converter. The converter was connected to the high-voltage power system, and its secondary terminal voltage could be controlled. Table A.1 lists the constant-power loads. The total capacity was 1.38 MW. Table A.2 lists the resistance and maximum currents of the branches. The line conductor parameter was determined by considering the voltage tolerance limits and line overloading when the bus real power was varied.

Table A.1 Load data for the test system

Bus No.	Bus Type	Load Capacity (kW)
1	Slack	0
2	Load	0
3	Load	200

4	Load	150
5	Load	80
6	Load	120
7	Load	200
8	Load	90
9	Load	300
10	Load	0
11	Load	80
12	Load	60
13	Load	100

Table A.2 Branch data for the test system

From Bus	To Bus	Resistance (Ω)	Maximum Current (A)
1	2	0.02940	1318
2	3	0.03460	760
2	5	0.03951	655
2	7	0.01358	1091
3	4	0.02195	655
5	6	0.06120	726
7	8	0.01730	760
7	10	0.03512	655
7	13	0.04390	655
8	9	0.01730	760
10	11	0.03073	655
10	12	0.03951	655

The voltage sensitivity was investigated as a function of the injected power at buses and the slack bus voltage. The approximate voltage sensitivity was calculated using (A.17) and (A.25). The exact voltage sensitivity as a function of the injected power at the buses was obtained from the inverse of the Jacobian matrix in (3.8), and the voltage sensitivity in response to changes in the slack bus voltage was calculated from the deviation of bus voltages and the slack bus voltage from a set of power flow solutions.

A.2.1 Verification of the Approximate Expression of Voltage Sensitivity with Regard to Bus Injected Power

The injected power at each bus was varied from −1 MW to 1 MW. Four cases

were considered, where the slack bus voltage was 0.6, 0.8, 1.0 and 1.2 pu; however, the bus voltage tolerance limit may be exceeded in some cases. Figure A.2 shows the maximum error of the approximate voltage sensitivity equation for each variation in the injected power at each bus. The controlled bus was the bus for which the injected power was varied.

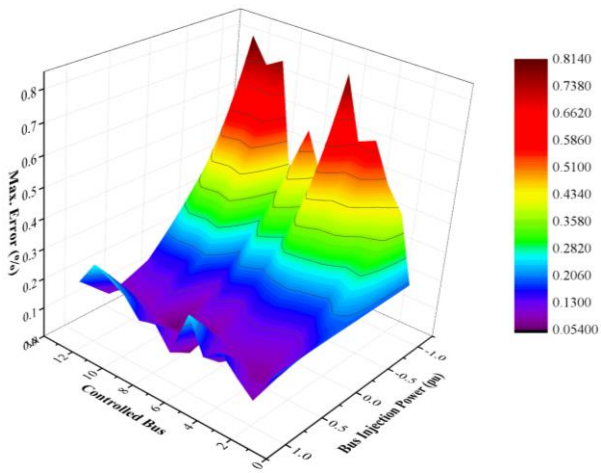

(**a**) V_{slack} = 0.6 pu

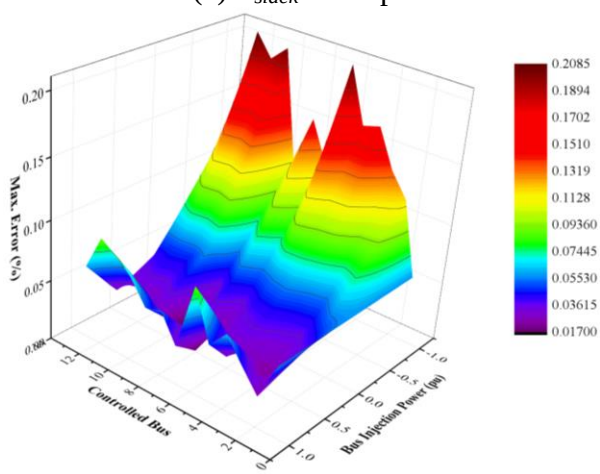

(**b**) V_{slack} = 0.8 pu

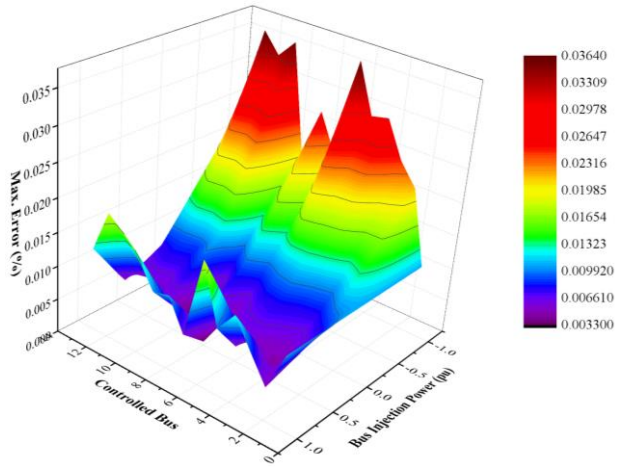

(**c**) V_{slack} = 1.0 pu

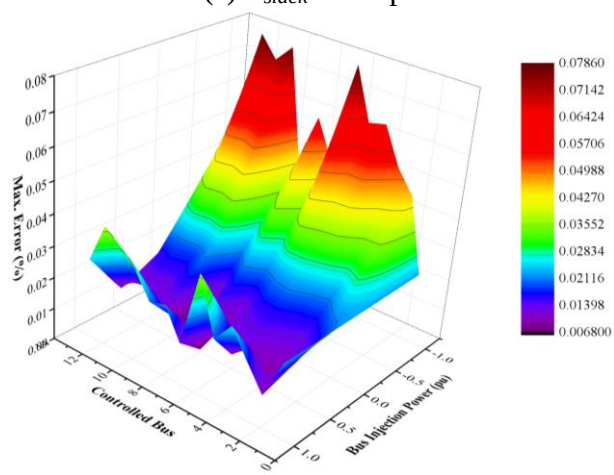

(**d**) V_{slack} = 1.2 pu

Figure A.2 The maximum error of the approximate expression for voltage sensitivity as a function of the injected power at the bus

The maximum error of the approximate expression for voltage sensitivity as a function of the injected power at the buses did not exceed 0.9% in any scenario, which indicates that the expression has good accuracy. The error increased as the negative injected power at the bus increased. This is because the voltage drop also increased due to power consumption. The later terms in (A.12) were neglected because it was assumed that the voltage drop between line conductors was much smaller than the bus voltage. The effect of neglecting these terms becomes larger as the voltage drop increases, increasing the error. Similarly, the slack bus voltage affects the accuracy of the approximate expression. A lower slack bus voltage will

lead to an increased load current, and hence an increase in the voltage drops over the conductors. Furthermore, the overall bus voltage will decrease as the slack bus voltage decreases. In addition, the ratio of the line voltage drop to the bus voltage increases, leading to an increase in the error due to the neglected terms. Consequently, the maximum error was small when slack bus voltage was maintained within the normal operating range, but increased as the slack bus voltage decreased.

A.2.2 Verification of the Approximate Expression of Voltage Sensitivity with Regard to the Slack Bus Voltage

The approximate expression was used to calculate the voltage sensitivity for slack bus voltages in the range 0.6–1.4 pu. The injected power was varied from −1 MW–1 MW at each bus. Figure A.3 shows the maximum error in the approximate expression for voltage sensitivity as a function of V_{slack} when the injected power was varied at buses 2, 7, 9 and 12.

The maximum error did not exceed 0.7%, and was approximately 0.05% when the bus voltage was maintained within the limits. The approximate expression for voltage sensitivity as a function of the slack bus voltage therefore has good accuracy. The error increased as the slack bus voltage decreased, and the negative injected power at the bus increased because the line voltage drop became larger than the limits of normal operating conditions. Therefore, the overall bus voltage also decreased, which is consistent with the assumptions in Equation (A.24).

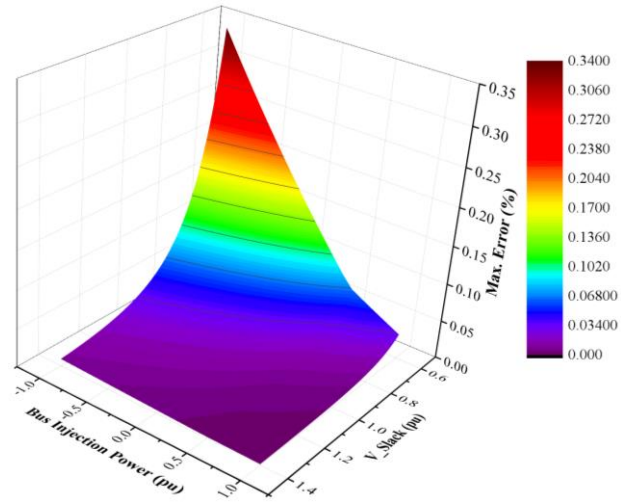

(**a**) Injected power varied at bus 2

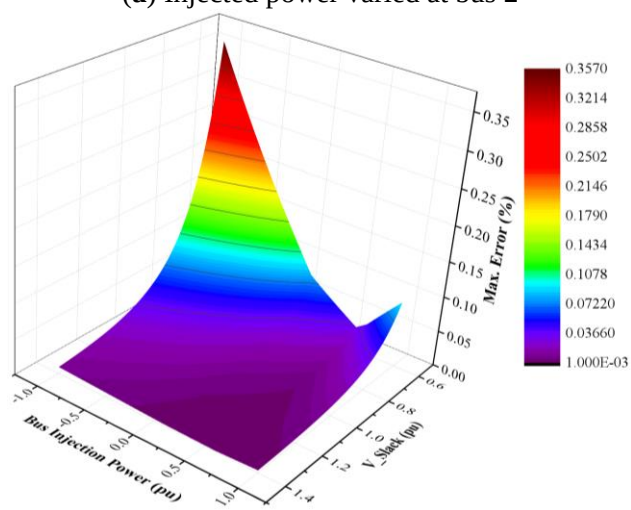

(**b**) Injected power varied at bus 7

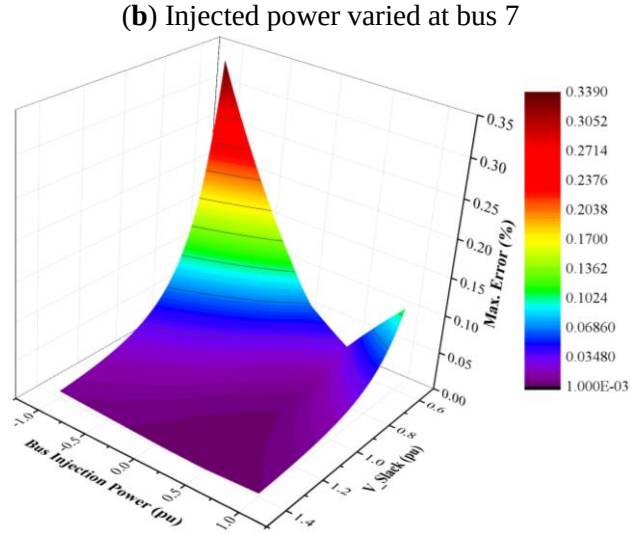

(**c**) Injected power varied at bus 9

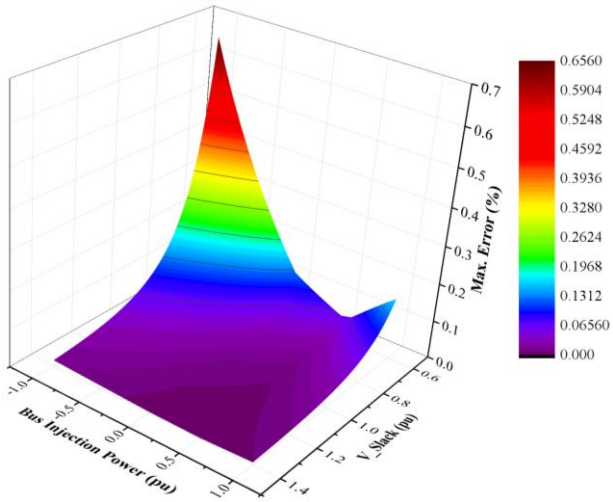

(**d**) Injected power varied at bus 12

Figure A.3 The maximum error in the approximate expression for voltage sensitivity as a function of V_{slack}

A.3 Analysis of Voltage Sensitivity

In this section, the relationships between the voltage sensitivity and various electrical quantities are analyzed using the approximate voltage sensitivity equations. The approximate equations are separated into several terms, which is helpful for examining how each variable affects the voltage sensitivity.

A.3.1 Analysis of the Approximate Expression of Voltage Sensitivity with Regard to Bus Injected Power

To analyze how the variables affect the voltage sensitivity, the expression in (A.17) is separated into the following four terms:

$$k_1 = \frac{V_i^2}{\left(V_i^2 + R_{ii}P_i\right)} \tag{A.26}$$

$$k_2 = \frac{1}{V_j} \tag{A.27}$$

$$k_3 = \sum_{k=1,k\neq j}^{n} \frac{R_{ik}R_{kj}P_k}{V_k^2 + R_{kk}P_k} \tag{A.28}$$

and

$$k_4 = R_{ij} \tag{A.29}$$

The denominator and the numerator in (A.26) have similar values because of the assumption in (A.14). In (A.26), the backward term in the denominator is equivalent to the voltage difference between the slack bus and bus *i*, which is induced by the bus real power at bus *i*, which should be significantly smaller than the bus voltage. Therefore, this term should be approximately 1.0, as long as the DC voltage tolerance is small; however, this assumption may not hold for large injected powers at buses or very low bus voltages. Figure A.4 shows the result of (A.26) when the injected power was varied at bus 13. When V_{slack} = 1.0 pu, the result was in the range 1–1.0062 (except at bus 13) and then increased as the negative injected power increased because of the increase in the negative injected power at bus 13 in response to a decrease in the voltage at other buses. The result of (A.26) at bus 13 was in the range 0.9791–1.0239, which is a larger deviation from 1.0 than at any of the other buses because of injected power variation at bus 13. Similar trends were found with V_{slack} = 0.6 pu. In this case, the result of (A.26) was in the range 0.9457–1.0810. The larger deviation from 1.0 was investigated because the overall bus voltage decreased as the difference between line voltages increased.

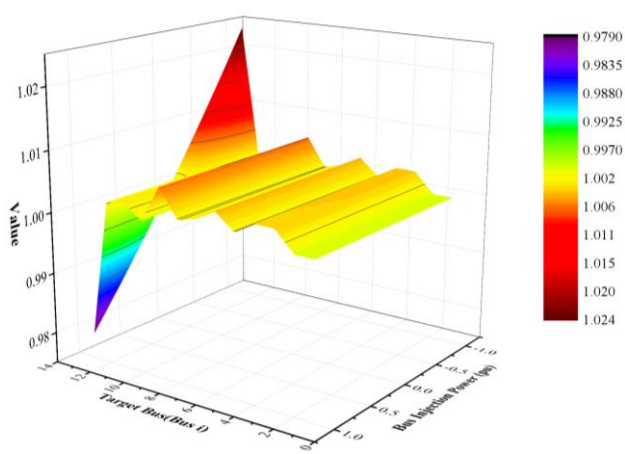

(**a**) V_{slack} = 1.0 pu

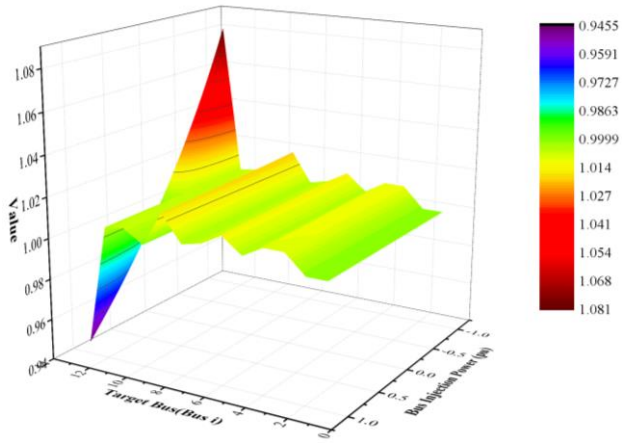

(**b**) V_{slack} = 0.6 pu

Figure A.4 The results of (A.26) as a function of the injected power at the bus

The expression in (A.27) is the inverse of the voltage at bus *j* (the output bus). If the voltage is within the tolerance limits (for example, within 10%), this term should be in the range 0.9091–1.1111. In the case study, it was in the range 0.9904–1.0360 for V_{slack} = 1.0 pu; however, it increased markedly as the bus voltage decreased, and was in the range 1.625–1.858 for V_{slack} = 0.6 pu, as shown in Figure A.5 (b). In addition, the result of (A.27) increases with increasing negative injected power, because this induces a decrease in the bus voltage. In this case, the voltage sensitivity to changes in the injected power at bus 13 exceeded that at the other buses because the injected power was varied at bus 13. For this reason, the variation in the injected power at bus 13 was larger than that at the other buses. This will be discussed further below.

Figure A.6 shows the results of (A.28) and Figure A.7 shows the result of (A.29). The former was much smaller than the latter. This follows because the relationship in (A.26) must be satisfied, and therefore the term in (A.28) may be neglected if a simple equation is required; however, an error of voltage sensitivity may increase. The term in (A.29) is identical to the element of the R-Bus matrix between buses *i* and *j*, and thus is constant regardless of the injected power at the bus and the slack bus voltage.

Consequently, the results of (A.28) is smaller than the result of (A.29), and so

the latter is the dominant term for the voltage sensitivity. The terms in (A.26) and (A.27) are in effect coefficients of the voltage sensitivities and have values of approximately 1.0, provided that the bus voltage is maintained within the tolerance limits. An increase in the negative injected power makes these terms larger because it decreases the overall voltage. In addition, a decrease in the slack bus voltage also makes the overall bus voltage smaller, and hence increases the value of these terms.

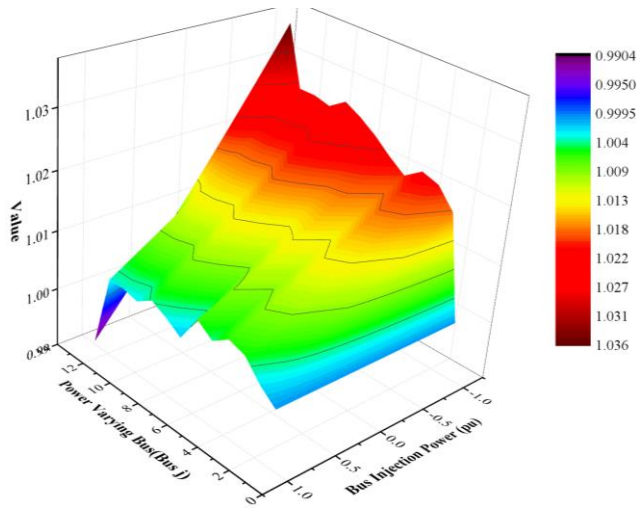

(**a**) V_{slack} = 1.0 pu

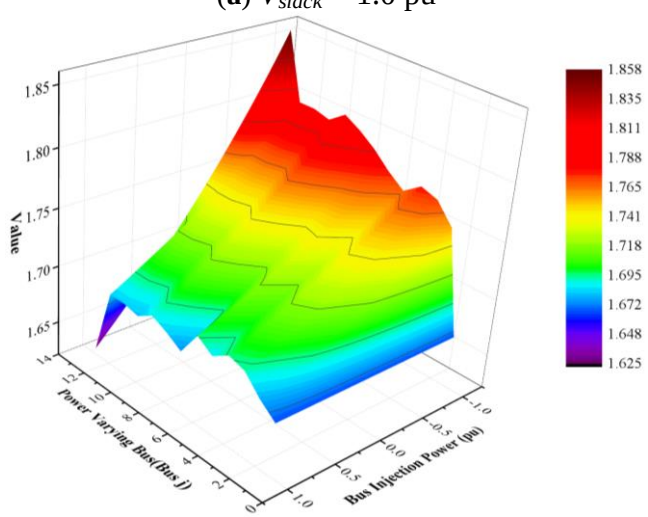

(**b**) V_{slack} = 0.6 pu

Figure A.5 The results of (A.27) as a function of the injected power at the bus

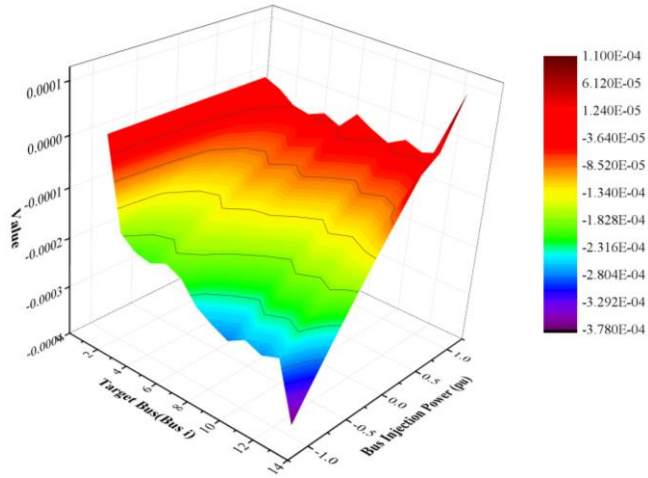

(a) V_{slack} = 1.0 pu

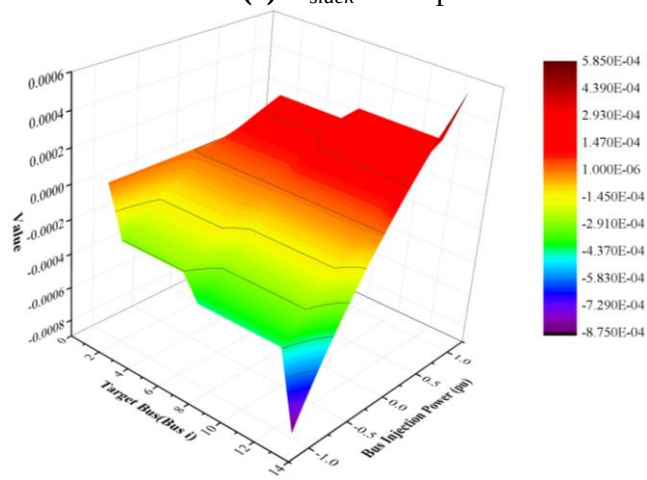

(**b**) V_{slack} = 0.6 pu

Figure A.6 The results of (A.28) as a function of the injected power at the bus

Figure A.8 shows the results for the exact calculated voltage sensitivity as a function of the injected power when the injected power was varied at bus 13. As shown in Figure A.8 (a), (b), the voltage sensitivity was largest at buses 9 and 12 because the term in (A.29) dominates the voltage sensitivity, and this term was largest at buses 9 and 12, respectively. As shown in Figure A.8 (c), (d), the forms of the voltage sensitivity curves were similar to those in Figure A.8 (a), (b), because the element of the R-Bus matrix influences the form of the voltage sensitivity curves. Therefore, the magnitudes of the voltage sensitivities were similar to the magnitudes of the R-Bus matrix elements. The increase in the injected power at bus

13 results in a small increase in the term in (A.26), as well as an increase in the voltage sensitivity. Overall, a low voltage results in increased voltage sensitivity, and the voltage sensitivity experiences larger changes due to variations in the injected power at the bus because a low bus voltage makes the terms in (A.26) and (A.27) more significant.

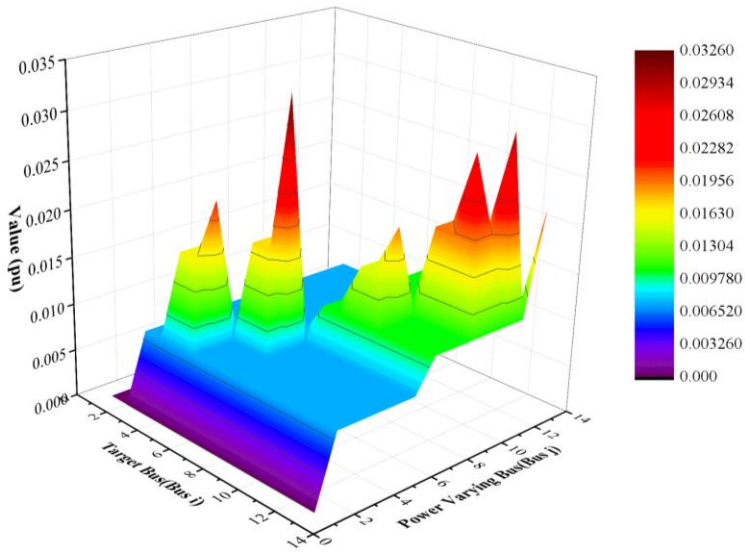

Figure A.7 The results of (A.29) as a function of the injected power at the bus.

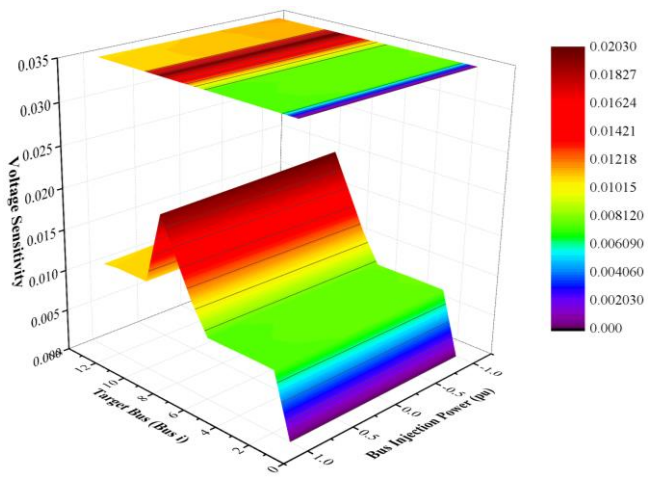

(**a**) j is bus 9 and V_{slack} = 1.0 pu

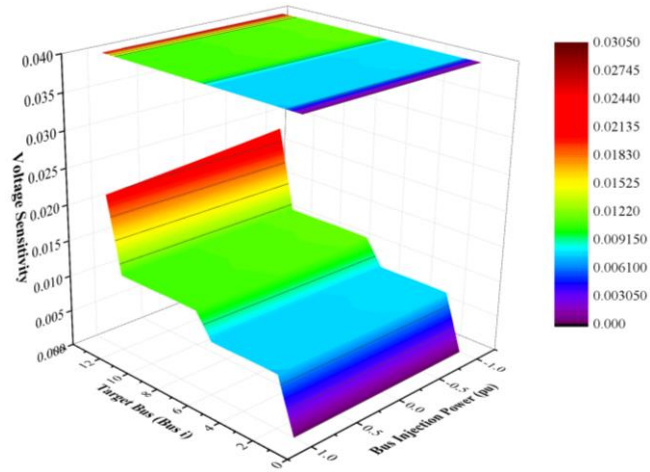

(**b**) j is bus 12 and V_{slack} = 1.0 pu

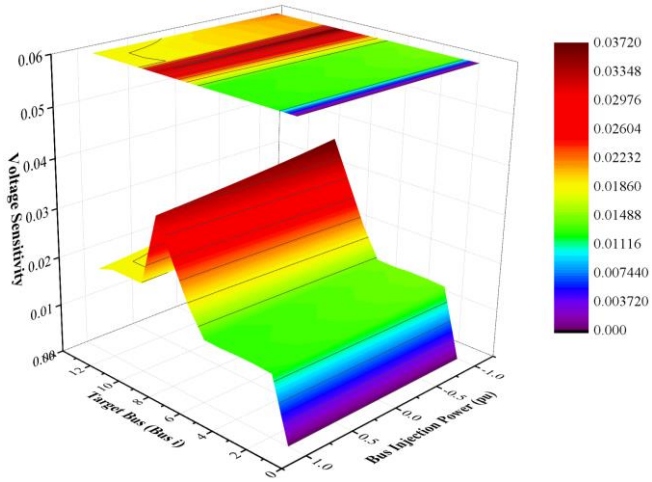

(**c**) j is bus 9 and V_{slack} = 0.6 pu

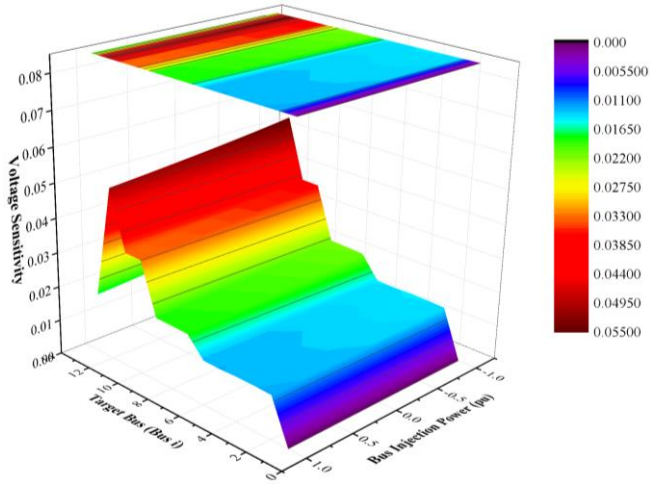

(**d**) j is bus 12 and V_{slack} = 0.6 pu

Figure A.8 The results of the exact calculation of the voltage sensitivity in response to changes in the bus injected power

A.3.2 Analysis of the Approximate Expression of Voltage Sensitivity with Regard to the Slack Bus Voltage

The approximate expression for voltage sensitivity to changes in slack bus voltage is composed of the following three terms:

$$k_5 = \frac{V_i^2}{\left(V_i^2 + R_{ii}P_i\right)} \tag{A.30}$$

$$k_6 = 1 \tag{A.31}$$

$$k_7 = \sum_{k=1,k\neq j}^{n} \frac{R_{ik}P_k}{V_k^2 + R_{kk}P_k} \tag{A.32}$$

As shown in Figure A.9, an increase in the negative injected power at the bus and a decrease in the slack bus voltage make the term in (A.30) larger. The term in (A.30) is close to 1.0 under most conditions, except when the slack bus voltage is very low and the negative injected power at the bus is very large. The magnitude of the term in (A.32), is much smaller than 1.0, because of the inequality in (A.16). Figure A.10 shows the result of the term in (A.32), which was much smaller than 1.0 at all operating points. Consequently, the approximate expression for the voltage sensitivity is equivalent to the term in (A.30), which is equivalent to term (A.26) if the term in (A.32) is neglected and the term in (A.30) dominates. The voltage sensitivity to the slack bus voltage is close to 1.0 because the term in (A.30) is close to 1.0.

Figure A.11 shows the results of the exact calculation of voltage sensitivity in response to changes in the slack bus voltage. The magnitude was close to 1.0 for all cases, as above. Both the form and the magnitude of the voltage sensitivity curve were similar to that given by the term in (A.30); however, the form of the exact calculation was smoother than the result of the term in (A.30) due to the effects of the term in (A.32). Figure A.11 (a), (c), (d), (f) show the effects of injected power at the bus. In these cases, the injected power was larger at buses 7 and 13 than at the other buses, which strongly affected the sensitivity. A large positive power

injected at buses 13 and 7 with these negative powers at the other buses resulted in voltage sensitivity at these buses of less than 1.0 (see Figure A.11 (c), (f)).

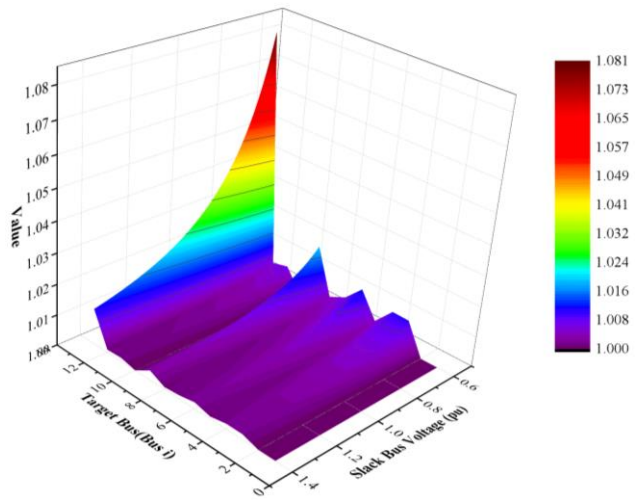

(**a**) The injected power at bus 13 is −1 MW

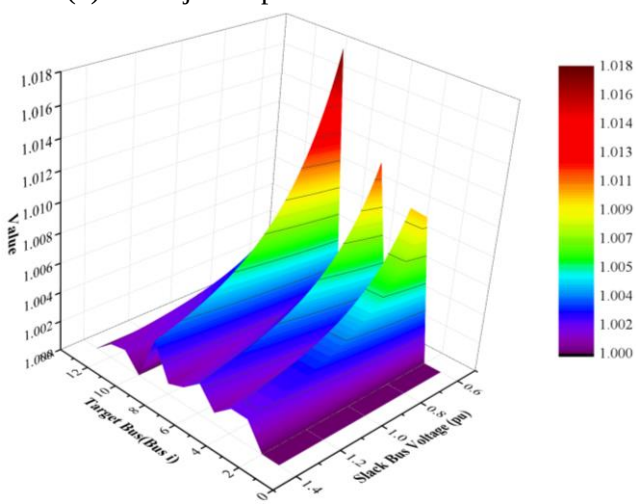

(**b**)) The injected power at bus 13 is 0 MW

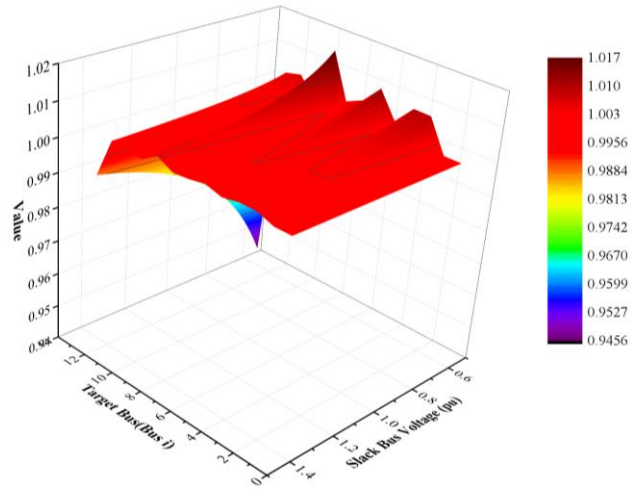

(**c**) The injected power at bus 13 is 1 MW

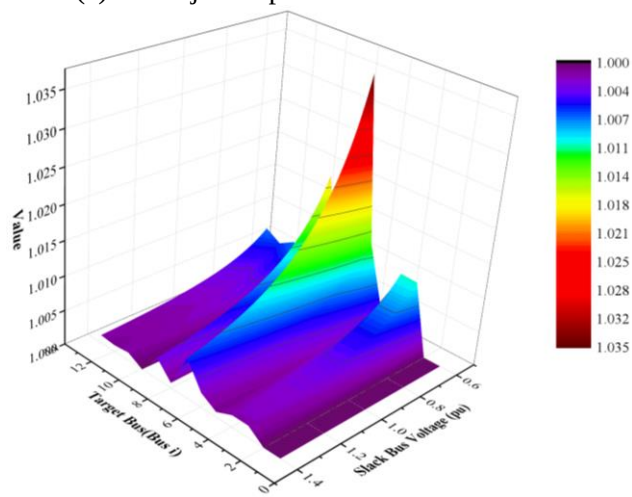

(**d**) The injected power at bus 7 is −1 MW

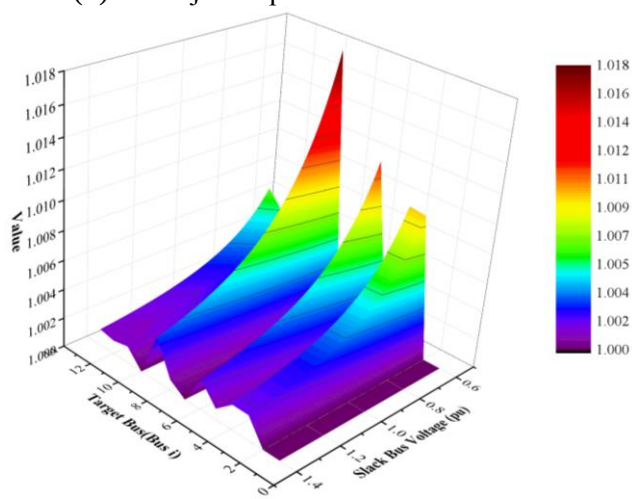

(**e**) The injected power at bus 7 is 0 MW

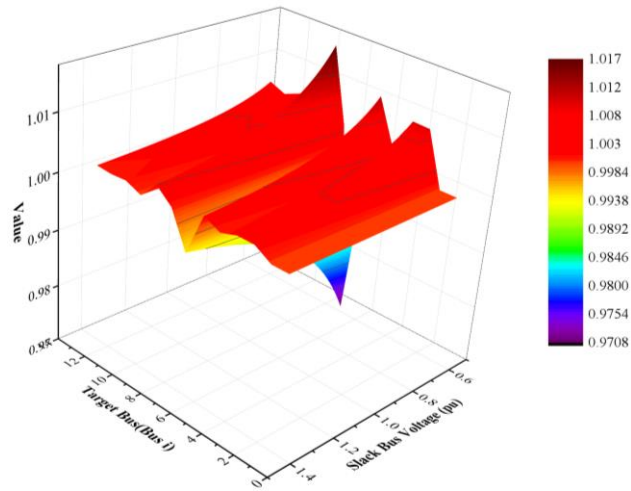

(**f**) The injected power at bus 7 is 1 MW

Figure A.9 The results of (40)

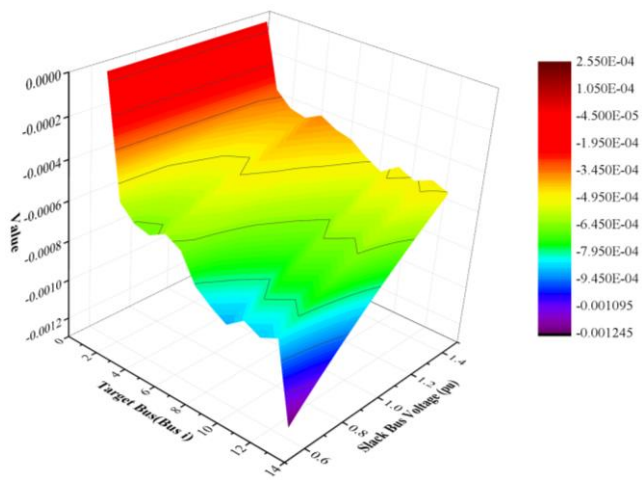

(**a**) The injected power at bus 13 is −1 MW

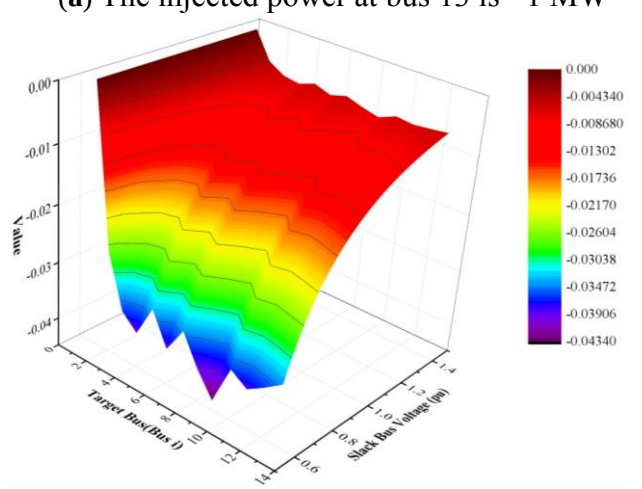

(b) The injected power at bus 13 is 0 MW

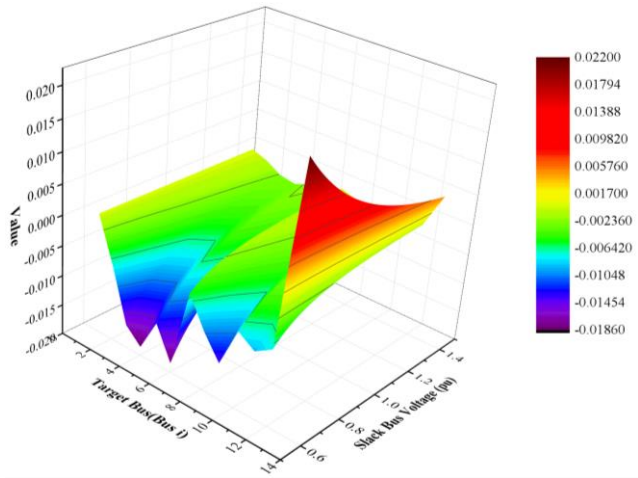

(**c**) The injected power at bus 13 is 1 MW

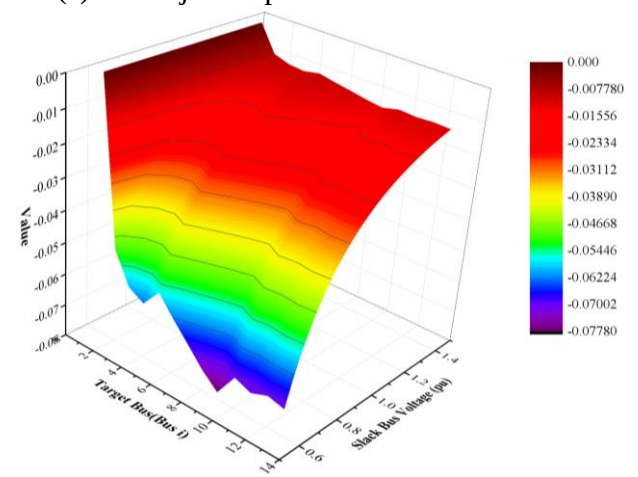

(**d**) The injected power at bus 7 is −1 MW

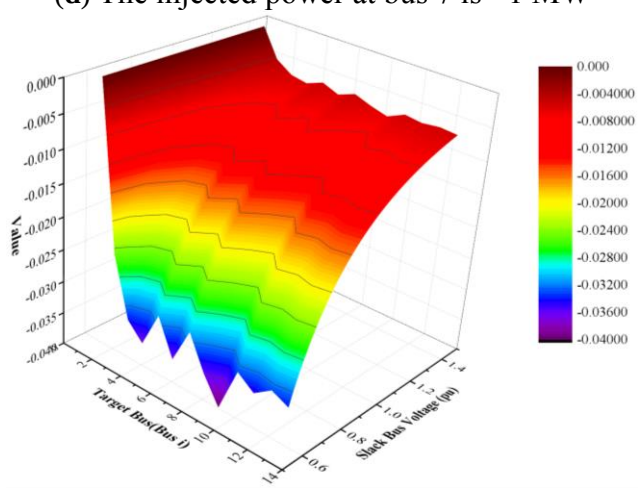

(**e**) The injected power at bus 7 is 0 MW

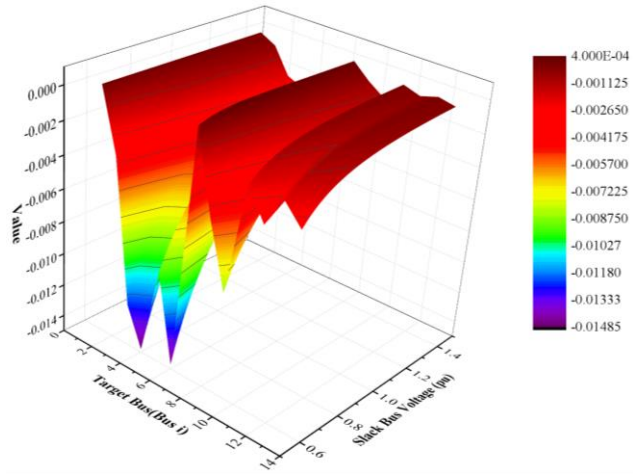

(**f**) The injected power at bus 7 is 1 MW

Figure A.10 The results of (42)

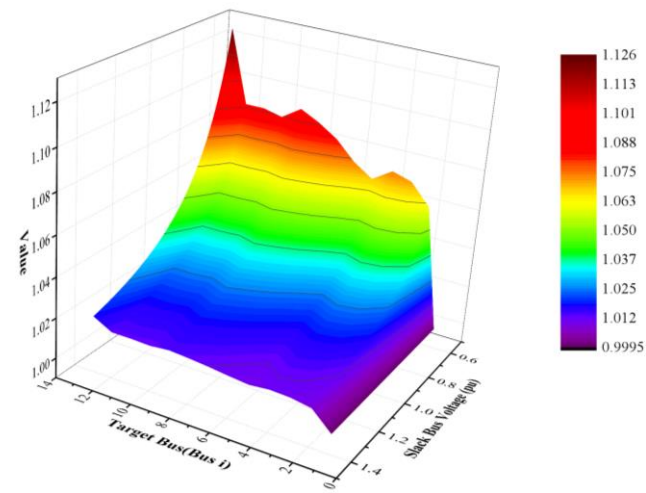

(**a**) The injected power at bus 13 is −1 MW

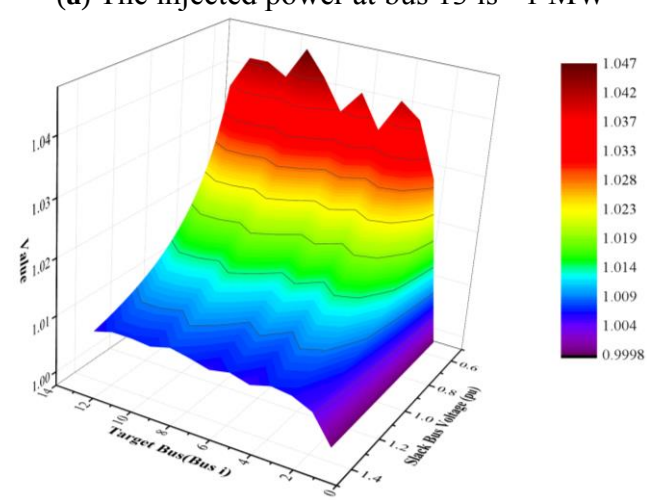

(**b**) The injected power at bus 13 is 0 MW

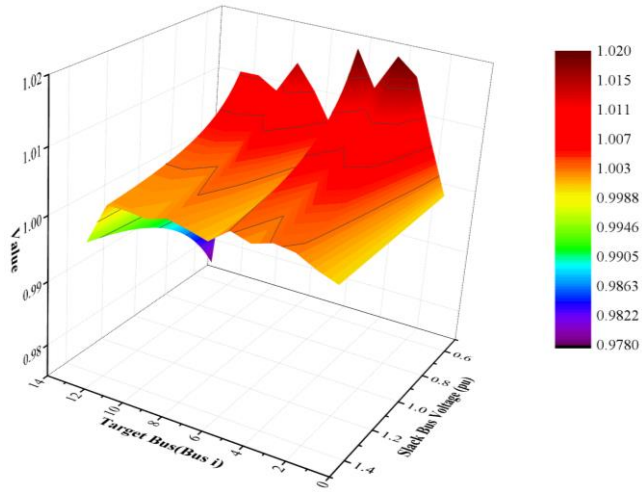

(**c**) The injected power at bus 13 is 1 MW

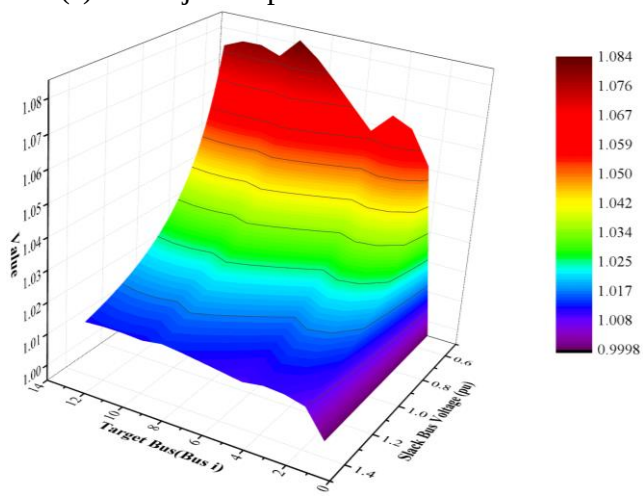

(**d**) The injected power at bus 7 is −1 MW

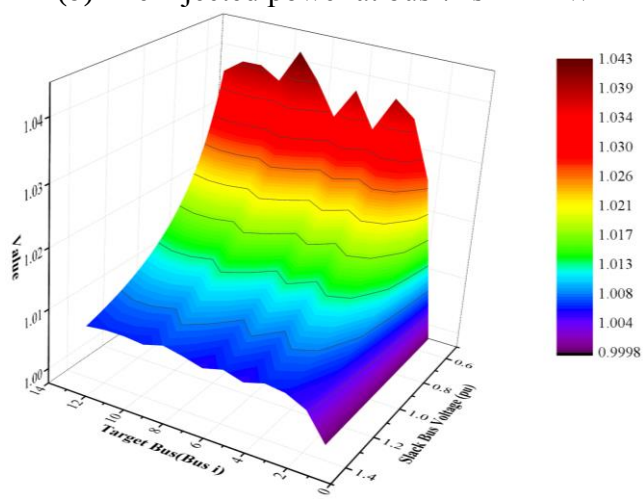

(**e**) The injected power at bus 7 is 0 MW

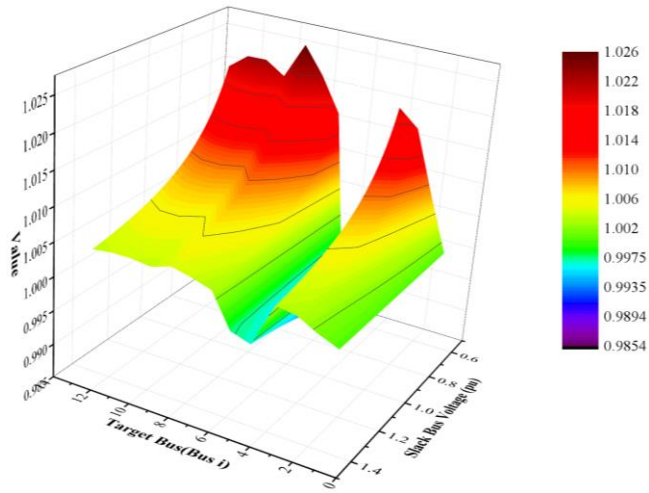

(**f**) The injected power at bus 7 is 1 MW

Figure A.11 The results of the exact calculation of the voltage sensitivity in response to changes in the slack bus voltage

Appendix B. Formulation for Approximated Expression for Loss Sensitivity in the Radial DC Distribution System

B.1 Approximate Expression for the Loss Sensitivity in a Radial DC Distribution System

This dissertation considers converter internal loss and loss over the line conductor. As mentioned above, there are researches modeling converter loss as equation by regression analysis. In this case, it is able to obtain loss sensitivity of converter internal loss by the partial derivative of a regression equation. However, loss sensitivity over the distribution line conductor is more complex and formulation in this dissertation focuses on it. Because GCC and DG is utilized as control equipment, two kinds of sensitivity are dealt with in this dissertation.

B.1.1 Conventional Calculation of Loss Sensitivity

The conventional calculation of loss sensitivity in the AC power system is presented in [65]. In a similar way, loss sensitivity in the DC power system can be calculated by use of the Jacobian matrix. Jacobian matrix in the DC power system is presented in (B.1) and loss sensitivity with respect to bus voltage is presented as (B.2):

$$J = \begin{bmatrix} \frac{\partial P_1}{\partial V_1} & \frac{\partial P_1}{\partial V_2} & \cdots & \frac{\partial P_1}{\partial V_n} \\ \frac{\partial P_2}{\partial V_1} & \frac{\partial P_2}{\partial V_2} & \cdots & \frac{\partial P_2}{\partial V_n} \\ \vdots & \vdots & \ddots & \vdots \\ \frac{\partial P_n}{\partial V_1} & \frac{\partial P_n}{\partial V_2} & \cdots & \frac{\partial P_n}{\partial V_n} \end{bmatrix} \tag{B.1}$$

$$\frac{\partial P_{loss}^{line}}{\partial V_i} = \sum_{k=1}^{n} \frac{\partial P_k}{\partial V_i} \quad for\ all\ k \tag{B.2}$$

GCC and DG are utilized for loss reduction control, and control variable of equipment is slack bus voltage and output power, respectively. Therefore, loss sensitivities with respect to bus injection power and slack bus voltage are analyzed to investigate changes in loss due to control. The loss sensitivity with respect to bus injection power and slack bus voltage is derived as (B.3) and (B.4).

$$\frac{\partial P_{line}^{loss}}{\partial P_i} = \sum_{k=1}^{n} \sum_{j=1}^{n} \frac{\partial V_j}{\partial P_i} \frac{\partial P_k}{\partial V_j} \quad for\ all\ k \tag{B.3}$$

$$\frac{\partial P_{line}^{loss}}{\partial V_{slack}} = \sum_{k=1}^{n} \frac{\partial P_k}{\partial V_{slack}} \quad for\ all\ k \tag{B.4}$$

B.1.2 Formulation of an Approximate Expression for Loss Sensitivity with Respect to Real Bus Power

The main purpose of this work is to obtain an approximate expression for loss sensitivity over the distribution line conductor. To formulate this, it is assumed that the variation in loss of distribution system can be used to describe the variation in real power at bus *j* (the controlled bus). Assumptions and linearization used in Appendix A is adopted to formulate an approximate loss sensitivity equation.

In a similar way as development of voltage sensitivity, line loss should be expressed as follows to derive sensitivities:

$$P_{line}^{loss} = f(P, V_{slack}) \tag{B.5}$$

Line loss is equivalent to a sum of bus injection power at all buses, including slack bus, and it is expressed as (B.6).

$$P_{line}^{loss} = \sum_{k=1}^{n} P_k \tag{B.6}$$

Bus injection power at slack bus is determined by the bus injection current of buses except slack bus. This is expressed as (B.7), and finally, the line loss equation is obtained as (B.8)

$$P_{slack} = -V_{slack} \sum_{\substack{k=1 \\ k \neq slack}}^{n} \frac{P_k}{V_k} \tag{B.7}$$

$$P_{line}^{loss} = \sum_{\substack{k=1 \\ k \neq slack}}^{n} P_k - V_{slack} \sum_{\substack{k=1 \\ k \neq slack}}^{n} \frac{P_k}{V_k} \tag{B.8}$$

From (B.8), if the real power at bus *j* were varied slightly, only small changes would be expected to occur in the bus voltages (except for the slack bus). Therefore, the deviation in the bus voltage and real power can be linearized because the sensitivity analysis deals with small variations in these parameters, allowing (B.8) to be re-written as:

$$P_{line}^{loss} + \Delta P_{line}^{loss} = \sum_{\substack{k=1 \\ k \neq slack,\, j}}^{n} P_k + P_j + \Delta P_j - V_{slack} \left(\sum_{\substack{k=1 \\ k \neq slack,\, j}}^{n} \frac{P_k}{V_k + \Delta V_k} + \frac{P_j + \Delta P_j}{V_j + \Delta V_j} \right) \tag{B.9}$$

where *j* is the index of the bus for which the real bus power is varied. The voltage deviation at the slack bus and bus injection power at buses except bus *j* are neglected because these are kept constant. To relate the deviation of the electrical quantities, the line loss deviation can be described by subtracting (B.8) from (B.9); *i.e.*,

$$\Delta P_{line}^{loss} = \Delta P_j - V_{slack} \left(\sum_{\substack{k=1 \\ k \neq slack,\, j}}^{n} \frac{-P_k \Delta V_k}{V_k^2 + V_k \Delta V_k} + \frac{V_j \Delta P_j - P_j \Delta V_j}{V_j^2 + V_j \Delta V_j} \right) \tag{B.10}$$

With assumption shown in (A.8), (B.10) can be approximated to (B.11).

$$\Delta P_{line}^{loss} \approx \left(1-\frac{V_{slack}}{V_j}\right)\Delta P_j + V_{slack}\sum_{\substack{k=1\\k\neq slack}}^{n}\frac{P_k \Delta V_k}{V_k^2} \tag{B.11}$$

From (B.11), line loss sensitivity in response to deviations in the real power at bus *j* is given by

$$\frac{\Delta P_{line}^{loss}}{\Delta P_j} \approx \left(1-\frac{V_{slack}}{V_j}\right) + V_{slack}\sum_{\substack{k=1\\k\neq slack}}^{n}\frac{P_k}{V_k^2}\frac{\Delta V_k}{\Delta P_j} \tag{B.12}$$

Derived loss sensitivity equation includes the voltage sensitivity of other buses and depends on it. To eliminate voltage sensitivity, the above equation is arranged as follows using (A.17):

$$\frac{\Delta P_{line}^{loss}}{\Delta P_j} \approx \left(1-\frac{V_{slack}}{V_j}\right) + V_{slack}\sum_{\substack{k=1\\k\neq slack}}^{n}\frac{P_k}{\left(V_k^2 + R_{kk}P_k\right)V_j}\left(R_{kj} - \sum_{\substack{k'=1\\k'\neq k}}^{n}\frac{R_{k'k}R_{k'j}P_{k'}}{V_{k'}^2 + R_{k'k'}P_{k'}}\right) \tag{B.13}$$

This equation can be simplified with the assumption in (A.16), and simple form of line loss sensitivity with respect to bus injection power is presented as follows:

$$\frac{\Delta P_{line}^{loss}}{\Delta P_j} \approx \left(1-\frac{V_{slack}}{V_j}\right) + V_{slack}\sum_{\substack{k=1\\k\neq slack}}^{n}\frac{R_{kj}P_k}{\left(V_k^2 + R_{kk}P_k\right)V_j} \tag{B.14}$$

B.1.3 Formulation of an Approximate Expression for Loss Sensitivity with Respect to Slack Bus Voltage

In this dissertation, the slack bus voltage is controlled by GCC for loss reduction and voltage regulation. Therefore, the slack bus voltage is considered as a controlled variable, which occurs variation in operating point of each equipment and distribution system, and influences variation in line loss over the conductors. To formulate an approximate expression for line loss sensitivity to slack bus voltage, the deviation of line loss in response to changes in the slack bus voltage.

In this case, a linearized form of line loss due to small variation in the slack bus voltage can be presented as follows:

$$P_{line}^{loss} + \Delta P_{line}^{loss} = \sum_{\substack{k=1 \\ k \neq slack}}^{n} P_k - \left(V_{slack} + \Delta V_{slack}\right) \sum_{\substack{k=1 \\ k \neq slack}}^{n} \frac{P_k}{V_k + \Delta V_k} \tag{B.15}$$

The Line loss deviation due to change in the slack bus voltage can be described by subtracting (B.14) from (B.15)

$$\Delta P_{line}^{loss} = V_{slack} \sum_{\substack{k=1 \\ k \neq slack}}^{n} \frac{P_k \Delta V_k}{V_k^2 + V_k \Delta V_k} - \Delta V_{slack} \sum_{\substack{k=1 \\ k \neq slack}}^{n} \frac{P_k}{V_k + \Delta V_k} \tag{B.16}$$

From above equation, the approximation is presented by Taylor series expansion as follows:

$$\frac{P_k}{V_k + \Delta V_k} \approx \frac{P_k}{V_k} - \frac{P_k}{V_k^2} \Delta V_k \tag{B.17}$$

The equation (B.16) can be approximated as follows using assumption shown in (A.8) and approximation shown in (B.17):

$$\Delta P_{line}^{loss} \approx V_{slack} \sum_{\substack{k=1 \\ k \neq slack}}^{n} \frac{P_k \Delta V_k}{V_k^2} - \Delta V_{slack} \sum_{\substack{k=1 \\ k \neq slack}}^{n} \frac{P_k}{V_k} \left(1 - \frac{\Delta V}{V_k}\right) \tag{B.18}$$

And the line loss deviation in the distribution system in response to changes in V_{slack} is given by

$$\frac{\Delta P_{line}^{loss}}{\Delta V_{slack}} \approx V_{slack} \sum_{\substack{k=1 \\ k \neq slack}}^{n} \frac{P_k}{V_k^2} \frac{\Delta V_k}{\Delta V_{slack}} - \sum_{\substack{k=1 \\ k \neq slack}}^{n} \frac{P_k}{V_k} \left(1 - \frac{\Delta V_k}{V_k}\right) \tag{B.19}$$

The backward term on the right-hand side of the equation includes ΔV_k, which is voltage deviation in response to changes in the slack bus voltage, and this variable is much smaller than 1 because voltage sensitivity with regard to the slack bus voltage is approximately 1.0 and deviation of the slack bus voltage is very small in sensitivity analysis. In addition, the variable V_k, which is voltage at bus k, also should be approximately 1.0 if bus voltage is maintained within tolerance limits. Therefore, this expression can be approximated as follows:

$$\frac{\Delta P_{line}^{loss}}{\Delta V_{slack}} \approx V_{slack} \sum_{\substack{k=1 \\ k\neq slack}}^{n} \frac{P_k}{V_k^2} \frac{\Delta V_k}{\Delta V_{slack}} - \sum_{\substack{k=1 \\ k\neq slack}}^{n} \frac{P_k}{V_k} \tag{B.20}$$

This expression is dependent on the voltage sensitivity of other buses to V_{slack}, which allows us to develop an approximate expression for voltage sensitivity as a function of the injected power at the buses. The following expression relates bus voltages to V_{slack}, and is arrived at via recursive substitution:

$$\frac{\Delta P_{line}^{loss}}{\Delta V_{slack}} \cong V_{slack} \sum_{\substack{k=1 \\ k\neq slack}}^{n} \frac{P_k}{V_k^2 + R_{kk} P_k} \left(1 - \sum_{k=1, k'\neq k}^{n} \frac{R_{kk'} P_{k'}}{V_{k'}^2 + R_{k'k'} P_k} \right) - \sum_{\substack{k=1 \\ k\neq slack}}^{n} \frac{P_k}{V_k} \tag{B.21}$$

This equation can be simplified with the assumption in (A.16), and simple form of line loss sensitivity with respect to bus injection power is presented as follows:

$$\frac{\Delta P_{line}^{loss}}{\Delta V_{slack}} \approx V_{slack} \sum_{\substack{k=1 \\ k\neq slack}}^{n} \frac{P_k}{V_k^2 + R_{kk} P_k} - \sum_{\substack{k=1 \\ k\neq slack}}^{n} \frac{P_k}{V_k} \tag{B.22}$$

B.2 Verification of the Approximate Loss Sensitivity Equation

To verify the proposed approximate expression for loss sensitivity, case studies are carried out to compare loss sensitivities derived using the proposed equation with values derived using exact calculations. The test system is identical to what used in verification of the approximate voltage sensitivity equation in Appendix A, it is shown in Figure A.1, Table A.1 and Table A.2.

The loss sensitivity was investigated as a function of the injected power at buses and the slack bus voltage. The approximate loss sensitivity was calculated using (B.13) and (B.21). The exact loss sensitivity as a function of the injected power at the buses was obtained from (B.3), and the voltage sensitivity in response to changes in the slack bus voltage was calculated from (B.4).

B.2.1 Verification of the Approximate Expression of Loss Sensitivity with

Regard to Bus Injected Power

The injected power at each bus was varied from −1 MW to 1 MW. Four cases were considered, where the slack bus voltage was 0.6, 0.8, 1.0 and 1.2 pu; however, the bus voltage tolerance limit may be exceeded in some cases. Figure B.1 shows the maximum error of the approximate loss sensitivity equation for each variation in the injected power at each bus. The controlled bus was the bus for which the injected power was varied.

Loss sensitivity has range from negative to positive values. Absolute percentage error can't evaluate an error if actual value is zero and an error becomes very large if actual value is close to zero. Therefore, an accuracy of loss sensitivity is evaluated normalized root mean squared error (NRMSE), which is defined as (B.23).

$$NRMSE(\%) = \frac{\sqrt{\sum_{i=1}^{n} \frac{\left(x_{actual,i} - x_{estimated,i}\right)^2}{n}}}{x_{actual,\max} - x_{actual,\min}} \times 100(\%) \tag{B.23}$$

In the studied cases, maximum NRMSE of the approximate expression for loss sensitivity as a function of the injected power at the buses is 4.1%, and accuracy isn't better than approximate voltage sensitivity. However, NRMSE didn't exceed 1.5% if voltage tolerance is limited within 10%, it is indicated that the approximate expression has quite good accuracy. Therefore, approximate loss sensitivity equation may be useful if bus voltage is maintained within allowed range. The error increased as the negative injected power at the bus increased or slack bus voltage is decreased due to effect of neglected term during approximation.

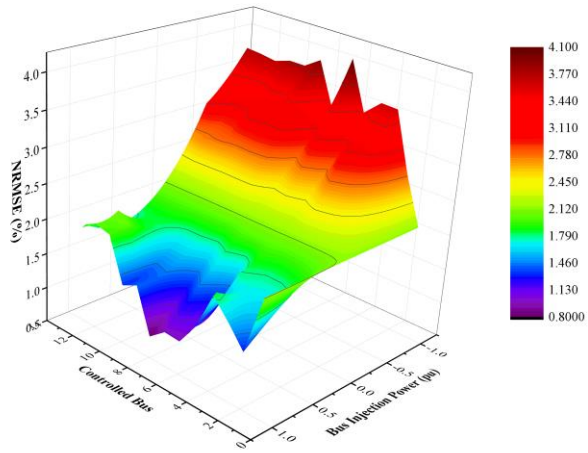

(**a**) V_{slack} = 0.6 pu

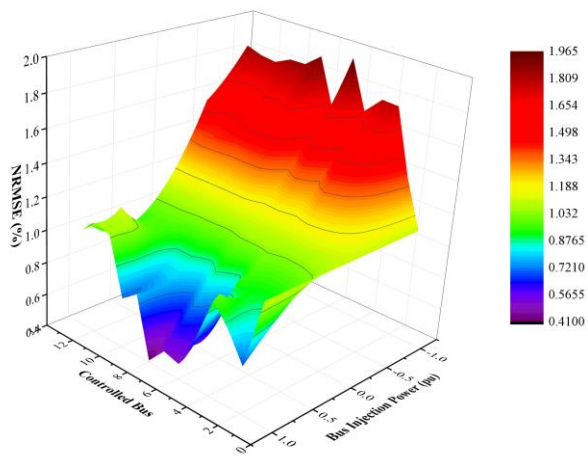

(**b**) V_{slack} = 0.8 pu

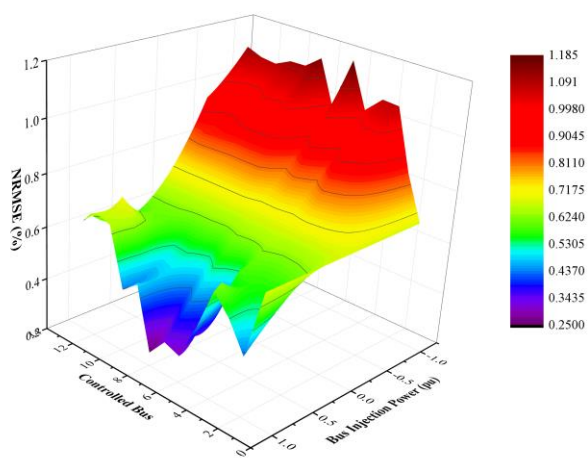

(**c**) V_{slack} = 1.0 pu

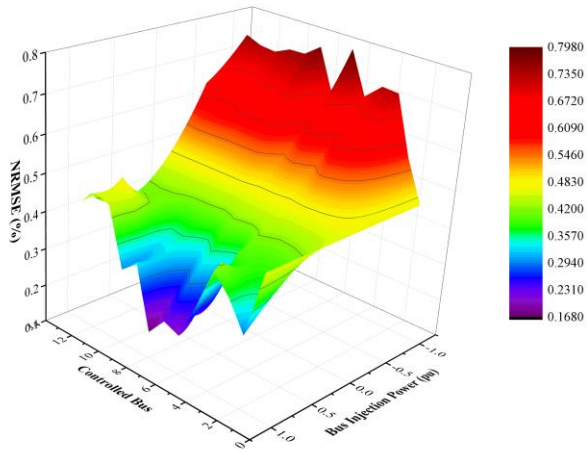

(**d**) V_{slack} = 1.2 pu

Figure B.1 The NRMSE of the approximate expression for loss sensitivity as a function of the injected power

B.2.2 Verification of the Approximate Expression of Loss Sensitivity with Regard to Bus Injected Power

The approximate expression (B.20) was used to calculate the voltage sensitivity for slack bus voltages in the range 0.6–1.2 pu. The exact value of loss sensitivity as a function of V_{slack} is calculated from a set of power flow solutions. Power flow solutions are calculated for each 0.001pu slack bus voltage deviation and loss sensitivity is calculated from loss deviation at each state. Figure B.2 shows the percentage error in the approximate expression for loss sensitivity as a function of V_{slack} when the injected power was varied at bus 2, 7, 9 and 12.

The maximum error did not exceed 0.25%. It is indicated that the approximate expression for voltage sensitivity as a function of the slack bus voltage has good accuracy. The error increased as the slack bus voltage decreased, the negative injected power at the bus increased, and the electrical distance from the slack bus increased because the line voltage drop became larger than the limits of normal operating conditions. The increased voltage drop affects the accuracy of voltage sensitivity as a function of the slack bus voltage in (B.20), as a result, an error increased due to large line voltage drop.

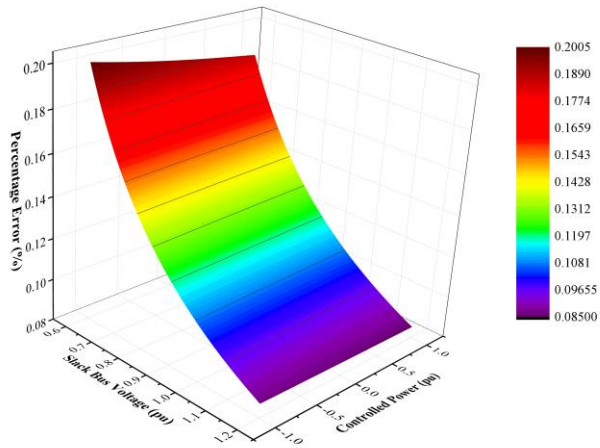

(**a**) Injected power varied at bus 2

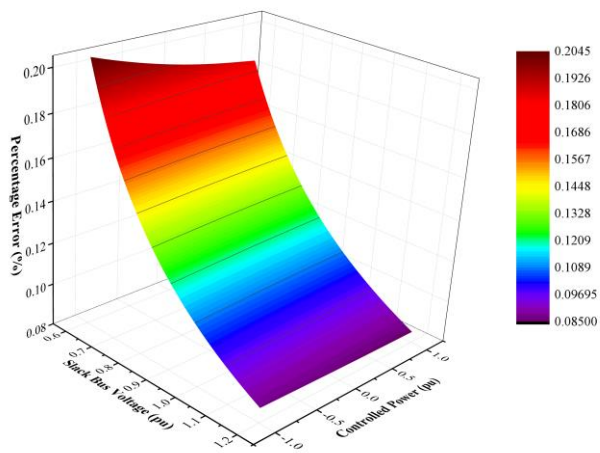

(**b**) Injected power varied at bus 7

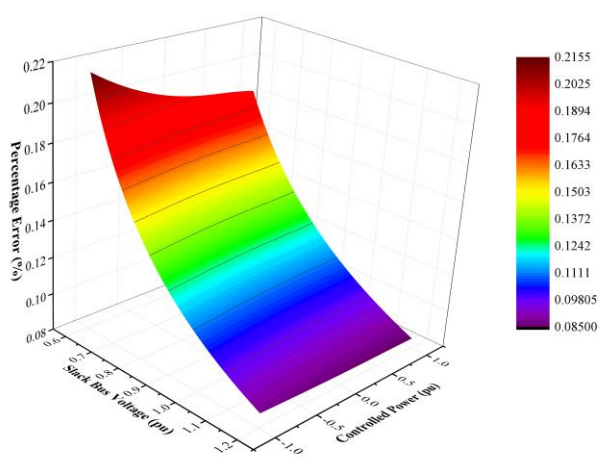

(**c**) Injected power varied at bus 9

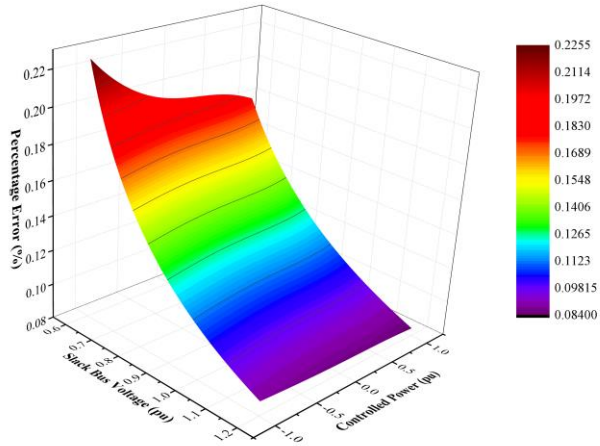

(**d**) Injected power varied at bus 12

Figure B.2 The percentage error of the approximate expression for loss sensitivity as a function of V_{slack}

Bibliography

[1] M. Starke, F. Li, L. M. Tolbert, and B. Ozpineci, "AC vs. DC distribution: maximum transfer capability," in *Power and Energy Society General Meeting-Conversion and Delivery of Electrical Energy in the 21st Century, 2008 IEEE*, 2008, pp. 1-6.

[2] T. Kaipia, P. Salonen, J. Lassila, and J. Partanen, "Possibilities of the low voltage DC distribution systems," in *Nordac, Nordic Distribution and Asset Management Conference*, 2006, pp. 1-10.

[3] X. Fang, S. Misra, G. Xue, and D. Yang, "Smart grid—The new and improved power grid: A survey," *Communications Surveys & Tutorials, IEEE,* vol. 14, pp. 944-980, 2012.

[4] D. J. Hammerstrom, "AC versus DC distribution systemsdid we get it right?," in *Power Engineering Society General Meeting, 2007. IEEE*, 2007, pp. 1-5.

[5] G. Byeon, T. Yoon, S. Oh, and G. Jang, "Energy management strategy of the DC distribution system in buildings using the EV service model," *Power Electronics, IEEE Transactions on,* vol. 28, pp. 1544-1554, 2013.

[6] A. Sannino, G. Postiglione, and M. H. Bollen, "Feasibility of a DC network for commercial facilities," *Industry Applications, IEEE Transactions on,* vol. 39, pp. 1499-1507, 2003.

[7] A. Monti, M. Colciago, P. Conti, M. Maglio, and R. Dougal, "Integrated simulation of communication, protection, and power in MVDC systems," in *Electric Ship Technologies Symposium, 2009. ESTS 2009. IEEE*, 2009, pp. 353-359.

[8] D. Salomonsson and A. Sannino, "Low-voltage DC distribution system for commercial power systems with sensitive electronic loads," *Power Delivery, IEEE Transactions on,* vol. 22, pp. 1620-1627, 2007.

[9] B. Zahedi and L. E. Norum, "Modeling and simulation of all-electric ships with low-voltage DC hybrid power systems," *Power Electronics, IEEE Transactions on,* vol. 28, pp. 4525-4537, 2013.

[10] J. G. Ciezki and R. W. Ashton, "Selection and stability issues associated with a navy shipboard DC zonal electric distribution system," *Power Delivery, IEEE Transactions on,* vol. 15, pp. 665-669, 2000.

[11] H. Kakigano, M. Nomura, and T. Ise, "Loss evaluation of DC distribution for residential houses compared with AC system," in *Power Electronics Conference (IPEC), 2010 International*, 2010, pp. 480-486.

[12] M. E. Baran and N. R. Mahajan, "DC distribution for industrial systems: opportunities and challenges," *Industry Applications, IEEE Transactions on,* vol. 39, pp. 1596-1601, 2003.

[13] M. Brenna, G. Lazaroiu, and E. Tironi, "High power quality and DG integrated low voltage dc distribution system," in *Power Engineering Society General Meeting, 2006. IEEE*, 2006, p. 6 pp.

[14] H. Kakigano, Y. Miura, and T. Ise, "Low-voltage bipolar-type DC microgrid for super high quality distribution," *Power Electronics, IEEE Transactions on,* vol. 25, pp. 3066-3075, 2010.

[15] A. Emadi, A. Khaligh, C. H. Rivetta, and G. A. Williamson, "Constant power loads and negative impedance instability in automotive systems: definition, modeling, stability, and control of power electronic converters and motor drives," *Vehicular Technology, IEEE Transactions on,* vol. 55, pp. 1112-1125, 2006.

[16] S. Grillo, V. Musolino, G. Sulligoi, and E. Tironi, "Stability enhancement in DC distribution systems with constant power controlled converters," in *Harmonics and Quality of Power (ICHQP), 2012 IEEE 15th International Conference on*, 2012, pp. 848-854.

[17] Y. Khersonsky, T. Ericsen, P. Bishop, J. Amy, M. Andrus, T. Baldwin, *et al.*, "Recommended Practice for 1 to 35 kV Medium Voltage DC Power Systems on Ships," 2010.

[18] F. Bignucolo, R. Caldon, and V. Prandoni, "Radial MV networks voltage regulation with distribution management system coordinated controller," *Electric Power Systems Research,* vol. 78, pp. 634-645, 2008.

[19] R. Aghatehrani and R. Kavasseri, "Reactive power management of a DFIG wind system in microgrids based on voltage sensitivity analysis," *Sustainable Energy, IEEE Transactions on,* vol. 2, pp. 451-458, 2011.

[20] L. Zhang, T. Wu, Y. Xing, K. Sun, and J. M. Gurrero, "Power control of DC microgrid using DC bus signaling," in *Applied Power Electronics Conference and Exposition (APEC), 2011 Twenty-Sixth Annual IEEE*, 2011, pp. 1926-1932.

[21] H. Kakigano, Y. Miura, and T. Ise, "Distribution voltage control for dc microgrids using fuzzy control and gain-scheduling technique," *Power Electronics, IEEE Transactions on,* vol. 28, pp. 2246-2258, 2013.

[22] T. Dragicevic, J. M. Guerrero, J. C. Vasquez, and D. Skrlec, "Supervisory control of an adaptive-droop regulated dc microgrid with battery management capability," *Power Electronics, IEEE Transactions on,* vol. 29, pp. 695-706, 2014.

[23] X. Lu, K. Sun, J. M. Guerrero, J. C. Vasquez, and L. Huang, "State-of-charge balance using adaptive droop control for distributed energy storage systems in DC microgrid applications," *Industrial Electronics, IEEE Transactions on,* vol. 61, pp. 2804-2815, 2014.

[24] Z. Ye, D. Boroyevich, K. Xing, and F. C. Lee, "Design of parallel sources in DC distributed power systems by using gain-scheduling technique," in *Power Electronics Specialists Conference, 1999. PESC 99. 30th Annual IEEE,* 1999, pp. 161-165.

[25] D. Chen and L. Xu, "Autonomous DC voltage control of a DC microgrid with multiple slack terminals," *Power Systems, IEEE Transactions on,* vol. 27, pp. 1897-1905, 2012.

[26] Y. Ito, Y. Zhongqing, and H. Akagi, "DC microgrid based distribution power generation system," in *Power Electronics and Motion Control Conference, 2004. IPEMC 2004. The 4th International*, 2004, pp. 1740-1745.

[27] W. Tang and R. Lasseter, "An LVDC industrial power distribution system without central control unit," in *Power Electronics Specialists Conference, 2000. PESC 00. 2000 IEEE 31st Annual*, 2000, pp. 979-984.

[28] J. Schönberger, R. Duke, and S. D. Round, "DC-bus signaling: A distributed control strategy for a hybrid renewable nanogrid," *Industrial Electronics, IEEE Transactions on,* vol. 53, pp. 1453-1460, 2006.

[29] J. Bryan, R. Duke, and S. Round, "Decentralized generator scheduling in a

nanogrid using DC bus signaling," in *Power Engineering Society General Meeting, 2004. IEEE*, 2004, pp. 977-982.

[30] M. o. T. I. a. Energy, "Standard for reliability and power quality in power system," ed, 2015.

[31] A. N. S. Institute, "ANCI C84.1: Electric power systems and equipment - voltage ranges," ed, 2011.

[32] M. Begovic, D. Novosel, B. Milosevic, and M. Kostic, "Impact of distribution efficiency on generation and voltage stability," in *System Sciences, 2000. Proceedings of the 33rd Annual Hawaii International Conference on*, 2000, p. 7 pp.

[33] D. Kirshner, "Implementation of conservation voltage reduction at Commonwealth Edison," *Power Systems, IEEE Transactions on,* vol. 5, pp. 1178-1182, 1990.

[34] Z. Wang and J. Wang, "Review on implementation and assessment of conservation voltage reduction," *Power Systems, IEEE Transactions on,* vol. 29, pp. 1306-1315, 2014.

[35] S. G. Naik, D. Khatod, and M. Sharma, "Optimal allocation of combined DG and capacitor for real power loss minimization in distribution networks," *International Journal of Electrical Power & Energy Systems,* vol. 53, pp. 967-973, 2013.

[36] S. K. Goswami and S. K. Basu, "A new algorithm for the reconfiguration of distribution feeders for loss minimization," *Power Delivery, IEEE Transactions on,* vol. 7, pp. 1484-1491, 1992.

[37] J.-H. Teng, S.-W. Luan, D.-J. Lee, and Y.-Q. Huang, "Optimal charging/discharging scheduling of battery storage systems for distribution systems interconnected with sizeable PV generation systems," *Power Systems, IEEE Transactions on,* vol. 28, pp. 1425-1433, 2013.

[38] C. Chen, S. Duan, T. Cai, B. Liu, and G. Hu, "Optimal allocation and economic analysis of energy storage system in microgrids," *Power Electronics, IEEE Transactions on,* vol. 26, pp. 2762-2773, 2011.

[39] T.-C. Ou, W.-M. Lin, C.-H. Huang, and F.-S. Cheng, "A hybrid programming for distribution reconfiguration of dc microgrid," in *Sustainable Alternative Energy (SAE), 2009 IEEE PES/IAS Conference on*,

2009, pp. 1-7.

[40] L. Meng, T. Dragicevic, J. M. Guerrero, and J. C. Vasquez, "Dynamic consensus algorithm based distributed global efficiency optimization of a droop controlled DC microgrid," in *Energy Conference (ENERGYCON), 2014 IEEE International*, 2014, pp. 1276-1283.

[41] J. Ma, F. He, and Z. Zhao, "Line loss optimization based OPF strategy by hierarchical control for DC microgrid," in *Energy Conversion Congress and Exposition (ECCE), 2015 IEEE*, 2015, pp. 6212-6216.

[42] H. Kakigano, Y. Miura, T. Ise, J. Van Roy, and J. Driesen, "Basic sensitivity analysis of conversion losses in a DC microgrid," in *Renewable Energy Research and Applications (ICRERA), 2012 International Conference on*, 2012, pp. 1-6.

[43] H. Mehrjerdi, S. Lefebvre, M. Saad, and D. Asber, "A decentralized control of partitioned power networks for voltage regulation and prevention against disturbance propagation," *Power Systems, IEEE Transactions on*, vol. 28, pp. 1461-1469, 2013.

[44] H. Ayres, W. Freitas, M. De Almeida, and L. Da Silva, "Method for determining the maximum allowable penetration level of distributed generation without steady-state voltage violations," *IET generation, transmission & distribution*, vol. 4, pp. 495-508, 2010.

[45] A. J. Flueck, R. Gonella, and J. R. Dondeti, "A new power sensitivity method of ranking branch outage contingencies for voltage collapse," *Power Systems, IEEE Transactions on*, vol. 17, pp. 265-270, 2002.

[46] J. Greatbanks, D. Popovic, M. Begovic, A. Pregelj, and T. Green, "On optimization for security and reliability of power systems with distributed generation," in *Power Tech Conference Proceedings, 2003 IEEE Bologna*, 2003, p. 8 pp. Vol. 1.

[47] P. Kankanala, S. C. Srivastava, A. K. Srivastava, and N. N. Schulz, "Optimal control of voltage and power in a multi-zonal MVDC shipboard power system," *Power Systems, IEEE Transactions on*, vol. 27, pp. 642-650, 2012.

[48] D. Popović, J. Greatbanks, M. Begović, and A. Pregelj, "Placement of distributed generators and reclosers for distribution network security and

reliability," *International Journal of Electrical Power & Energy Systems*, vol. 27, pp. 398-408, 2005.

[49] W. R. Wagner, A. Keyhani, S. Hao, and T. C. Wong, "A rule-based approach to decentralized voltage control," *Power Systems, IEEE Transactions on*, vol. 5, pp. 643-651, 1990.

[50] P. A. Ruiz and P. W. Sauer, "Voltage and reactive power estimation for contingency analysis using sensitivities," *Power Systems, IEEE Transactions on*, vol. 22, pp. 639-647, 2007.

[51] C. Vournas, "Voltage stability and controllability indices for multimachine power systems," *Power Systems, IEEE Transactions on*, vol. 10, pp. 1183-1194, 1995.

[52] R. Yan and T. K. Saha, "Voltage variation sensitivity analysis for unbalanced distribution networks due to photovoltaic power fluctuations," *Power Systems, IEEE Transactions on*, vol. 27, pp. 1078-1089, 2012.

[53] K. Christakou, J. LeBoudec, M. Paolone, and D.-C. Tomozei, "Efficient computation of sensitivity coefficients of node voltages and line currents in unbalanced radial electrical distribution networks," *Smart Grid, IEEE Transactions on*, vol. 4, pp. 741-750, 2013.

[54] J.-C. Choi, H.-Y. Jeong, J.-Y. Choi, D.-J. Won, S.-J. Ahn, and S.-i. Moon, "Voltage Control Scheme with Distributed Generation and Grid Connected Converter in a DC Microgrid," *Energies*, vol. 7, pp. 6477-6491, 2014.

[55] A. A. Hamad, M. A. Azzouz, and E. F. El-Saadany, "Multiagent Supervisory Control for Power Management in DC Microgrids," *Smart Grid, IEEE Transactions on*, vol. PP, pp. 1-1, 2015.

[56] T. P. Hai, I.-Y. Chung, J.-Y. Kim, and J. Cho, "Voltage Control in Low-Voltage Distribution System Based on Distribution Control," in *The International Conference on Electrical Engineering 2015*, Hong Kong, 2015, pp. 1-6.

[57] P. Kundur, N. J. Balu, and M. G. Lauby, *Power system stability and control* vol. 7: McGraw-hill New York, 1994.

[58] I. o. Electrical and E. Engineers, *IEEE Recommended Practice for Industrial and Commercial Power Systems Analysis*: IEEE, 1990.

[59] K. Mamandur and R. Chenoweth, "Optimal control of reactive power flow

for improvements in voltage profiles and for real power loss minimization," *Power Apparatus and Systems, IEEE Transactions on*, pp. 3185-3194, 1981.

[60] M. Braun, "Reactive Power supplied by PV Inverters–Cost-Benefit-Analysis," in *22nd European Photovoltaic Solar Energy Conference and Exhibition*, 2007, pp. 3-7.

[61] A. E.-M. M. M. Aly and A. El-Aal, "Modelling and simulation of a photovoltaic fuel cell hybrid system," 2005.

[62] Y. Wang, S. Mao, and R. M. Nelms, *Online Algorithms for Optimal Energy Distribution in Microgrids*: Springer, 2015.

[63] *Korea power exchange - Load forecasting*. Available: http://kpx.co.kr/KOREAN/htdocs/main/sub/bidForegenList.jsp

[64] *Korea power exchange - SMP*. Available: http://kpx.co.kr/KOREAN/htdocs/main/sub/bidSmpList.jsp

[65] H. Happ, "Optimal power dispatch," *Power Apparatus and Systems, IEEE Transactions on*, pp. 820-830, 1974.

국문 초록

방사형 직류 배전계통에서 손실을 고려한 계통 연계 컨버터와 분산전원의 민감도 기반 협조 운영 기법

서울대학교

전기 · 컴퓨터 공학부

정 호 용

본 학위논문은 방사형 DC 배전 계통에서 선로 및 변환 손실을 고려한 계통 연계 컨버터와 분산전원의 협조 제어 기법을 제안하고 전압 민감도와 손실 민감도 근사식에 대한 정식화를 새롭게 제안한다.

DC 배전 계통의 장점이 부각됨에 따라 이에 대한 관심이 집중되고 가능성이 열리고 있다. DC 배전 계통은 AC 계통에 비해 송전 가능한 전력이 더 크고 계통의 전체적인 손실이 더 작게 나타난다. DC 배전 계통은 또한 에너지 효율, 지속가능성, 유연성 측면에서 스마트 그리드 환경에 적합하며 이러한 점들은 스마트 그리드의 중요한 기술적인 문제와 관련이 있다. 여러 연구에서 DC 배전 계통의 가능성과 타당성에 대해 다뤘으나, 아직 안정적이고 경제적인 계통 운영 측면에서 고려해야 할 기술적인 문제들이 다수 존재한다. DC 배전 계통에서는 DC/AC 또는

DC/DC 컨버터를 통해 전력을 공급받기 때문에 정전력 부하 특성을 나타나며, 정전력 부하의 negative incremental resistance 특성으로 인해 전압 안정도 문제가 야기된다. 전압 안정도 문제를 방지하기 위해 전압 제어기법들이 연구 되어왔다. 그러나 이러한 연구들은 전압 제어 능력 및 효율적인 전압 제어에서 한계를 보이고 있다. 특히, DC 배전 계통의 효율적인 운영관점에서 선로 및 변환 손실은 중요한 요소이나, 대부분의 기존 연구들에서는 선로 손실과 변환 손실 저감을 고려하지 못하고 있다.

본 학위논문의 연구는 방사형 DC 배전 계통에서 전체 손실 저감을 고려하면서 전압을 적정전압 내로 유지하는 것을 목적으로 한다. 제어 전략을 수립하기 전에 선형 근사를 이용하여 전압과 선로 손실에 대한 새로운 민감도 식을 정식화 하였다. 제안된 수식에 대한 검증이 이루어졌으며 제안된 수식의 정확도가 양호함을 확인하였다. 전압민감도의 해석적 분석이 수행되었고 분석 결과는 전압 제어 전략을 수립하는데 활용되었다. 또한, 민감도 근사식은 민감도 계산시 연산량을 감소 시킬 수 있기 때문에 빠른 응답 특성을 지닌 제어기 구현에 유용하게 적용될 수 있다.

민감도 근사식과 근사식 분석 결과를 바탕으로 방사형 DC 배전 시스템에서 전체 손실을 고려한 협조 전압 제어 전략을 제안하였다. 전체적인 제어 전략을 구조를 제시하였으며, 전압 제어기기의 역할과 상호 작용에 대해 기술하였다. 최적 스케쥴링 모델과 함께 목적함수 및 제약조건에 대한 모델링을 수행하였다. 손실 저감 및 전압 제어를 위한 제어 전략을 수립하였으며, 이를 구현하기 위한 제어 모듈을 설계하였다. 또한 각 전압 제어기기의 전기적 변수의 변화에 따른 전체 손실 변화를 나타내는 전압 제어기기에 대한 전체 손실 민감도를 정식화 하였다.

제안된 기법의 검증을 위해 MATLAB과 PSCAD/EMTDC 상에

시험 계통을 구성하여 다양한 조건하에서 모의를 수행하였다. 결과를 통해 부하 및 신재생 발전량이 변화하는 조건하에서 전체 모선 전압을 제어하면서 효과적으로 손실을 저감시킬 수 있음을 확인하였다. 이에 따라, 제안된 협조 전압 제어 전략은 방사형 시스템에서 안정도와 경제성을 고려한 계통 운영에 유용하게 적용될 수 있다.

핵심어: DC 배전 계통, 협조 전압 제어, 손실 저감, 전압 민감도, 손실 민감도

학번: 2009-20897